宇宙現象を用いた究極理論探査 (IV)

● 京大基研　小玉英雄

首都大東京集中講義

2017/11/15 - 16

講義計画

第1章 宇宙論の基礎

1.1 膨張する宇宙

1.2 熱いビッグバン宇宙

1.3 加速する宇宙

1.4 4次元インフレーション宇宙モデルの概観

第2章 究極理論

2.1 究極理論の候補

2.2 超弦理論と超重力理論

2.3 D-Brane

第3章 インフレーションによる究極理論探査

3.1 問題点

3.2 加速膨張に対するNO-GO定理

3.3 超弦理論に基づくインフレーションモデル

第4章 Axion Cosmophysicsによる究極理論探査

4.1 What is axion?

4. 2 String Axions

4. 3 Direct Search

4. 4 Axion Cosmophysics

4. 5 重力波によるアクシオン探査

4. 6 ガンマ線天文学によるアクシオン探査

第4章　Axion Cosmophysicsによる究極理論探査

4.1 What is axion?

QCD Axion

A psued-NG boson arising from the SSB of the Peccei-Quinn chiral symmetry to resolve the strong CP problem.

- **Basic features of the invisible QCD axion**
  - **P&CP-odd, very weak coupling to matter**

$$g_{aq}\, a\,(\bar{q}\gamma_5 q): \quad g_{aq} \approx m_q/f_a;\;\; f_a \gtrsim 10^9\text{GeV}$$

$$g_{a\gamma}\, a\, F\wedge F: \quad g_{a\gamma} \approx 1/f_a$$

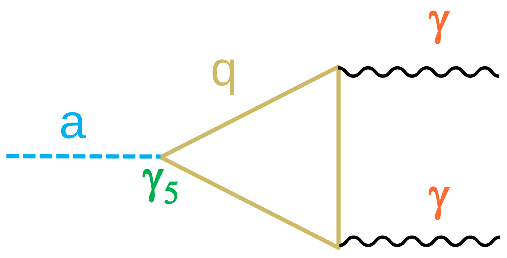

  - **Small mass by the QCD instanton effect:**

$$m_a = 10^{-3}\ \text{eV}\left(\frac{10^{10}\text{GeV}}{f_a}\right)$$

  - **Dark matter candidate:** $\Omega_a \simeq 0.01\left(\frac{f_a}{10^{10}GeV}\right)^{1.175}$

Axion

Axion = Pseudo NG boson associated with SB of chiral shift/U(1) symmetry

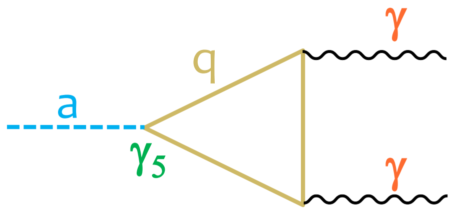

ϕ: CP Odd

$$\mathscr{L}_\phi = -\frac{1}{2}(\partial\phi)^2 - V(\phi) + \phi\sum_\alpha \frac{\xi_\alpha}{f_a}\frac{g_\alpha^2}{16\pi^2} F^{(\alpha)}\cdot\tilde{F}^{(\alpha)} + \partial_\mu\phi\sum_j \frac{y_j}{f_a}\bar{\Psi}_j\gamma^\mu\gamma_5\Psi_j$$

Chern-Simons coupling to EM

$$g_{a\gamma}\phi\boldsymbol{E}\cdot\boldsymbol{B};\quad g_{a\gamma}\sim\frac{10^{-3}}{f_a}$$

Derivative coupling to fermions

$$V(\phi) = \Lambda^4\left(1-\cos\left(\frac{\phi}{f_a}\right)\right) = \frac{\Lambda^4}{2f_a^2}\phi^2 - \frac{\Lambda^4}{6f_a^4}\phi^4 + \cdots$$

attractive self-interaction

axion mass $m_a = \frac{\Lambda^2}{f_a}$

axion decay constant f_a

アクシオン作用積分の一般的構造

- カイラルU(1)/シフト変換

$$\phi \to \phi + \lambda f_a \Rightarrow \quad U = e^{i\lambda Q_5}$$

f_a: アクシオン崩壊定数 ← $\mathscr{L} = -\frac{1}{2}(\nabla\phi)^2 + \cdots$

- 作用積分

アクシオンの作用積分は、スピノール場Ψはそのままにして、スカラ場を

$$\Phi = e^{i(\phi(x)/f_a)Q_5}\Phi_0$$

と置き換えることにより得られる。このとき、湯川結合に$e^{-i(\varphi(x)/f_a)Q_5}$の因子が残る。これを消すために、スピノール場 Ψ に対して 変換

$$Q_5 = t\gamma_5 \Rightarrow \quad \Psi \mapsto e^{i(\phi(x)/f_a)t\gamma_5}\Psi$$

を施す。ここで t はエルミート行列。$\phi(x)$が定数のとき、以上の変換は

ラグランジアンを変えないので、結局、アクシオンのラグランジアンは

$$e^{-1}\mathscr{L}_{\phi,0} = -\frac{1}{2}(\nabla\phi)^2 + \frac{1}{f_a}\partial_\mu\phi J_5^\mu; \quad J_5^\mu = \bar{\Psi}\gamma^\mu\gamma_5 t\Psi$$

Chiral Anomaly

カイラルカレントは，それを構成しているフェルミ粒子がゲージ相互作用すると，一般的に量子効果によりアノーマリーが生じ，カレントの保存則に位相的なゲージ補正項が加わる [Bell JS, Jackiw R (1969); Adler SL (1969)].

- 可換ゲージ場のTriangle Anomaly

Lagrangian

$$\mathscr{L} = -i\bar{\psi}(\gamma^{\mu} D_{\mu} - m)\psi - \frac{1}{4} F_{\mu\nu} F^{\mu\nu},$$
$$D_{\mu} = \partial_{\mu} + ieA_{\mu}$$

は、古典的ではつぎの対称性をもつ。

– achiralな対称性： $\psi \mapsto e^{i\alpha}\,\psi$

– chiralな対称性（質量$m = 0$のとき): $\psi \mapsto e^{i\beta\gamma_5}\,\psi$

- 保存則(量子論)

$$J^\mu = \bar{\psi}\gamma^\mu\psi \quad : \quad \partial_\mu J^\mu = 0,$$

$$J_5^\mu = \bar{\psi}\gamma^\mu\gamma_5\psi \quad : \quad \partial_\mu J_5^\mu = -2m\bar{\psi}\gamma_5\psi + \frac{e^2}{8\pi^2}F^{\mu\nu}\tilde{F}_{\mu\nu}.$$

anomaly

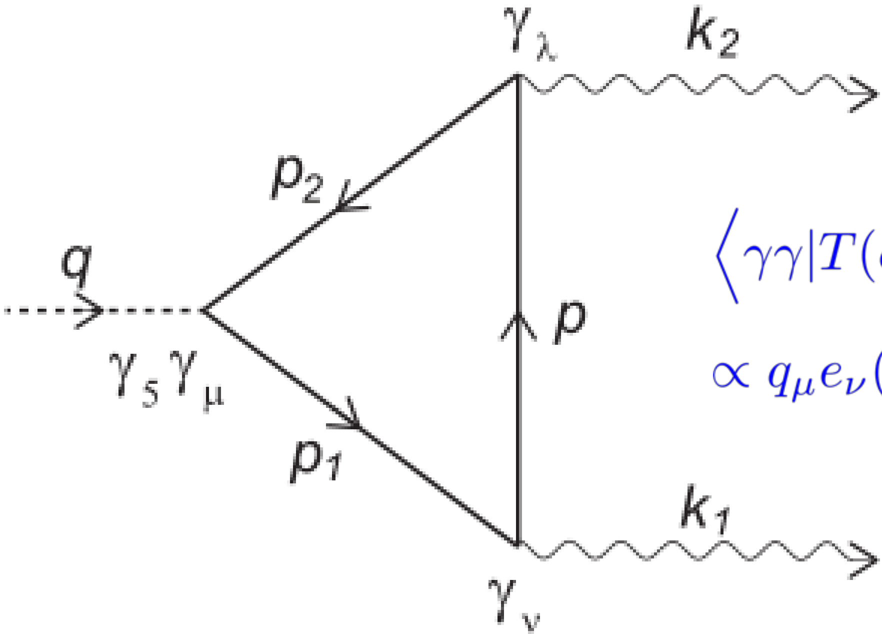

$$\left\langle \gamma\gamma | T(e^{iS_I} q_\mu \hat{J}_5^\mu(q)) | 0 \right\rangle$$

$$\propto q_\mu e_\nu(k_1) e_\lambda(k_2) \left\langle 0 | T(\hat{J}_5^\mu(q) \hat{J}^\nu(k_1) \hat{J}^\lambda(k_2)) | 0 \right\rangle$$

- ABJ anomaly
  - 不可避性 : 正則化においてベクトルカレントの保存を要請すると，軸性ベクトルカレントの保存則にはanomalyが発生し，その値は正則化の方法に依存しない.
  - 非くり込み定理 : くり込みにより形を変えない. [Adler-Bardeenの定理]
  - 普遍性 : 非可換ゲージ場，重力場との結合もカイラルアノマリーを生む.

$$D_\mu = \nabla_\mu - ig t_a A^a_\mu, \quad J^\mu_5 = \bar{\psi}\gamma^\mu\gamma_5 t\psi$$

$$\Rightarrow \quad \partial_\mu J^\mu_5 = \cdots + \frac{g^2}{8\pi^2}\mathrm{Tr}(t t_a t_b) F^a_{\mu\nu}\tilde{F}^{b\mu\nu} + \frac{1}{384\pi^2}\mathrm{Tr}(t) R_{\mu\nu\lambda\sigma}\tilde{R}^{\mu\nu\lambda\sigma}$$

- 様々な証明法
  - 摂動計算 : Cut offによる正則化, Pauli-Villars正則化、Point-splitting正則化.
  - 藤川による経路積分法:PI measureの正則化とAthiya-Singer指数定理.

アクシオンとゲージ場のChern-Simon結合

- 量子論では、正則化に伴うアノマリーのため、カイラル変換に対して有効ラグランジアンは次のように変換する:

$$e^{-1}\delta\mathscr{L}_{\rm eff} = \lambda\mathscr{P};$$
$$\mathscr{P} = \sum_{a,b}\mathrm{Tr}(tt_a t_b)\frac{1}{16\pi^2}F^a\cdot\tilde{F}^b \equiv \sum_{a,b}\mathrm{Tr}(tt_a t_b)\frac{1}{64\pi^2}\epsilon^{\mu\nu\lambda\sigma}F^a_{\mu\nu}F^b_{\lambda\sigma};$$

したがって、$\mathscr{P}\neq 0$ならば理論の不変性が破れる。ここで、ゲージ場$A^a = A^a_\mu dx^\mu$は次のように規格化されているものとする:

$$D_\mu\Psi = \left(\partial_\mu - iA^a_\mu t_a\right)\Psi,$$
$$e^{-1}\mathscr{L}_A = -\sum_a \frac{1}{2g_a^2}F^a\cdot F^a; \quad F^a = dA^a - \frac{i}{2}f^a_{bc}A^b\wedge A^c.$$

ただし, aはゲージ場のすべての成分を走るものとする. したがって, a, bが同じゲージ群に対するゲージ場の成分を表すとき, $g_a = g_b$となる.

- この変換を局所化し$\lambda = \lambda(x)$とすると, 有効Lagrangianは次のように変化する:

$$e^{-1}\delta\mathscr{L}_{\rm eff} = J_5^\mu \partial_\mu \lambda + \lambda \mathscr{P},$$

ここで, J_5^μはカイラル変換 $e^{i\lambda t\,\gamma_5}$に対するカレントである. 分配関数Zに対する経路積分による表示では, この局所変換は単に経路積分変数の変数変換なのでZに影響しない:

$$Z = \int [d\Psi d\bar{\Psi}\cdots]e^{iS} = \int [d\Psi' d\bar{\Psi}'\cdots]e^{iS'} = \int [d\Psi d\bar{\Psi}\cdots]e^{i(S+\delta S)}.$$

- これより次式を得る:

$$\langle \nabla_\mu J_5^\mu \rangle = \mathscr{P}$$

- TreeレベルLagrangianに付加項　$(\phi/f_a)\mathscr{P}$を加えることにより，この保存則の変更と場の方程式がtree levelで整合的となる．これより、（多成分）アクシオンに対する一般的な有効Lagrangianは次式で与えられる：

$$e^{-1}\mathscr{L}_a = -\frac{1}{2}\sum_{\alpha\beta}K^{\alpha\beta}\nabla\phi_\alpha\cdot\nabla\phi_\beta + \sum_\alpha \frac{1}{f_\alpha}\partial_\mu\phi_\alpha(\bar{\Psi}\gamma^\mu\gamma_5 t_\alpha\Psi)$$
$$+\sum_\alpha\frac{\phi_\alpha}{f_\alpha}\left(\sum_{a,b}\frac{\xi^\alpha_{ab}}{16\pi^2}F^a\cdot\tilde{F}^b + \frac{\mathrm{Tr}(t_\alpha)}{568\pi^2}R_{\mu\nu\lambda\sigma}\tilde{R}^{\mu\nu\lambda\sigma}\right);$$

ここで，t_αはカイラル変換$e^{i\lambda_\alpha t_\alpha\gamma_5}$を定義する行列, ϕ_αはそれに対するアクシオンで、$\xi^\alpha_{ab}=\mathrm{Tr}(t_\alpha\, t_a t_b)$である。

ポテンシャルの計算：インスタントン法

- CS作用積分

アクシオン場ϕ_α が一様なとき，$G = \mathrm{SU}(n)$ゲージ場$A = A^a t_a$に対するCS作用積分は，規格化$\mathrm{Tr}(t_a t_b) = \delta_{ab}/2$のもとで，

$$S_{CS} = \int \frac{\theta}{8\pi^2}\mathrm{Tr}(F \wedge F),$$

で与えられる．θが定数の時、この作用積分はゲージバンドルの第1Pontrjagin数p_1

$$p_1 = \int \frac{1}{8\pi^2}\mathrm{Tr}(F \wedge F) \in \mathbb{Z},$$

に比例する位相数となる．ここで，θは定数θ_0とアクシオン場を用いて

$$\theta = \theta_0 + \sum_\alpha \frac{\xi_A^\alpha}{f_\alpha}\phi_\alpha; \quad \mathrm{Tr}(t_\alpha t_a t_b) = \xi_A^\alpha \delta_{ab}.$$

と表される．ここで、Aはゲージ場を区別するラベル。

- インスタントン解
  - $p_1 \neq 0$ となるゲージ場の古典解。ユークリッド時空でのみ存在。
  - $\pi_3(G)$の類により分類される。
  - $\pi_3\big(\mathrm{SU}(1)\big) = 0$より、可換ゲージ場はインスタントン解を持たない。
  - $\pi_3\left(\mathrm{SU}(n)\right) = \mathbb{Z}(n \geq 2)$より、非可換ゲージ場のインスタントン解は整数$n \in \mathbb{Z}$（インスタントン数=ポントリャーギン数）により分類され、各インスタントン数に対して、SDないしASDとなるものが最小の作用積分をもつ。
  - $\mathrm{G} = \mathrm{SU}(2)$に対して、$n = \pm 1$となるSD/ASDインスタントン解は具体的表式が知られている（BPST解）。

$$A = \frac{r^2}{r^2 + R^2} U^{-1} dU; \quad U - \frac{1}{r}\left(x^4 \sigma_0 + i x^j \sigma_j\right) \ \in \mathrm{SU}(2)$$

● アクシオンポテンシャル

BPSTインスタントン解は，時空併進とdilationに対応するモジュライ自由度を持つので，その分配関数Zへの寄与は

$$Z_1 = \tilde{\Lambda}^5 \int d^4x \int dR e^{-S_E},$$

とあらわされる．ここで，$\tilde{\Lambda}$はある質量スケール．Rはインスタントンサイズである．また，S_Eは

$$S_E = \int d^4x \frac{1}{g^2} \mathrm{Tr}(*F \wedge F) = \pm \frac{1}{g^2} \int d^4x \mathrm{Tr}(F \wedge F) = \frac{8\pi^2}{g^2} |p_1|.$$

一般のインスタントン解を，p個のBPST解とq個のanti-BPST解の重ね合わせにより近似すると（dilute gas 近似), $n = p - q$より

$$Z_{\text{inst}} = \sum_{p,q \geq 0} \frac{Z_1^p}{p!} \frac{Z_{-1}^q}{q!} e^{i(p-q)\theta} = \exp\left[\tilde{\Lambda}^5 \int d^4x \int dR e^{-8\pi^2/g^2} (e^{i\theta} + e^{-i\theta})\right].$$

これは，インスタントンが非摂動論的ポテンシャル

$$V = -\Lambda^4 \cos\theta + \text{const} = -\Lambda^4 \cos\left(\theta_0 + \sum_\alpha \xi^\alpha \phi_\alpha / f_\alpha\right) + \text{const},$$

を生み出すことを意味する．ここで，

$$\Lambda^4 = 2\tilde{\Lambda}^5 \int dR e^{-8\pi^2/g^2(1/R)}.$$

この表式より，IR極限 $R \to \infty$ でゲージ場が強結合となると，大きなポテンシャルが生成されることが分かる．しかし，一般には，この強結合効果を計算するのは困難である．Colorゲージ場の場合には，次の方法によりその計算が可能で，Λ はパイ中間子の質量程度となる．

- ## 2成分以上の強結合ゲージ場がアクシオンと結合する場合

アクシオンポテンシャルは各ゲージ場からの寄与の和となる:

$$V = -\sum_A \Lambda_A^4 \cos\left(\theta_{A,0} + \sum_\alpha \xi_A^\alpha \phi_\alpha / f_\alpha\right) + \mathrm{const.}$$

ここで, $\theta_{A,0}$はフェルミ粒子の質量行列のCP位相と各非可換ゲージ場の真空のθ角の和である.

- ## アクシオンの質量

アクシオンの質量は, $\theta_{A,0} = 0$とおいて, Vをϕ_αについて2次まで展開することにより得られる:

$$V_2 = \frac{1}{2}\sum_{\alpha\beta}\left(\sum_A \Lambda_A^4 \xi_A^\alpha \xi_A^\beta\right)\frac{\phi_\alpha \phi_\beta}{f_\alpha f_\beta}.$$

この表式より, 一般に, アクシオン質量は, 最も大きな強結合スケールΛとアクシオン崩壊定数f_aを用いて

$$m_a \sim \frac{\Lambda^2}{f_a}$$

と表される.

ポテンシャル計算:カイラル有効理論法

- θ位相の除去

まず，SU(3)ゲージ場に対するCS項のθ位相（アクシオンを含む）を，カイラル変換

$$(u, d) \to (e^{iy_u\theta\gamma_5}u, e^{iy_d\theta\gamma_5}d)(\ y_u + y_d = -1)$$

により，クォーク質量行列に移動させる．すると，クォーク質量行列は

$$im_u\bar{u}u + im_d\bar{d}d \to im_u\bar{u}e^{2iy_u\theta\gamma_5}u + im_d\bar{d}e^{2iy_d\theta\gamma_5}d,$$

と変化し，クォークの運動項は新たなクォーク･アクシオン結合

$$\partial_\mu\theta(y_u\bar{u}\gamma^\mu\gamma_5u + y_d\bar{d}\gamma^\mu\gamma_5d).$$

を生み出す．

カイラル縮退

強結合領域では，クォーク場の積が真空期待値を持ち，カイラル対称性が自発的に破れる：

$$-i\left\langle \bar{u}u\right\rangle = -i\left\langle \bar{d}d\right\rangle = v_c \cos\left(2\pi^0/f_\pi\right),$$
$$-i\left\langle \bar{u}\gamma_5 u\right\rangle = i\left\langle \bar{d}\gamma_5 d\right\rangle = -iv_c \sin\left(2\pi^0/f_\pi\right),$$
$$\left\langle \bar{u}\gamma_\mu\gamma_5 u\right\rangle = -\left\langle \bar{d}\gamma_\mu\gamma_5 d\right\rangle = \frac{1}{2}f_\pi\partial_\mu\pi^0,$$

ここで，π^0は中性パイ中間子場，f_πはパイ中間子崩壊定数である．これにより，クォーク質量項よりポテンシャルが生み出される：

$$V_{a\pi} = -v_c m_u \cos\left(y_u\theta - 2\pi^0/f_\pi\right) - v_c m_d \cos\left(y_d\theta + 2\pi^0/f_\pi\right),$$

さらに，アクシオンとフェルミ粒子の微分結合は，アクシオンとπ^0の混合

$$\frac{1}{2}\left\{\sum_\alpha \frac{\nabla_\mu\phi_\alpha}{f_\alpha}(z_u^\alpha - z_d^\alpha) + \nabla_\mu\theta(y_u - y_d)\right\} f_\pi\nabla^\mu\pi^0,$$

を生み出す．ここで，$t_{\alpha u} = z_u^\alpha u$，$t_{\alpha d} = z_d^\alpha d$である．

- アクシオン質量

アクシオンが1成分（QCDアクシオン）のみの場合，(y_u, y_d)の値は，$y_u + y_d = -1$ およびアクシオン―パイオン混合が消えるという要請から一意的に決まる．これにより，アクシオンとパイ中間子に対する標準的な質量公式を得る:

$$
\begin{aligned}
m_\pi^2 &\simeq 4 v_c \frac{m_u + m_d}{f_\pi^2}, \\
m_a^2 &\simeq v_c \frac{\xi^2}{f_a^2} \frac{m_u m_d}{m_u + m_d} \simeq \left(\frac{\xi f_\pi}{2 f_a}\right)^2 \frac{m_u m_d}{(m_u + m_d)^2} m_\pi^2;
\end{aligned}
$$

ここで，$f_a \gg f_\pi$（invisible axion condition)を仮定した.

なお、2つ以上のアクシオンがSU(3)ゲージ場と結合する場合，y_uとy_dの選択でaxion-pion混合を消せない．代わりに，QCDアクシオン以外のアクシオンの定義をπ^0に比例した項だけずらすことにより取り除かれる．このため，axion-pion混合はアクシオン質量に影響を与えない。

4. 2 String Axions

Find phenomena characteristic to string theory!!

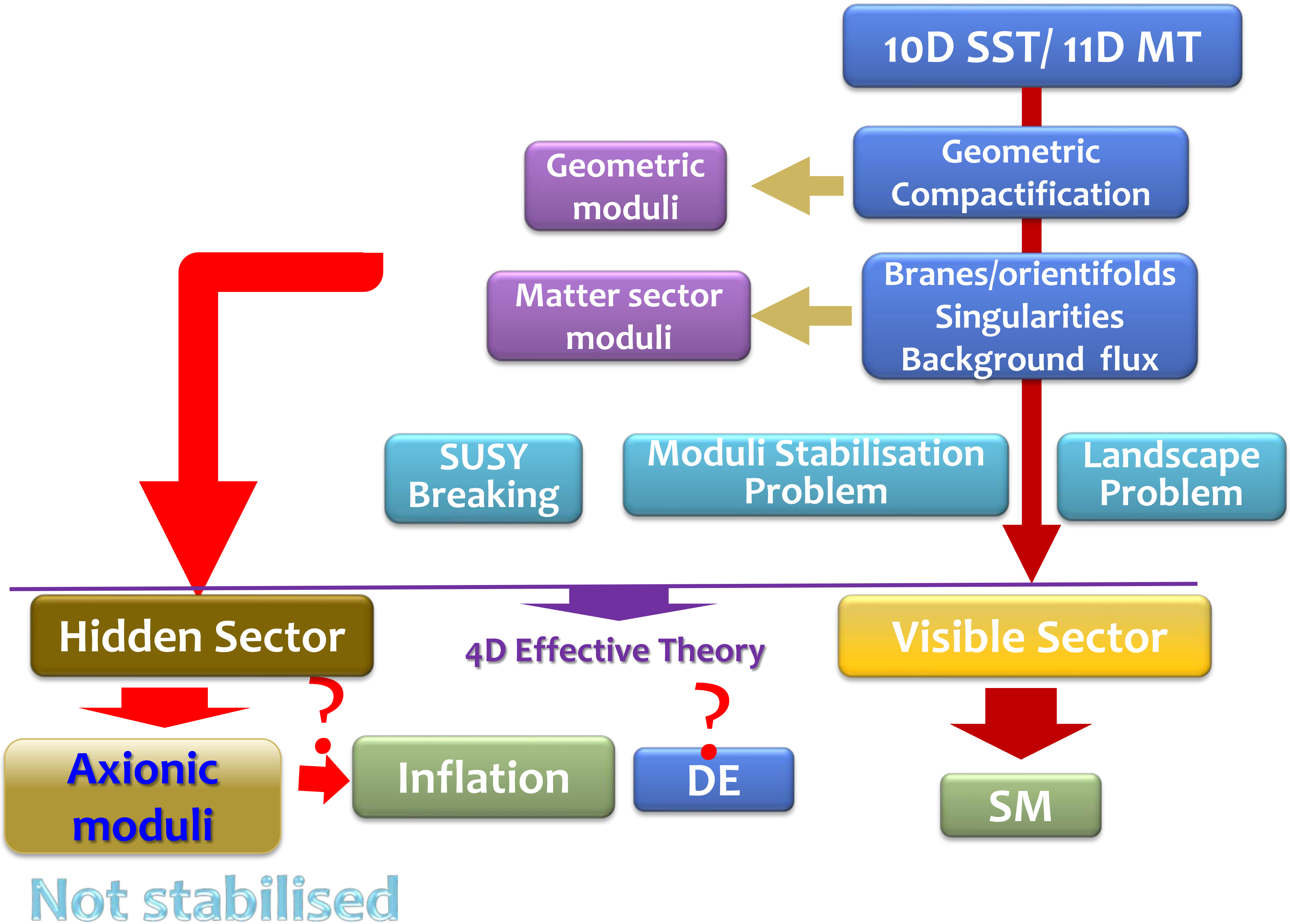

M-theory

- Bosonic Fields
  - Metric : g_{MN}
  - 3-form potential: C_{MNL} => $G=dC$

P & CP odd

- Action of the bosonic part

Chern-Simons term

$$2\kappa^2 S = \int_{M_{11}} \left[*1R - \frac{1}{2} *G \wedge G - \frac{1}{6} C \wedge G \wedge G \right]$$

This action is invariant under the gauge transformation

$$\delta C_3 = d\Lambda_2 \Rightarrow \quad d\Lambda \wedge G \wedge G = d(\Lambda \wedge G \wedge G)$$

- Compactification

$$M_{11} = X_4 \times Y_7 \text{ (no warp)}$$

- Massless fields in 4D spacetime from the form potential C_4

Harmonic forms on Y_7 : $\omega_1^a(y),\ \omega_2^\alpha, (y),\ \omega_3^m(y)$

$$C_3 = c_3(x) + b_2^a(x) \wedge \omega_1^a(y) + A_1^\alpha(x) \wedge \omega_2^\alpha(y) + a^m(x)\omega_3^m(y)$$

- Effective 4D action

$$4\kappa^2 S_B = \int_{X_4} \Big[-\mathrm{vol}(Y_7) * dc_3 \wedge dc_3 - K_{1ab} * h_3^a \wedge h_3^b - K_{3mn} * da^m \wedge da^n$$
$$-K_{2\alpha\beta} * F^\alpha \wedge F^\beta - A_{m\alpha\beta} a^m F^\alpha \wedge F^\beta + B_{amn} a^m da^n \wedge h_3^a \Big]$$

where $h_3^a = db_2^a$, $F^\alpha = dA_1^\alpha$ and

$$K_{npq} = \int_{Y_7} \omega_n^p \cdot \omega_n^q \Omega(Y_7),$$

$$A_{m\alpha\beta} = \int_{Y_7} \omega_3^m \wedge \omega_2^\alpha \wedge \omega_2^\beta, \quad B_{amn} = \int_{Y_7} \omega_3^m \wedge \omega_3^n \wedge \omega_1^a.$$

- Transformation $b_2^a \rightarrow b_a$

$$S'_B = S_B(c_3, a, h_3, F) + \frac{1}{2\kappa^2}\int_{X_4} b_i dh_3^i$$

$$\delta_{h_3} S'_B = 0 \Rightarrow \quad -K_{1ij} * h_3^j = Db_i \equiv db_i - \frac{1}{2} B_{imn} a^m da^n$$

$$2\kappa^2 S_{\text{eff}} = \int_{X_4} \frac{1}{2}\Big[-\text{vol}(Y_7) * dc_3 \wedge dc_3 - K_{2\alpha\beta} * F^\alpha \wedge F^\beta$$
$$-K_{3mn} * da^m \wedge da^n - K_2^{ij} * Db_i \wedge Db_j - A_{m\alpha\beta} a^m F^\alpha \wedge F^\beta \Big]$$

- Axions

$$b_i \rightarrow b_i + c_i, \quad a^m \rightarrow a^m$$
$$a^m \rightarrow a^m + c^m, \quad b_i \rightarrow b_i + B_{imn} c^m a^n$$

- b_i: parity even X
- a^m: parity odd O (m=1,…, $b_1(Y_7)$)

Type I Sugra in 10D

- Fundamental fields
  - Gravity multiplet
    - Bose fields: g_{MN}, ϕ, B_2
    - Majorana 3/2-field $\psi_M \in \mathbf{16} \otimes \mathbf{10}$; $\Gamma_{11}\psi_M = \pm\psi_M$
    - 1/2-field $\lambda \in \mathbf{16}$; $\Gamma_{11}\lambda = \mp\lambda$
  - Gauge multiplet
    - Gauge field $A_1 \in \mathrm{ad}(G)$ (Gauge group G can be arbitrary)
    - Majorana 1/2-field $\chi \in \mathrm{ad}(G) \otimes \mathbf{16}$

- Action for the bosonic part

$$S_{10} = \frac{1}{2\kappa^2}\int_{M_{10}} e^{-2\phi}\left[R * 1 + 4 * d\phi \wedge d\phi - \frac{1}{2} * H_3 \wedge H_3 - \frac{\alpha'}{4}\mathrm{tr}_v(*F \wedge F)\right]$$

$$H_3 = dB_2 - \frac{\alpha'}{4}\left(\omega^G_{\mathrm{CS}} - \omega^L_{\mathrm{CS}}\right)$$

$$\omega_{\mathrm{CS}}(A) = \mathrm{tr}\left(A \wedge dA + \tfrac{2}{3} A \wedge A \wedge A\right).$$

$$dH_3 = \frac{\alpha'}{4}\left[\mathrm{Tr}(\mathscr{R} \wedge \mathscr{R}) - \mathrm{Tr}(F \wedge F)\right]$$

アノーマリー相殺条件

- Calabi-Yau compactification

$$ds^2(M_{10}) = ds^2(X_4) + ds^2(Y_6).$$

$$B = \ell_s^2 \sum_{i=1}^{b_2(Y)} \alpha_i(x)\eta_2^i(y) + \beta_2(x), \quad e^{\phi} = g_s$$

Harmonic 2-form basis

- Effective action

$$2\kappa_{10}^2 S_B = -\frac{V_Y}{2g_s^2}\int_{X_4} \Big[\sum Y^{ij} * d\alpha_i \wedge d\alpha_j + *h \wedge h + \frac{\theta}{\pi}\left\{dh - \ell_s^2 (4\pi)^{-2}\left(\mathrm{Tr}(F\wedge F) - \mathrm{tr}(\mathscr{R}\wedge\mathscr{R})\right)\right\}\Big],$$

where

$$Y^{ij} = \ell_s^4 V_Y^{-1} \int_{Y_6} *\eta^i \wedge \eta^j$$

- Duality transformation: $d\theta = 2\pi * h$

$$S_a = \int_{X_4} \Big[-\frac{1}{2}\sum Y^{ij} * da_i \wedge da_j - \frac{1}{2} * da \wedge da + \frac{\lambda}{f_a} a \left\{\mathrm{Tr}(F\wedge F) - \mathrm{tr}(\mathscr{R}\wedge\mathscr{R})\right\}\Big],$$

Model-independent axion

$$a = f_a\theta: \quad f_a = \frac{\sqrt{V_Y}}{2\sqrt{2}\pi\kappa_{10} g_s} = \frac{L^3}{\sqrt{2}\pi g_s \ell_s^4} = \frac{m_{\rm pl}}{2\sqrt{2}\pi}, \quad \lambda = \frac{\ell_s^2 f_a^2}{2\pi^2} = \frac{m_{\rm pl}^2\ell_s^2}{16\pi^3}.$$

- ## Model-dependent axions

10D Type-I theory requires the Green-Schwarz counter term

$$S = \int_{M_{11}} B \wedge X_8(F, \mathscr{R});$$

$$X_8 = \mathrm{tr}(R_2^4) + \frac{[\mathrm{tr}(R_2^2)]^2}{4} - \frac{\mathrm{Tr}_a(F_2^2)\mathrm{tr}(R_2^2)}{30} + \frac{\mathrm{Tr}_a(F_2^4)}{3} - \frac{[\mathrm{Tr}_a(F_2^2)]^2}{900}$$

in order to cancel the quantum gauge anomaly in the gauge and gravity sector:

$$\delta H_3 = 0 \quad \Rightarrow \quad \begin{aligned} &\delta A_1 = d\lambda - i[A_1, \lambda], \quad \delta\omega_1 = d\Theta + [\omega_1, \Theta], \\ &\delta B_2 = \frac{\alpha'}{4}\left[\mathrm{tr}(\lambda dA_1) - \mathrm{tr}(\Theta d\omega_1)\right] \end{aligned}$$

This counter term produces the CS coupling of the model-dependent aions:

- Correspondence to D=4 N=1 Sugra

HET		Gravity	$h^{1,1}$ chiral	$h^{2,1}$ chiral	Chiral
G_{MN}	$\rightarrow$	$g_{\mu\nu}$	$h^{1,1}$ Kähler	$2h^{2,1}$ complex str.	
B_{MN}	$\rightarrow$		$a_i \eta_2^i(y)$		$a(B_{\mu\nu})$
ϕ	$\rightarrow$				ϕ

$$B = \frac{\ell_s^2}{f_a} \sum_{i=1}^{b_2(Y)} a_i(x) \eta_2^i(y) + \beta_2(x)$$

$$da = 2\pi f_a * d\beta_2$$

Type IIB Sugra in 10D

- Fundamental fields

Bose fields

– NS-NS fields: $g_{MN}, \quad \phi, \quad B_2$

– RR fields: C_0, C_2, C_4

Spinor fields

– Two Majorana 1/2-fields: $\lambda = \lambda^{(1)} + i\lambda^{(2)}, \ \Gamma_{11}\lambda = \pm\lambda$

– Two Majorana 3/2-fields: $\psi_M = \psi_M^{(1)} + i\psi_M^{(2)}, \ \Gamma_{11}\psi_M = \mp\psi_M$

- Action (Bosonic part: impose $*F_5=F_5$ after variation) in the Einstein frame:

$$2\kappa^2 S_{\rm IIB} = \int *1\left[R - \frac{\nabla\tau\cdot\nabla\bar\tau}{2({\rm Im}\,\tau)^2}\right] - \frac{1}{2{\rm Im}\,\tau} *G_3\wedge\bar G_3 - \frac{1}{4}*\tilde F_5\wedge\tilde F_5$$
$$\pm\frac{i}{4{\rm Im}\,\tau}C_4\wedge G_3\wedge\bar G_3.$$

where

$$\tau = C_0 + ie^{-\phi},$$
$$G_3 := \tau H_3 - F_3;\quad F_3 = dC_2,\quad H_3 = dB_2,$$
$$\tilde F_5 = dC_4 - \frac{1}{2}C_2\wedge H_3 + \frac{1}{2}B_2\wedge F_3$$

Correspondence to D=4 N=2 Sugra

IIB		Gravity	$h^{2,1}$ Vector	$h^{1,1}$ Hyper	Hyper
G_{MN}	$\rightarrow$	$g_{\mu\nu}$	$2h^{2,1}$ complex str.	$h^{1,1}$ Kähler	
B_{MN}	$\rightarrow$			$a_i\eta_2^i(y)$	$a\,(B_{\mu\nu})$
ϕ	$\rightarrow$				ϕ
C_0	$\rightarrow$				$c(C_0)$
C_2	$\rightarrow$			$\gamma_i\eta_2^i(y)$	$\chi(C_{\mu\nu})$
C_4	$\rightarrow$	$V_1 \wedge \Omega_3$	$V_{1K} \wedge \alpha^K$	$c_i * \eta_2^i(y)$	

$$B_2 = \frac{\ell_s^2}{f_a} a_i(x)\eta_2^i(y) + \beta_2(x), \quad da = 2\pi f_a * d\beta_2$$

$$\tau = C_0 + ie^{-\phi}$$

$$C_2 = \gamma_i(x)\eta_2^i(y) + C_2(x); \quad d\chi = *dC_2$$

$$\begin{aligned} C_4 \;=\;& V(x) \wedge \mathrm{Re}\,\Omega(y) - \tilde{V}(x) \wedge \mathrm{Im}\,\Omega(y) + V_K(x) \wedge \alpha^K(y) + \tilde{V}^K(x) \wedge \beta_K(y) \\ & + c_i(x) * \eta_2^i(y) + \tilde{c}^i(x) \wedge \eta_2^i \end{aligned}$$

D-Brane fields

Bose fields :

– $U(N_a)$-gauge fields F_a

Spinor fields

– BG magnetic fields/intersections

$\Rightarrow U(N_a) \times \overline{U(N_b)}$-bifundamental chiral fermions χ_{ab}

Chern-Simons coupling of axions

$$S_{\rm CS} = \mu_p \left[\int_{B_{p+1}} C_{p+1} + (2\pi\alpha') \int_{B_{p+1}} C_{p-1} \wedge {\rm tr} F \right. \\ \left. + \frac{(2\pi\alpha')^2}{2} \int_{B_{p+1}} C_{p-3} \wedge {\rm tr} F^2 - \frac{1}{24(8\pi^2)} \int_{B_{p+1}} C_{p-3} \wedge {\rm tr} R^2 + \cdots \right]$$

– NS-axions a, a_i : no CS coupling

– RR-axions c, c_i : CS couplings to F & R $\Leftarrow$ D3, D7

- アクシオンの種類(数)
  - モデル依存型アクシオンは，内部空間が位相的に複雑になるほど多種になる．特に，IIB型理論のフラックスコンパクト化では，ワープのためにadS真空のupliftに膨大な数の2サイクルが必要となり，対応して非常に多種のアクシオンが生成されることになる[Douglas M, Kachru S 2007].
  - ヘテロ型理論でも，Betti数 $b_2(Y)$ に対する明確な制限は得られていないが，トーリック型CYの組織的な探査研究では，一般的なCYでは $b_2(Y)$が非常に大きくなることが知られている[Kreuzer M 2010].

Type IIA Sugra in 10D

- Fundamental fields

Bose fields

- NS-NS fields: $g_{MN}, \quad \phi, \quad B_2$
- RR fields: $C_1, \quad C_3$

Spinor fields

- Two Majorana 1/2-fields: $\lambda \in \mathbf{16}, \quad \lambda' \in \mathbf{16}'$
- Two Majorana 3/2-fields: $\psi_M \in \mathbf{16} \otimes \mathbf{10}, \ \psi'_M \in \mathbf{16}' \times \mathbf{10}$

- Action (string frame)

$$
\begin{aligned}
S_{\text{IIA,bosonic}} &= S_{\text{NS}} + S_{\text{R}} + S_{\text{CS}}; \\
S_{\text{NS}} &= \frac{1}{2\kappa_{10}^2} \int d^{10}x(-g)^{1/2} e^{-2\phi} \left(R + 4(\nabla\phi)^2 - \frac{1}{2} H_3 \cdot H_3 \right), \\
S_{\text{R}} &= -\frac{1}{4\kappa_{10}^2} \int d^{10}x(-g)^{1/2} \left(\tilde{F}_2 \cdot \tilde{F}_2 + \tilde{F}_4 \cdot \tilde{F}_4 \right), \\
S_{\text{CS}} &= -\frac{1}{4\kappa_{10}^2} \int B_2 \wedge F_4 \wedge F_4 .
\end{aligned}
$$

where

$$
H_3 = dB_2, \quad F_2 = dC_1 + m_0 B_2, \quad F_4 = dC_3,
$$
$$
\tilde{F}_4 = F_4 - C_1 \wedge H_3 . - \frac{m_0}{2} B_2 \wedge B_2
$$

- Correspondence to D=4 N=2 Sugra

IIA		Gravity	$h^{1,1}$ Vector	$h^{2,1}$ Hyper	Hyper
G_{MN}	$\rightarrow$	$g_{\mu\nu}$	$h^{1,1}$ Kähler	$2h^{2,1}$ complex str.	
B_{MN}	$\rightarrow$		$a_i \eta_2^i(y)$		$a\ (B_{\mu\nu})$
ϕ	$\rightarrow$				ϕ
C_1	$\rightarrow$	C_μ			
C_3	$\rightarrow$		$C_{i\mu}\eta_2^i(y)$	$c_j \eta_{2,1}^j(y)$	$c\Omega_3(y)$

$$B = \frac{\ell_s^2}{f_a} \sum_{i=1}^{b_2(Y)} a_i(x)\eta_2^i(y) + \beta_2(x), \quad da = 2\pi f_a * d\beta_2$$

$$C_3 = c(x)\Omega_3(y) + c_j(x)\eta_{2.1}^j(y) + C_{1i} \wedge \eta_2^i(y) + \text{cc}$$

Stringy Axion Mass

- If the shift symmetry is not violated at the tree level by flux, branes and compactification (i.e., by moduli stabilisation), it can be preserved by perturbative quantum corrections (for supersymmetric states).
- However, axions acquire small mass by non-perturbative effects such as
  - **CS-coupled gauge field instanton/gaugino condensates**
  - **WS instantons**
  - **Euclidean D-brains (D-instanton)**
- If a light QCD axion really exists, it is natural that there survive lots of other light axions coming from the large number of non-trivial cycles in extra-dimensions, which can be order of several hundreds or more.

WS Instanton ⇒ NSNS axion mass

- 弦に対するEuclid作用積分のボソン部分

$$S_E = \frac{1}{4\pi\alpha'} \int_\Sigma d^2\sigma \sqrt{h} \left\{ (h^{ab} g + \epsilon^{ab} B)(\partial_a X, \partial_b X) + \alpha' R_s \phi \right\}$$

- 背景場のモジュライ自由度
  - Kaehler moduli: $g_{i\bar{j}} = \sum_\alpha r_\alpha b^\alpha_{i\bar{j}}$
  - Axion moduli: $B_{[2]} = \sum_\alpha \theta_\alpha b^\alpha$

ここで, b^α $(\alpha = 1, \cdots, b_2)$は $H^{(1,1)}(Y_6)$ の基底で, $H_2(Y_6)$の基底 Σ_αの双対基底である:

$$\int_{\Sigma_\beta} b^{(\alpha)} = \delta^\alpha_\beta .$$

● モジュライに対する有効作用積分

Dilaton ϕ が定数のとき，flat gauge $h_{ab}\,d\sigma^a d\sigma^b = dz\,d\bar{z}$ のもとで，

$$S_E = \frac{1}{\pi\alpha'}\int dz d\bar{z}\sum_\alpha b^{(\alpha)}_{i\bar{j}}\left\{r_\alpha\left(\partial X^i\bar{\partial}X^{\bar{j}}+\bar{\partial}X^i\partial X^{\bar{j}}\right)-i\theta_\alpha\left(\partial X^i\bar{\partial}X^{\bar{j}}-\bar{\partial}X^i\partial X^{\bar{j}}\right)\right\}$$
$$+\chi_\Sigma\phi$$

ここで，

$$\hat{b}^{(\alpha)} = X^* b^{(\alpha)} = b^{(\alpha)}_{i\bar{j}}\left(\partial X^i\bar{\partial}X^{\bar{j}}-\bar{\partial}X^i\partial X^{\bar{j}}\right)dz\wedge d\bar{z}$$

はWS Σ 上の閉形式となるので，θ_αが z に依存しないときには，S_E の第2項は位相不変量となる：

$$S_E \Rightarrow \sum_\alpha\left(r_\alpha I^{(\alpha)}-i\theta_\alpha Q^{(\alpha)}\right)+\chi_\Sigma\phi;$$

$$I^{(\alpha)} = \frac{1}{\pi\alpha'}\int dz d\bar{z} b^{(\alpha)}_{i\bar{j}}\left(\partial X^i\bar{\partial}X^{\bar{j}}+\bar{\partial}X^i\partial X^{\bar{j}}\right),$$

$$Q^{(\alpha)} = \frac{1}{\pi\alpha'}\int_\Sigma \hat{b}^{(\alpha)}.$$

シフト対称性の非摂動論的破れ

- WS Σのイメージが Y_6 でゼロホモローグなとき、S_E はθ_αに関してシフト対称性 $\theta_\alpha \rightarrow \theta_\alpha + const$ をもつ。
- WS Σ が非自明な2サイクルを覆うとき、位相不変量 $Q^\alpha \neq 0$なら，この シフト対称性は非摂動論的に破れる.

状況は，4次元理論でのアノーマリーによるアクシオンCS項 $a\, F \wedge F$ と完全に対応しており，同様の議論により，この $\theta_\alpha Q^\alpha$項が非摂動論的ポテンシャルを生み出す.

Holomorphic/anti-holomorphic instantons

b^α が正定値(例えば、$b^\alpha = J_{1,1}$)とすると、$I^\alpha \geq |Q_\alpha|$ なので、

$$Q_{(\alpha)} = \pm I^{(\alpha)} \quad \Leftrightarrow \quad \partial X^i = 0 \text{ or } \bar{\partial} X^i = 0$$

の時 S_E は最小。

● インスタントンの生み出すアクシオンポテンシャル

$$e^{-S_E} = g^{-\chi_\Sigma} e^{-\sum_\alpha (r_\alpha \mp i\theta_\alpha) I^{(\alpha)}} = e^{-I + i\sum_\alpha \theta_\alpha Q^{(\alpha)}}$$

となるので，4次元理論が $N = 1$ sugraとなるときには，

$$\delta W = \sum_\alpha A_\alpha e^{-R_\alpha / f_\alpha}$$

となる．対応するポテンシャルは

$$V_a = \sum_\alpha \Lambda_\alpha^4 \cos(a_\alpha / f_\alpha); \quad \Lambda_\alpha^4 = M_\alpha^4 e^{-I^{(\alpha)}}.$$

ここで，$a_\alpha / f_a = \theta_\alpha / (\pi\alpha')$で，$f_a$は a_αが標準的な運動項を持つという条件で決まる.

D- Instanton ⇒ RR axion mass

- RR axions

  IIA: $C_3 = c_i\,(x)\omega_3^i(y)$, IIB: $C_4 = (1+*)c_i(x)\omega_4^i(y)$

- D-instanton action

$$S_{Dp}^E = \frac{\mu_p}{g_s}\int_{\Sigma_{p+1}} \sqrt{\det G} - i\mu_p \int_{\Sigma_{p+1}} C_p$$

- Chiral fields: $T_i = (\tau_i, c_i)$, $t_i = \mathrm{vol}(\sigma_i)$, $\int_{\sigma_i} \omega^j = \delta_i^j$

$$S_{EDp} = \frac{\mu_p}{g_s} n^j \tau_j - i\mu_p c_j n^j = \frac{T_j}{f_j} n^j, \quad n^j \in \mathbb{Z}$$

- NP superpotential

$$\delta W = \sum_i A_i e^{-T_i/f_i}$$

Rough Estimates

- Lagrangian of an axion

$$\mathscr{L} = -\frac{1}{2} f_a^2 (\partial\theta)^2 - \Lambda^4 U(\theta); \quad \Lambda^4 \approx M^4 e^{-S}$$

where S is the instanton action.

- From the relations

$$C_{p+1} = \frac{a}{f_a \mu_p} \omega_{p+1} \;\Rightarrow\; S \sim \frac{\mu_p}{g_s} \ell^{p+1}, \quad f_a \sim \frac{L^3/\ell^{p+1}}{\ell_s^4 \mu_p}$$

we have

$$S f_a \sim \frac{L^3}{\ell_s^4 g_s} \sim m_{\rm pl} \Rightarrow \quad f_a \sim \frac{m_{\rm pl}}{S}$$

Hence,

$$m_a \approx \Lambda^2 / f_a \sim (M^2 / m_{\rm pl}) S e^{-S/2}$$

- The total potential for the axion is in general the sum of the QCD contribution and the stringy contribution:

$$V = V_{\rm QCD} + V_{\rm s} :$$

$$V_{\rm QCD} = \frac{a^2}{8f_a^2} r^2 F_\pi^2 m_\pi^2 \frac{m_u m_d}{(m_u + m_d)^2};$$

$$V_{\rm s} = \Lambda^4 \cos\left(\frac{a}{f_a} + \psi\right).$$

- If we require that this stringy effect is less than the QCD instanton effect for the QCD axion, we have

$$\frac{a}{f_a} \approx \frac{M^4 e^{-S}}{m_\pi^2 F_\pi^2} < 10^{-10} \quad \Rightarrow \quad S \gtrsim 200 \Rightarrow \quad \begin{array}{l} f_a \lesssim 10^{16}\mathrm{GeV} \\ m_a \lesssim 10^{-15}\mathrm{eV} \end{array}$$

Thus, it is expected that there are lots of superlight axions whose mass spectrum is homogeneous in log m, producing the axiverse.

Anthropic QCD axion cosmology

The PQ symmetry breaking scale f_a can be as large as the GUT scale or string scale if the initial amplitude of the axion field is much smaller than the mean value:

$$\Omega_a \approx 0.01 \left(\frac{f_a}{10^{16}\mathrm{GeV}} \right)^{1.175} \times \left(\frac{\theta_i}{3 \times 10^{-4}} \right)^2$$

- This requires the low scale inflation from the isocurvature constraint if the QCD axion makes non-negligible contribution to DM.
- This problem can be evaded if the axion abundance is diluted by the entropy production due to moduli decay.

So-Young Pi: Phys. Rev. Lett. 52 (1984) 1725;
A. D. Linde: Phys. Lett. B 201 (1988) 437;
M. Tegmark, A. Aguirre, M. Rees, F. Wilczek: Phys. Rev. D 73 (2006) 023505.
M.F. Herzberg, M. Tegmark, F. Wilczek: Phys. Rev. D78 (2008) 083507.
….

4. 3 Direct Search

Experimental Searches

Laser Experiment

- LSW: ALPS@DESY(2010), PVLAS@Italy(2006/2007)
- Birefringence: PVLAS@Italy(2006/2007), OSQAR@CERN

Helioscope

- Large magnet: SUMICO@UTokyo, CAST@CERN ⇒ IAXO
- Bragg scattering: SOLAX, COSME

Haloscope

- Microwave cavity: ADMX-I&II@Washington, X3@Yale, CULTASK@Korea
- Toroidal magnet: ABRACADABRA@MIT
- NMR-type: CASPEr@Mainz (2014/2017)
- Solid state: MADMAX@Munich, ORPHEUS@Seattle, QUAX@Italy

Various Experimental Bounds

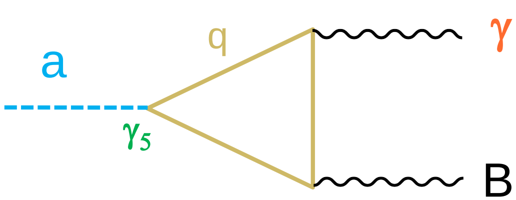

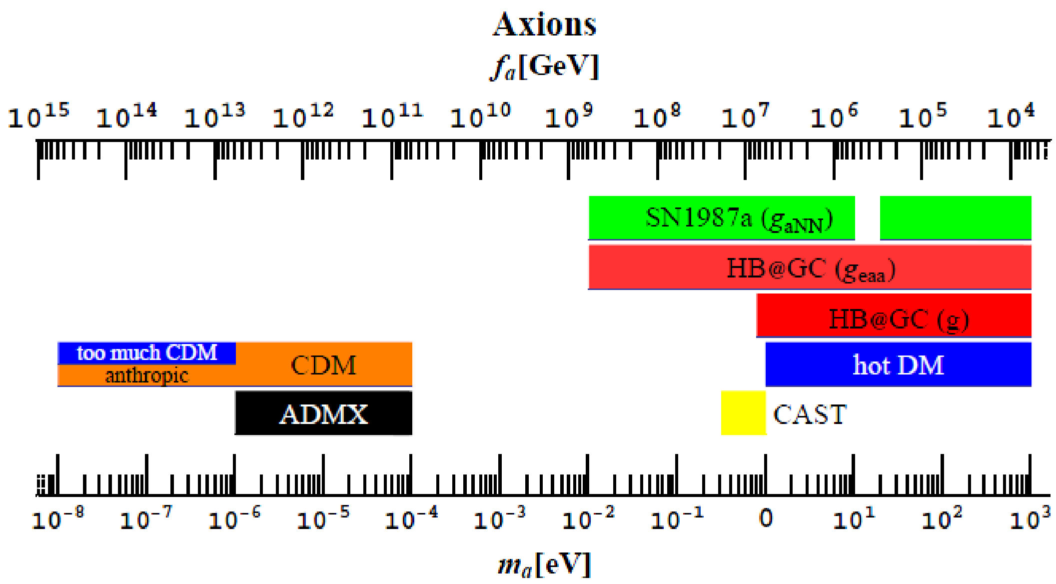

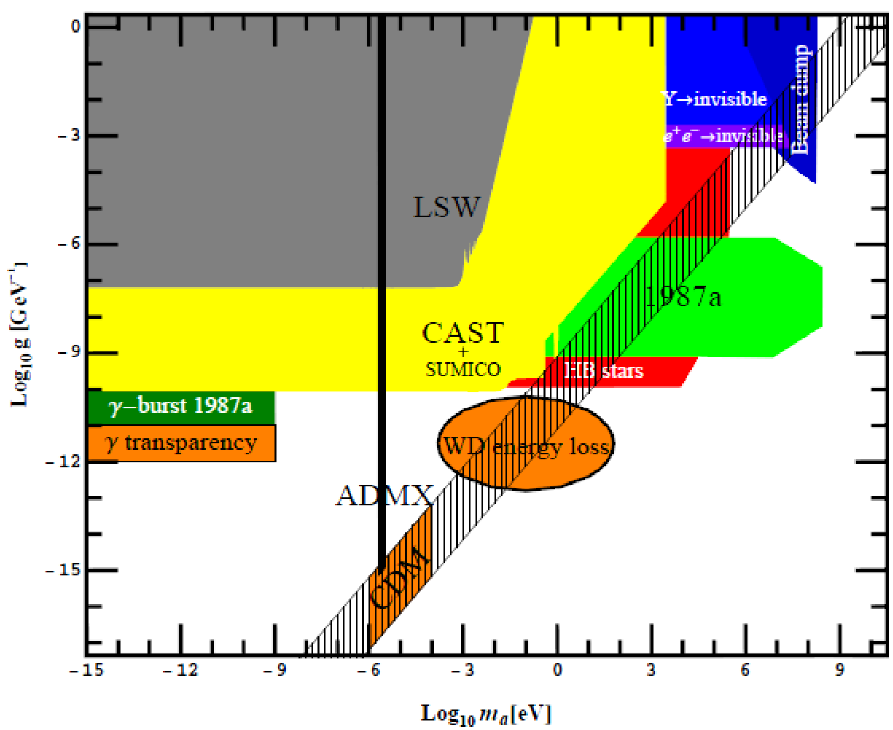

J. Jaeckel, A. Ringwald:
Ann.Rev.Nucl.Part.Sci. 60 (2010) 405
[arXiv:1002.0329]
The Low-Energy Frontier of Particle Physics

ALPS@DESY

Axion-Like Particle Search

arXiv: 1004.1313 [hep-ex]

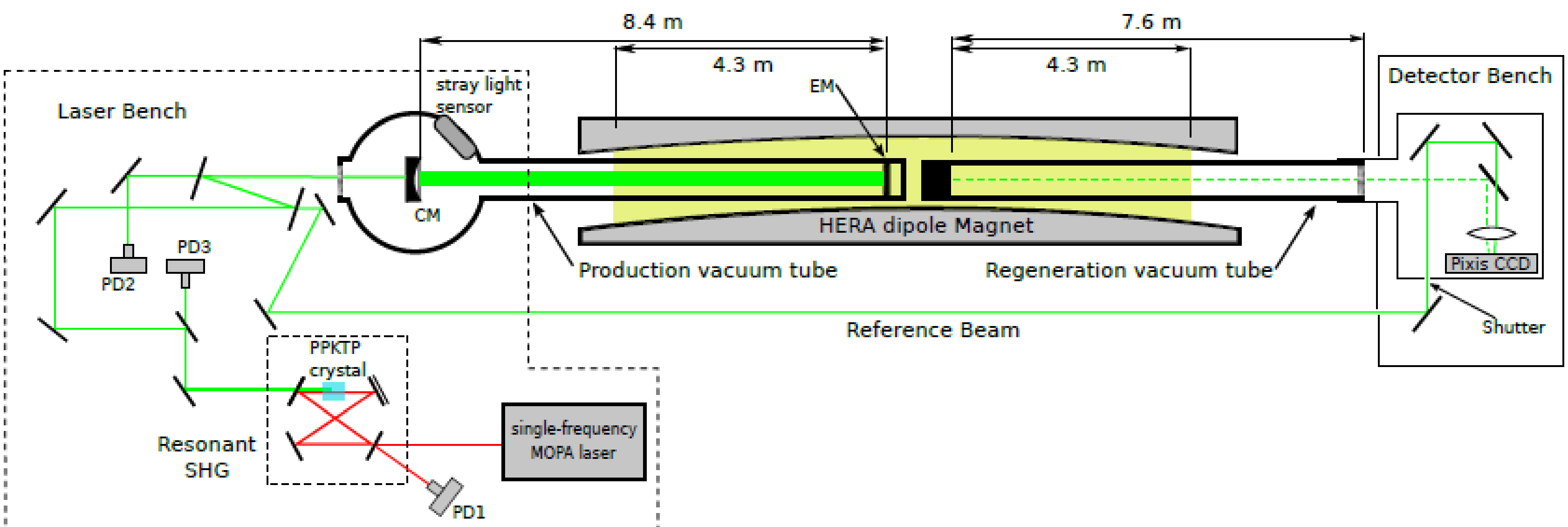

太陽アクシオン

Axion Helioscope
(Sikivie 1983)

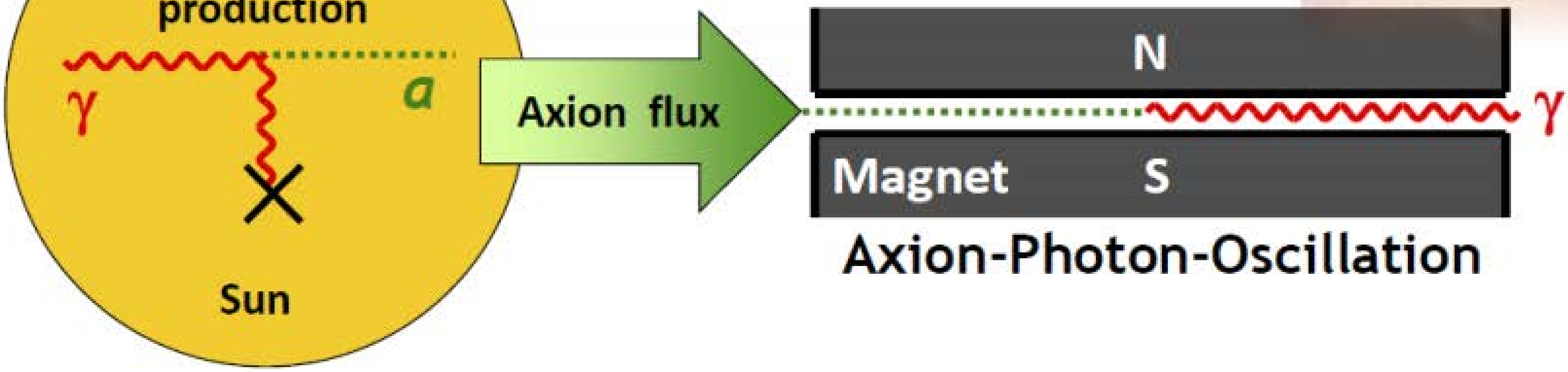

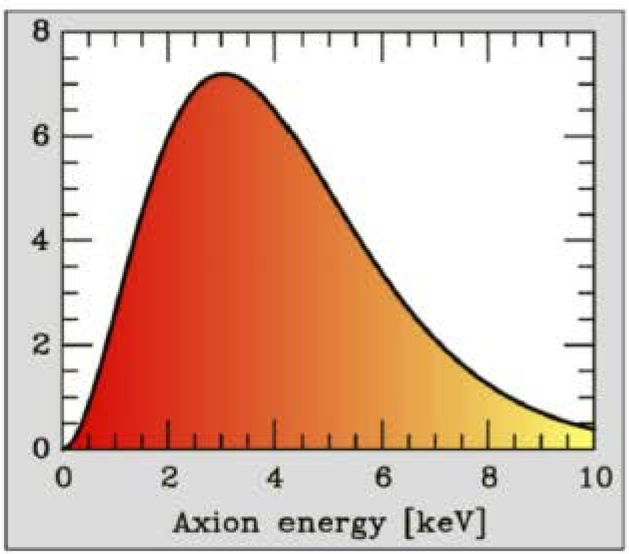

- Tokyo Axion Helioscope ("Sumico")
  (Results since 1998, up again 2008)
- CERN Axion Solar Telescope (CAST)
  (Data since 2003)

Alternative technique:
Bragg conversion in crystal
Experimental limits on solar axion flux from dark-matter experiments (SOLAX, COSME, DAMA, CDMS ...)

Axion Helioscope
Sumico & CAST

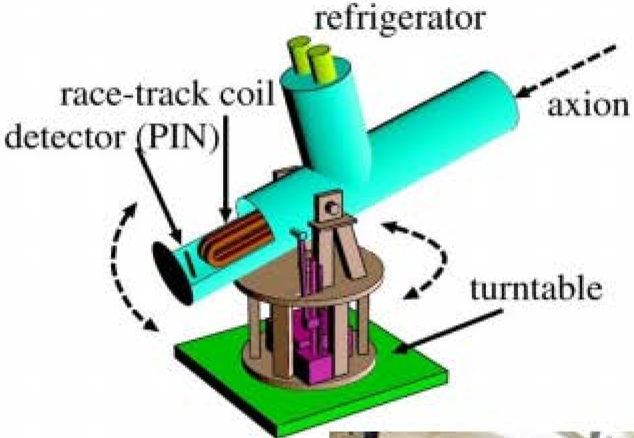

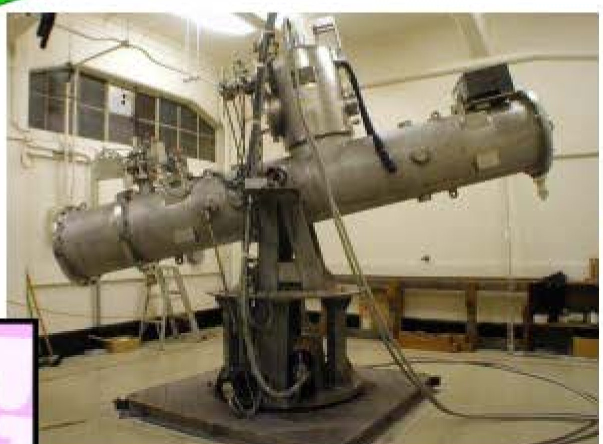

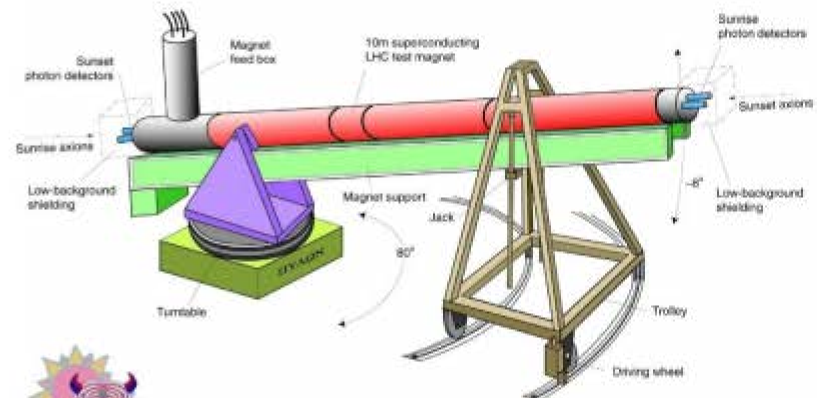

Cern Axion Solar Telescope

From: 小川泉@IRCC20130912

International Axion Observatory

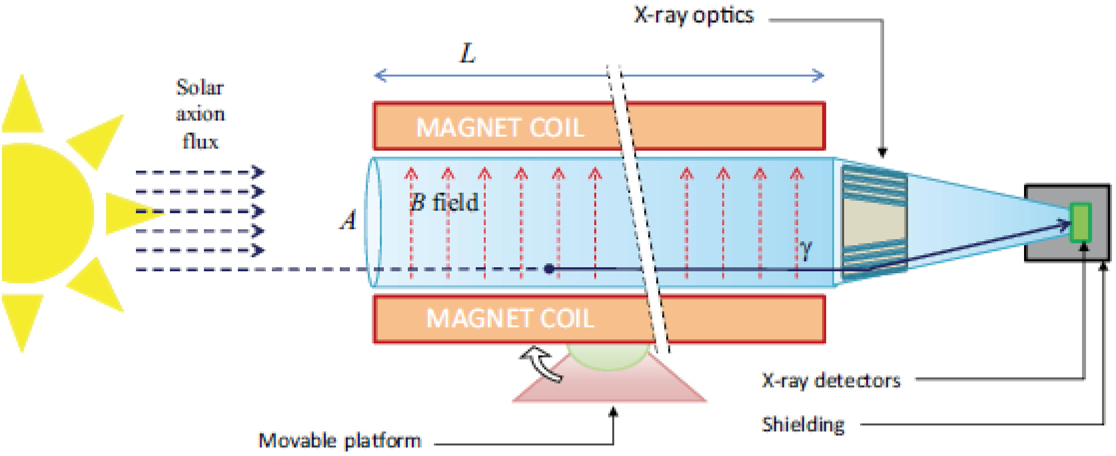

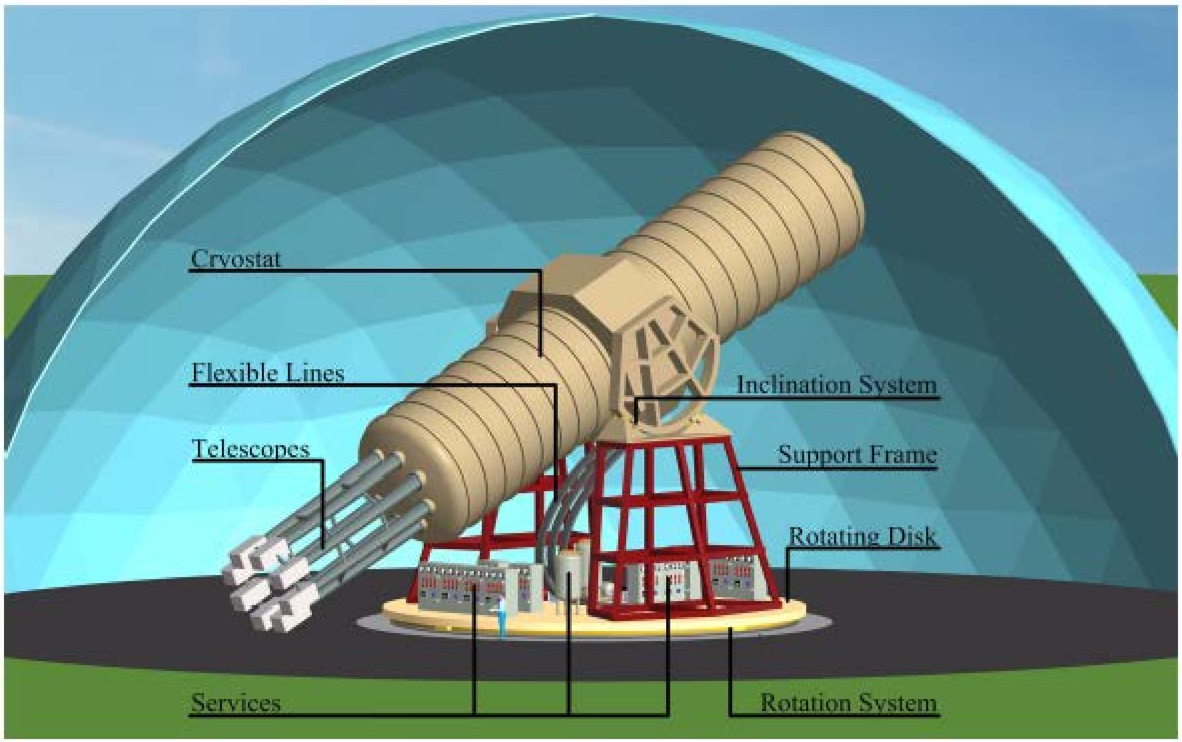

IAXO Conceptual Design Report: arXiv:1401.3233

Axions in Astrophysics

- **Key point**

  Axions are converted to and from photos by mixing:

  $$L = g_{a\gamma}\, a\, \boldsymbol{E}\cdot\boldsymbol{B}$$

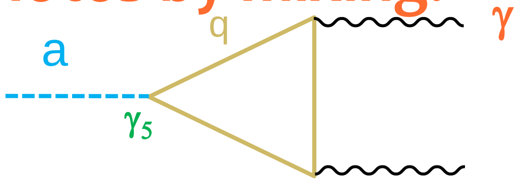

- **Solar axions due to the Primakov effect:**
  - **CAST experiment at CERN(2007, 2008)**

$$\begin{aligned} g_{\alpha\gamma} \quad < \quad & 9\times 10^{-11}\mathrm{GeV}^{-1}\ (m_a < 0.02\mathrm{eV}), \\ & 2\times 10^{-10}\mathrm{GeV}^{-1}(m_a < 0.7\mathrm{eV}) \end{aligned}$$

Cast Collaboration (2011) PRL 107 (2011) 261302 [arXiv:1106.3919]

CAST Bounds

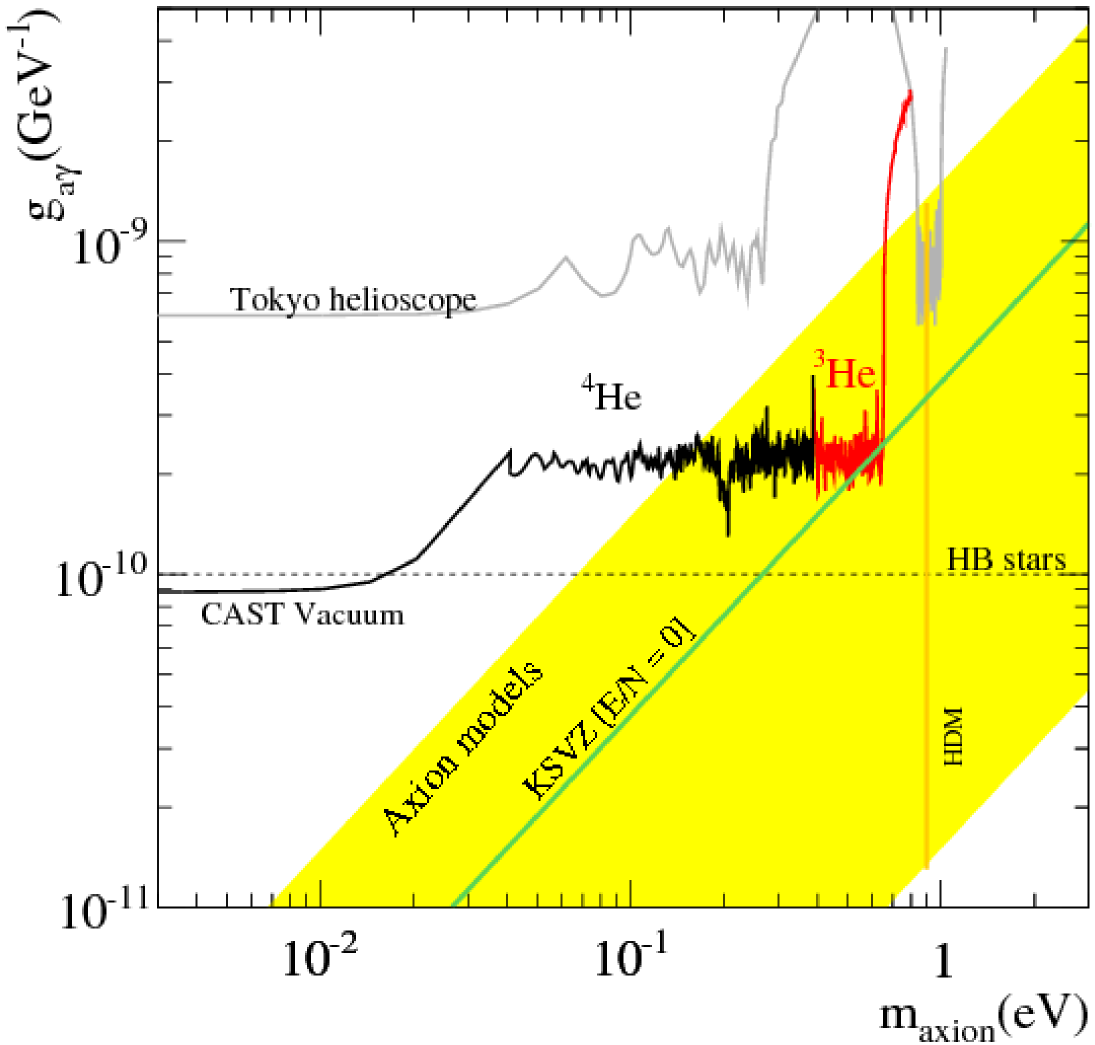

CAST Collaboration
(2011) arXiv:1106.3919

ADMX

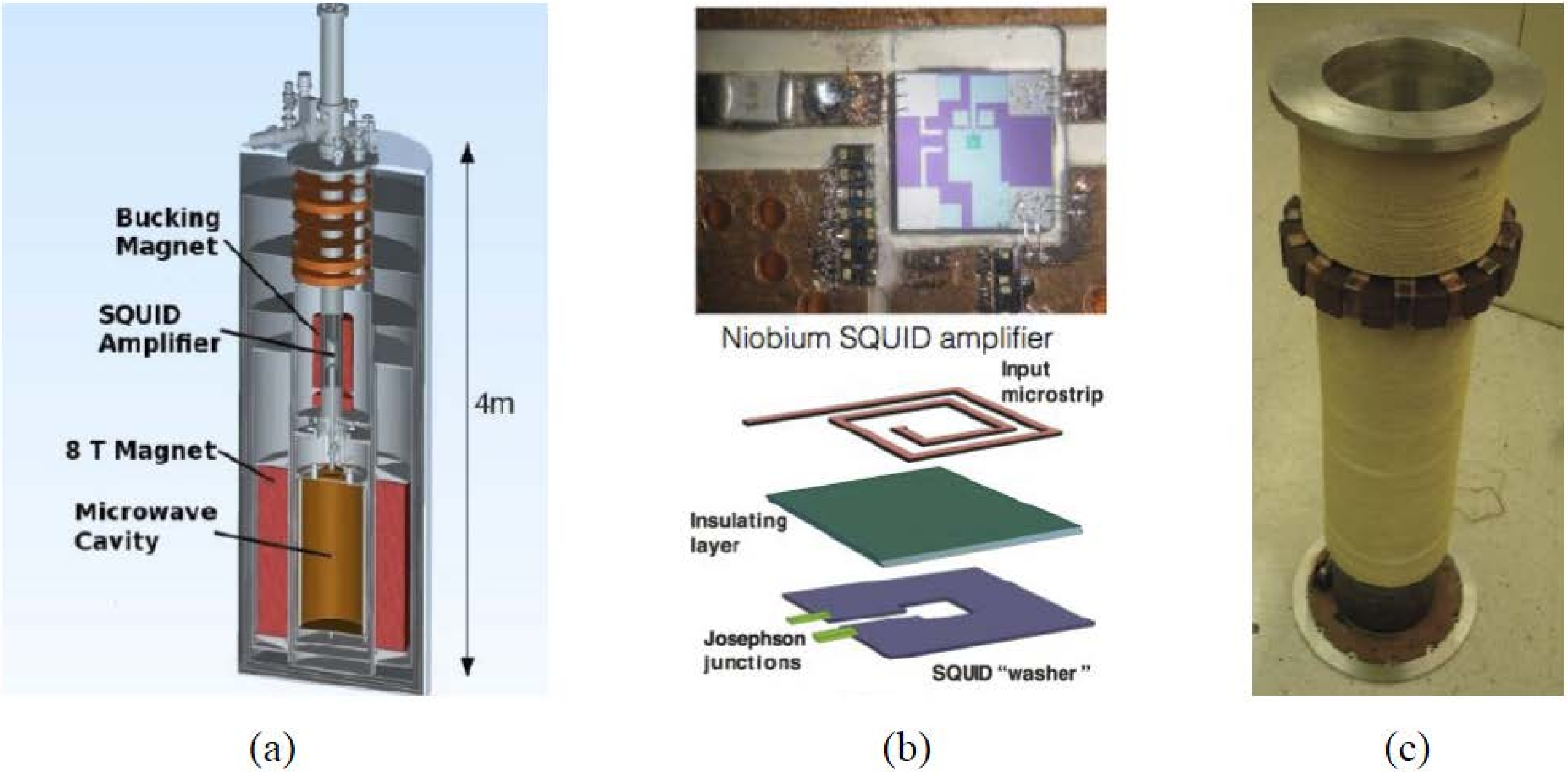

FIGURE 4. a) Graphic illustration of ADMX experiment. b) Top: photograph of a SQUID amplifier. Bottom: graphic illustration of a SQUID amplifier. c) Superconducting solenoid "bucking" magnet.

I. Stern, arXiv:1612.08296 [physics.ins-det].

ADMX: Projected Sensitivity

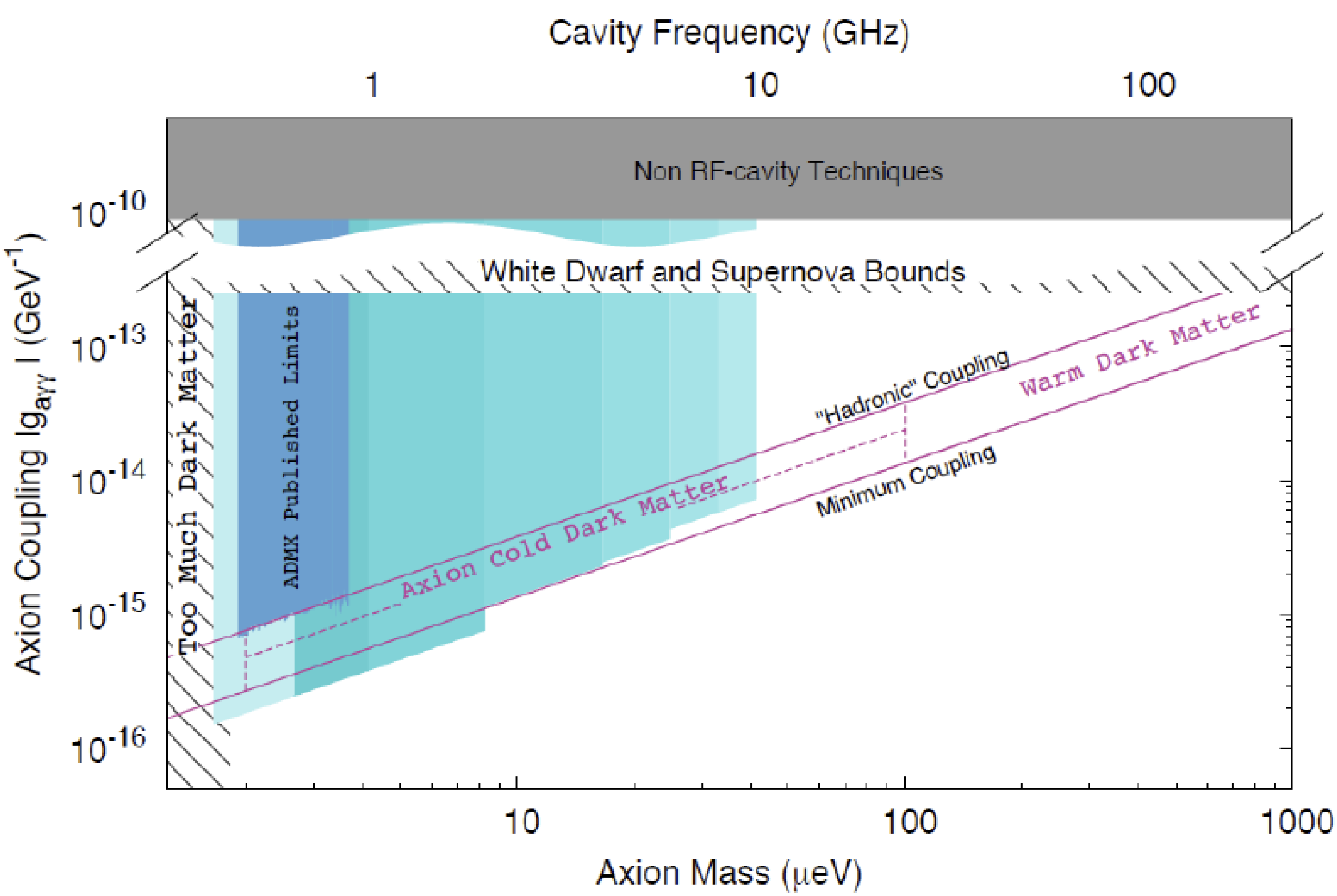

FIGURE 9. Projected sensitivity of ADMX Gen 2. Searches are scheduled to be complete by 2022.

I. Stern, arXiv:1612.08296 [physics.ins-det].

CASPEr: Sensitivity

$$H_{aNN} = g_{aNN}\sqrt{2\rho_{DM}}\cos(m_a t)\ \boldsymbol{v}\cdot\boldsymbol{\sigma}_N\ ;\quad g_{aNN} = q_{5N}/f_a$$

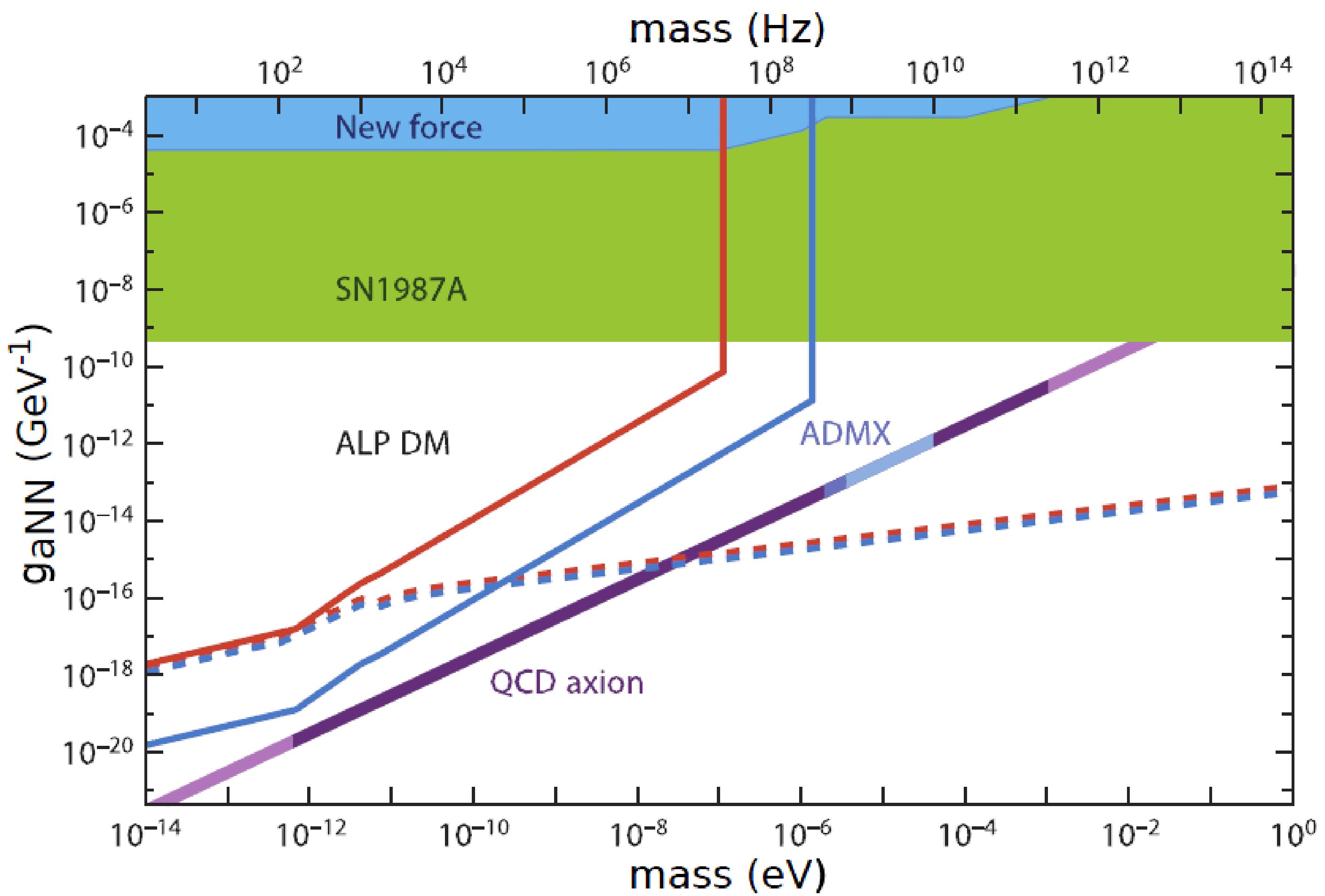

Garcon A && (CASPEr): arXiv:1707.05312

ABRACADABRA

$$\boldsymbol{J}_{\text{eff}} = g_{a\gamma\gamma}\sqrt{2\rho_{\text{DM}}}\cos(m_a t)\,\boldsymbol{B}_0$$

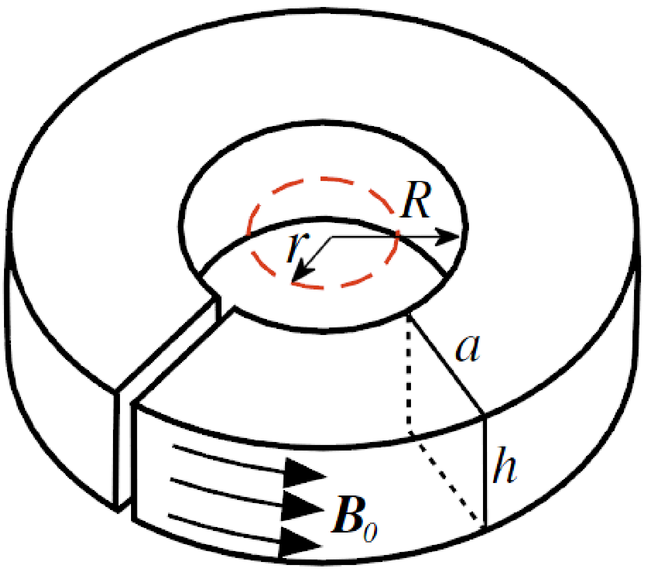

FIG. 1. A (gapped) toroidal geometry to generate a static magnetic field $\mathbf{B}_0$. The dashed red circle shows the location of the superconducting pickup loop of radius $r \leq R$. The gap ensures a return path for the Meissner screening current; see discussion in main text.

ABRACADABRA: sensitivity

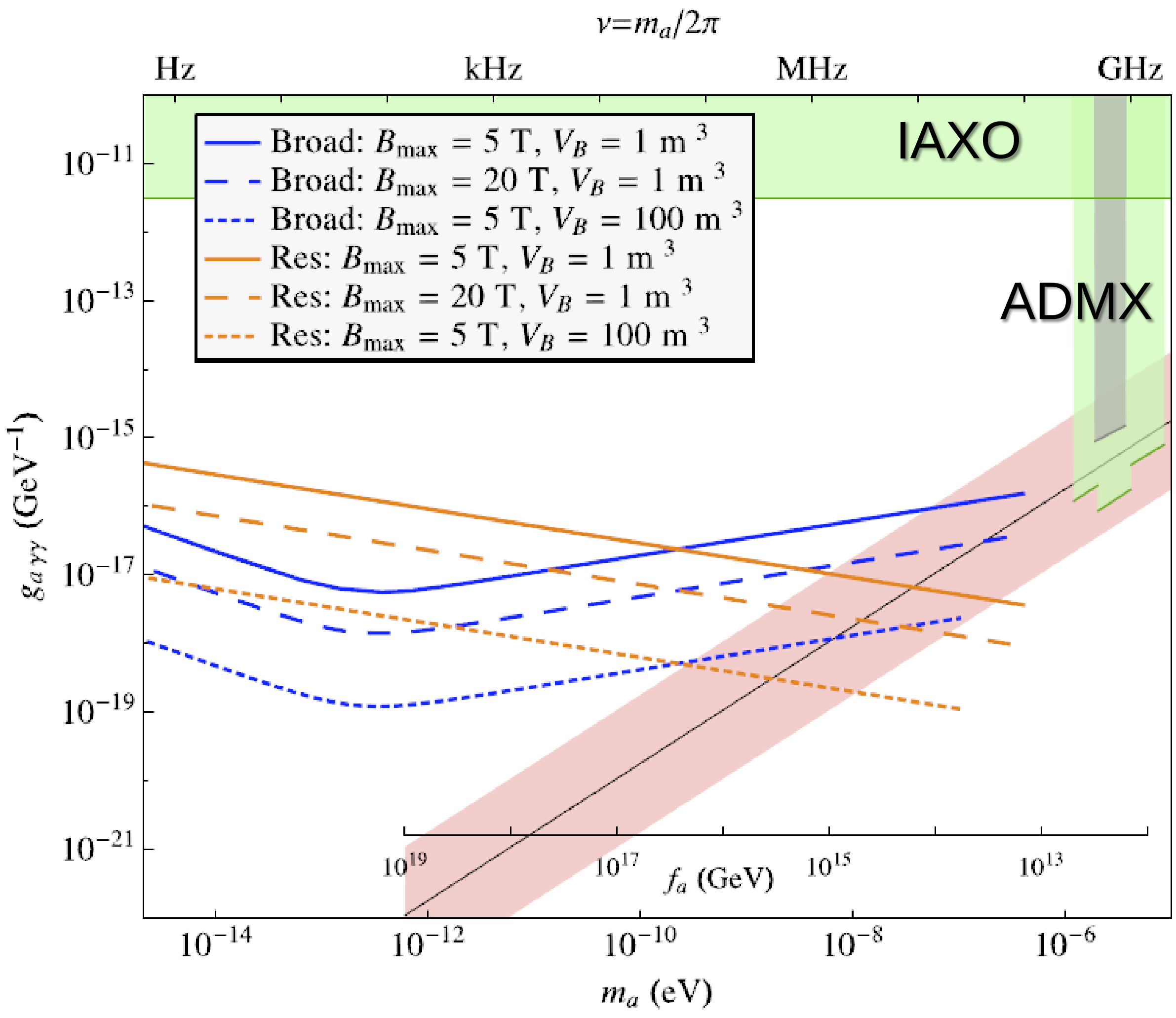

Kahn Y, Safdi BR, Thaler J: PRL117, 141801 (2016)

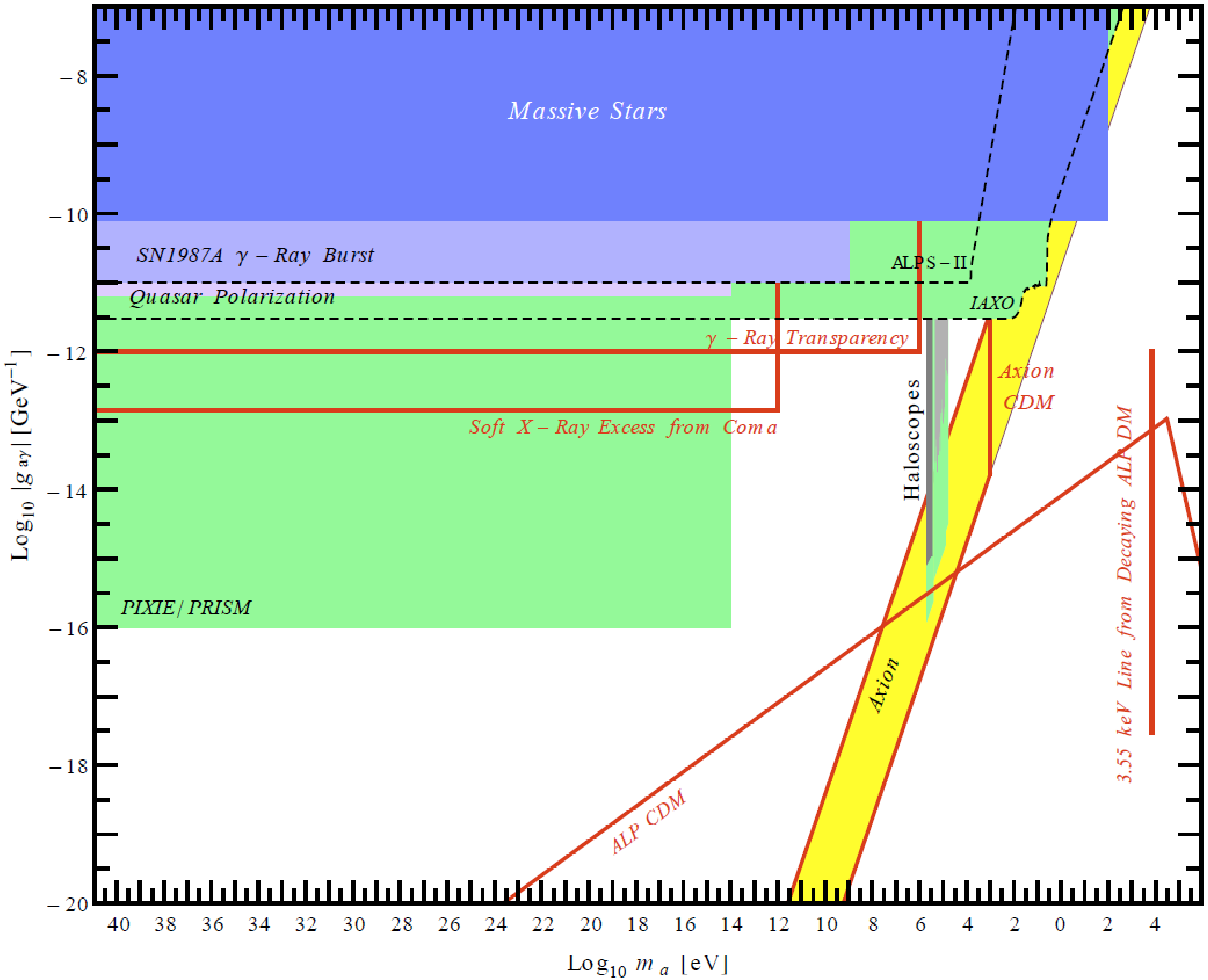

Ringwald A: arXiv:1407.0546

4. 4 Axion Cosmophysics

Characteristic Mass Scales

- Compton wavelength= Horizon size (m=3H)
  - Present $t=t_0$: $m_0=4.5\times 10^{-33}$ eV
  - CMB last scattering $t=t_{ls}$: $m_{ls}=0.7\times 10^{-28}$ eV
  - H recombination $t=t_{rec}$: $m_{rec}=1.2\times 10^{-28}$ eV
  - Equidensity time $t=t_{eq}$: $m_{eq}=0.9\times 10^{-27}$ eV
- Compton wavelength= BH size ($1/m=M_{pl}^2/M$)
  - Supermassive BH $M=10^{10}\,M_\odot$: $m_{bh,max}=1.3\times 10^{-20}$ eV
  - Solar mass BH $M=1\,M_\odot$: $m_{bh,min}=1.3\times 10^{-10}$ eV
- QCD axion $m \approx \Lambda_{QCD}^2/f_a$
  - $f_a=10^{16}$ GeV: $m \sim 10^{-9}$ eV
  - $f_a=10^{12}$ GeV: $m \sim 10^{-5}$ eV

$$\text{Cf. } m_a = 1\text{eV} \times \left(\frac{6\times 10^6\,\text{GeV}}{f_a}\right)$$

Axion Cosmophysics

Super-light axionic fields produce a rich variety of new cosmophysical phenomena and provide a new window to string compacitification!!

Phenomena irrelevant to abundance

- **Instabilities of black hole systems**
- **Influence on high-energy gamma ray propagation**
- **Solar activity/heat transport**
- **……**

Phenomena sensitive to abundance

- **Deformation of the cosmological power spectrum**
- **Rotation of the CMB polarisation**
- **Dark matter/ Dark radiations**
- **Dark energy**
- **……**

UHE gamma rays from AGNs can penetrate the CBR barrier

EM axion: $F_a \sim 10^{10}$ GeV

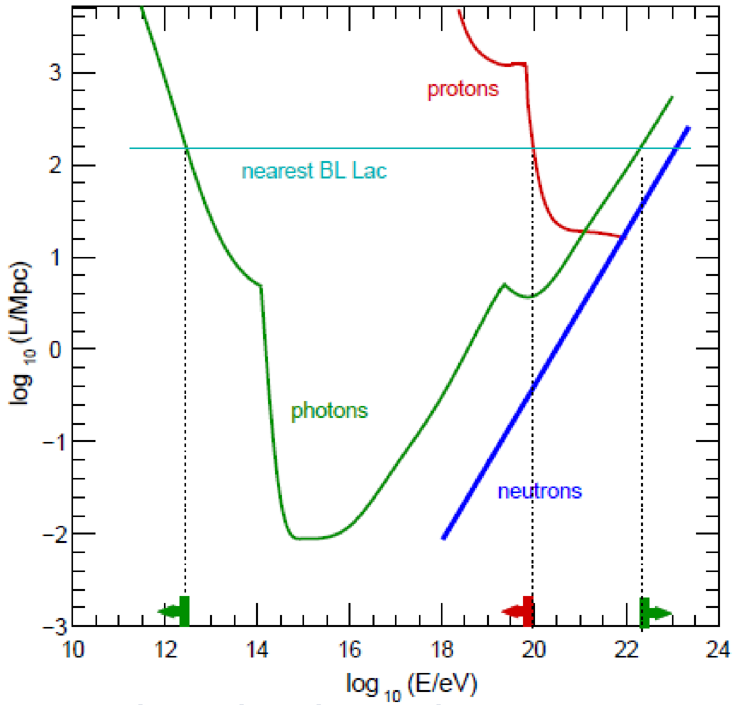

Optical depth against CMB

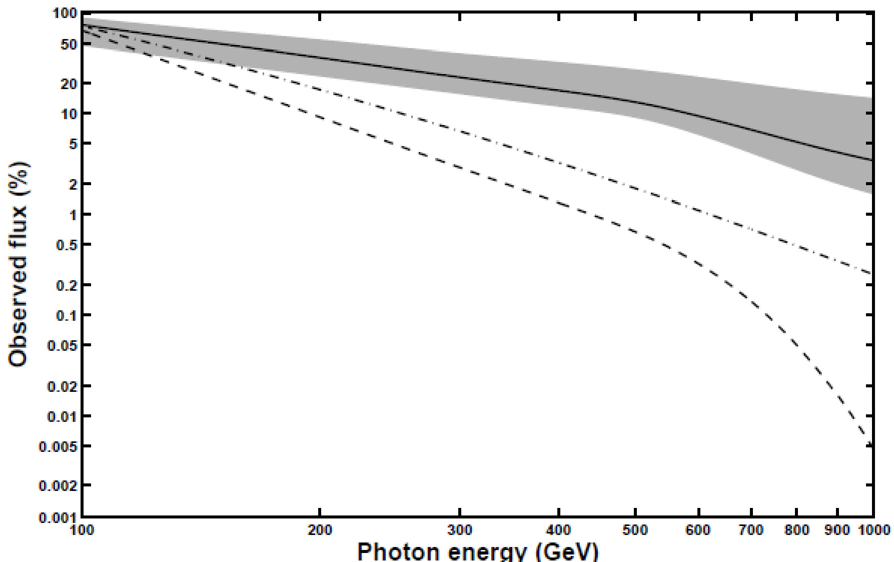

Expected flux from 3C279

$$B = 10^{-9}\mathrm{G}, \quad L_{\mathrm{dom}} \sim 1\mathrm{Mpc}$$

Fairbairn, Rashba, Troitsky 2009; Roncadelli, de Angelis, Mansutti 2009

UHE gamma rays from AGNs can penetrate the CBR barrier

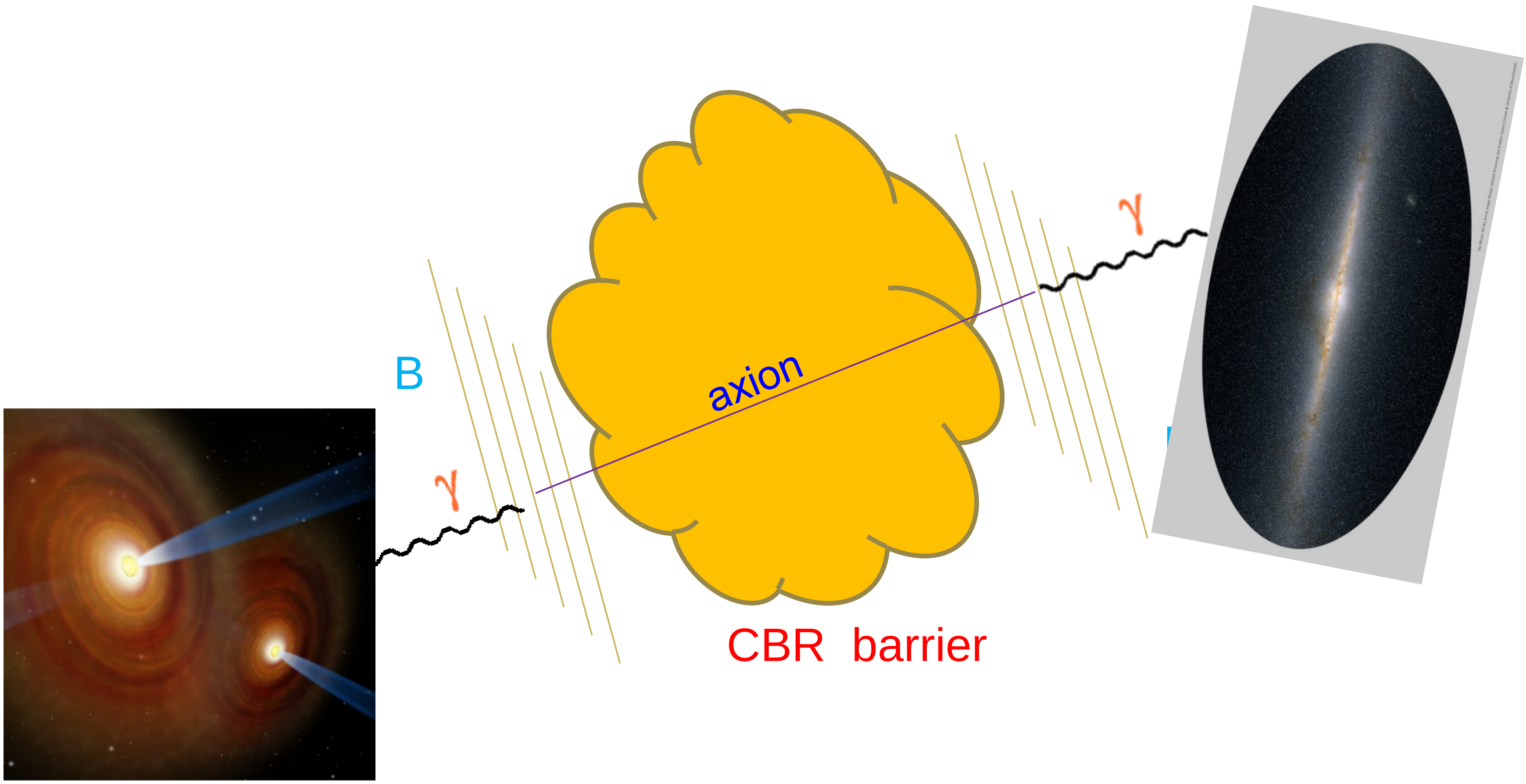

New Activities in Astrophysical Black Hole Systems

Any axion: $m_a = 10^{-10} \sim 10^{-20}$ eV

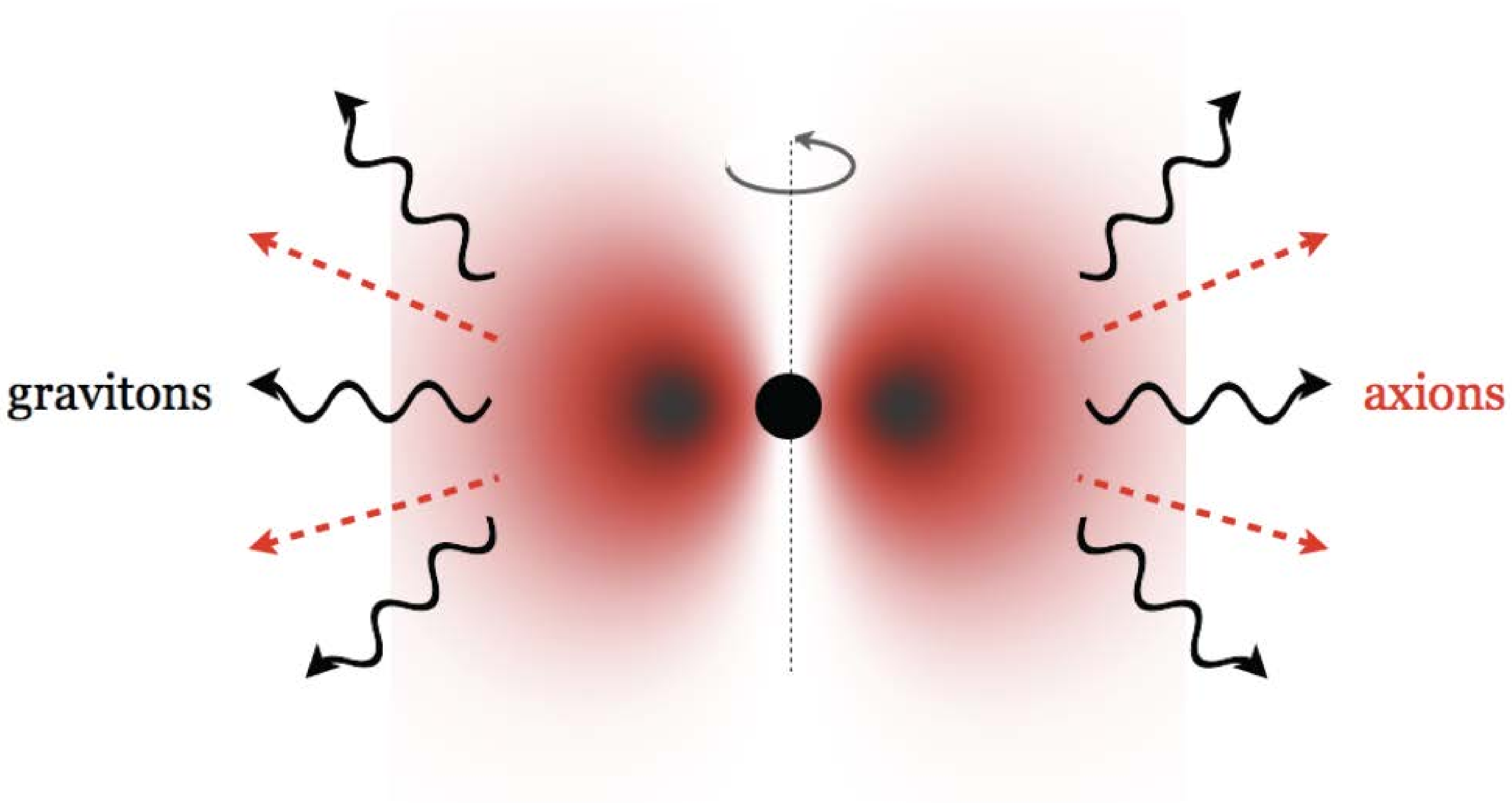

Arvanitaki A, Dubovsky S:
arXiv:1004.3558

Cosmological Birefringence

EM axion: $m_a = 10^{-28} \sim 10^{-33}$ eV

- **ϕ F∧F term induces the rotation of the CMP polarisation when $d\phi/dt \neq 0$.**

⇒ Generates B-modes from E-modes after recombination.

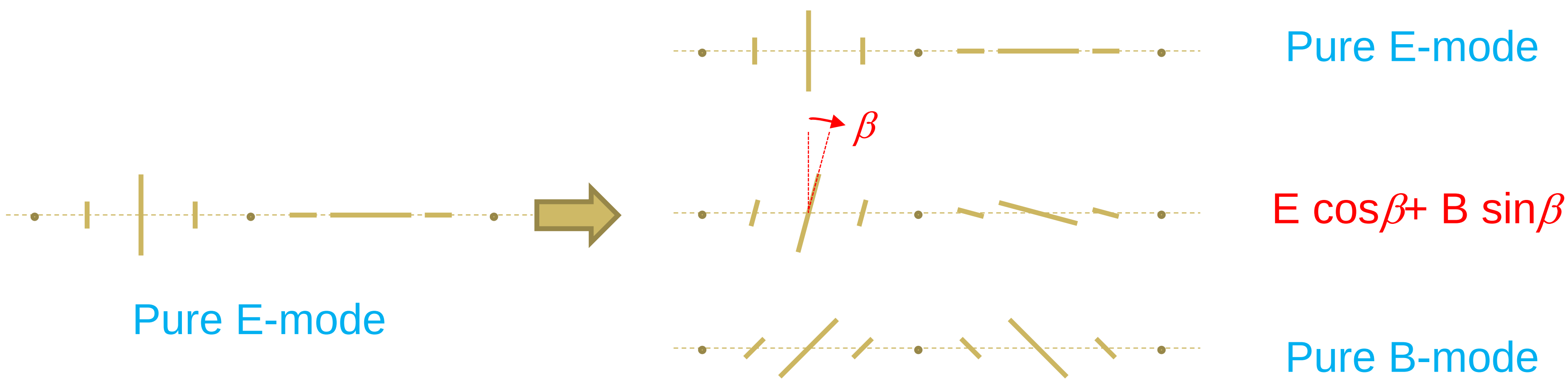

Lue, Wang, Kamionkowski 1999

Axions behave both as DE and CDM

Any axion: $m_a = 0 \sim 10^{-3}$eV

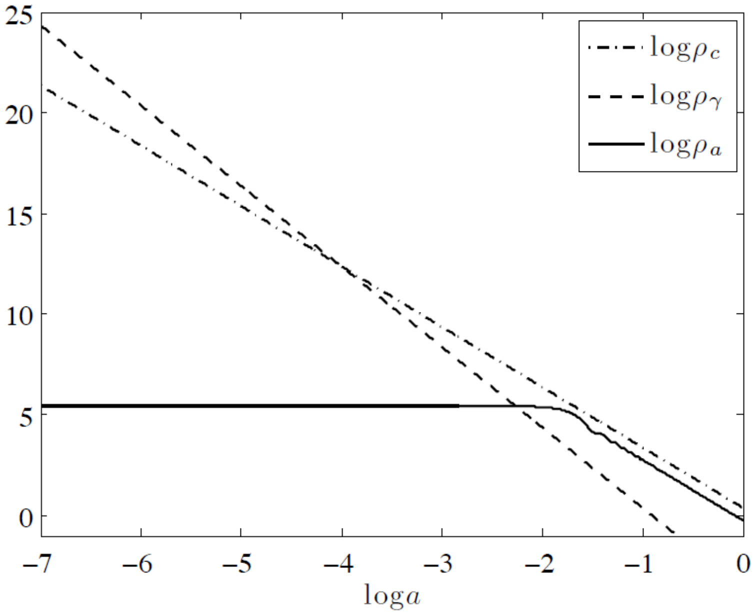

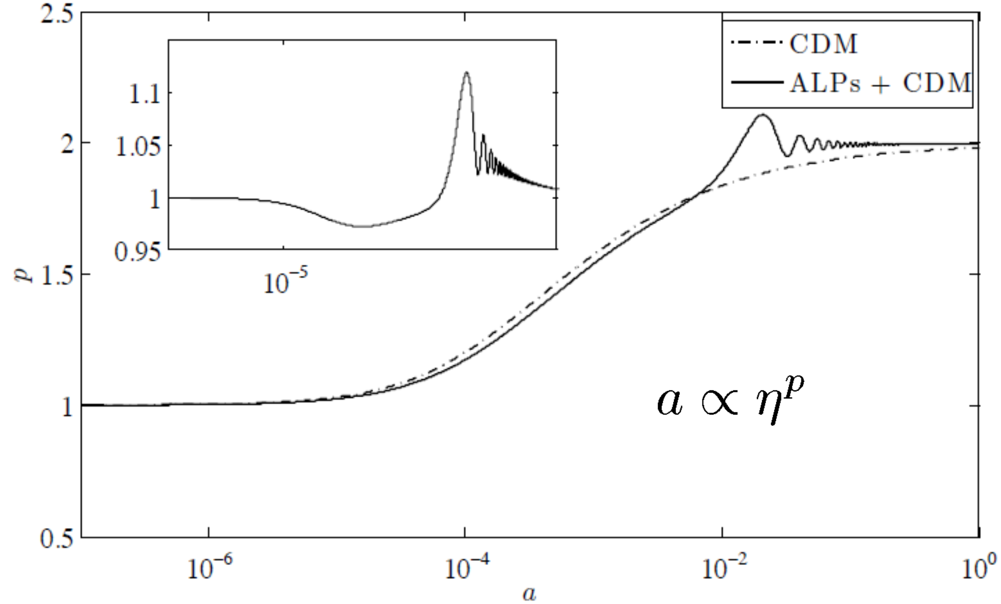

$$m/H_0 = 10^3, \quad \Omega_c = 0.8, \quad \Omega_\Lambda = 0$$

Marsh DJE, Ferreira PG:
arXiv:1009.3501

Deformations of Cosmologial LSS

Any axion: m_a = $10^{-20}$$\sim$ 0^{-28} eV

Transfer function:

$$T^2(k) := \frac{P(k)_{\mathrm{ALPs+CMD}}}{P(k)_{\mathrm{CMD}}}$$

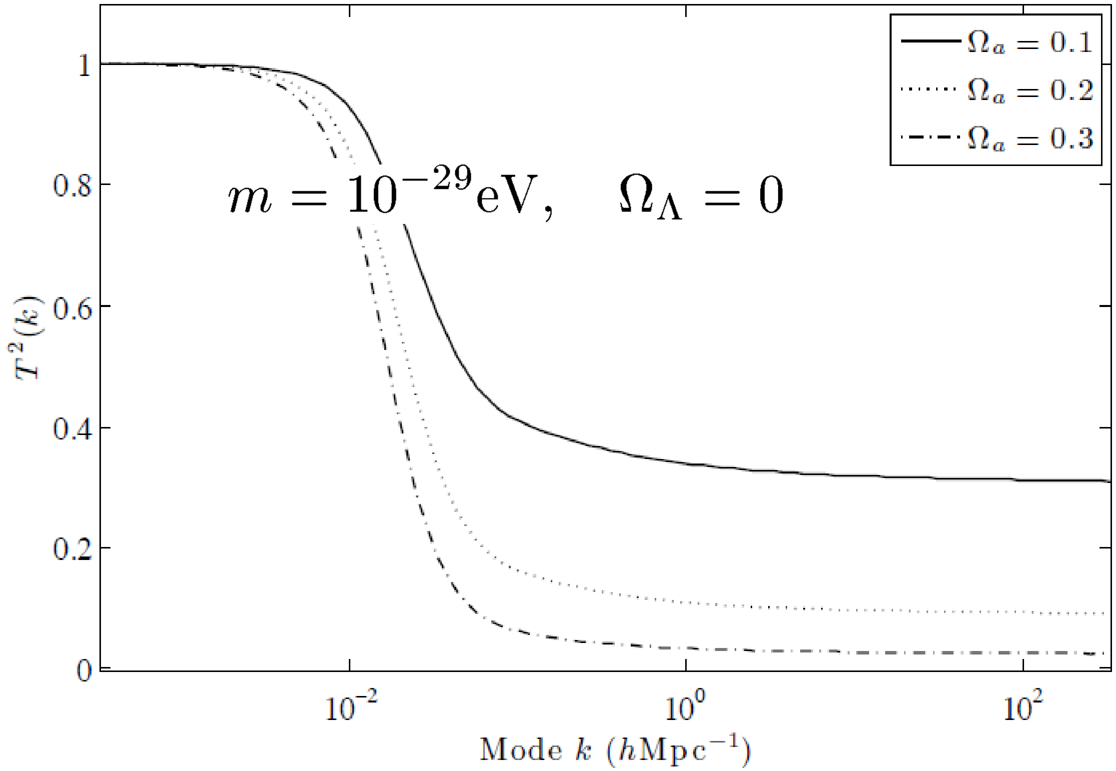

$m_a - f_a$ plane

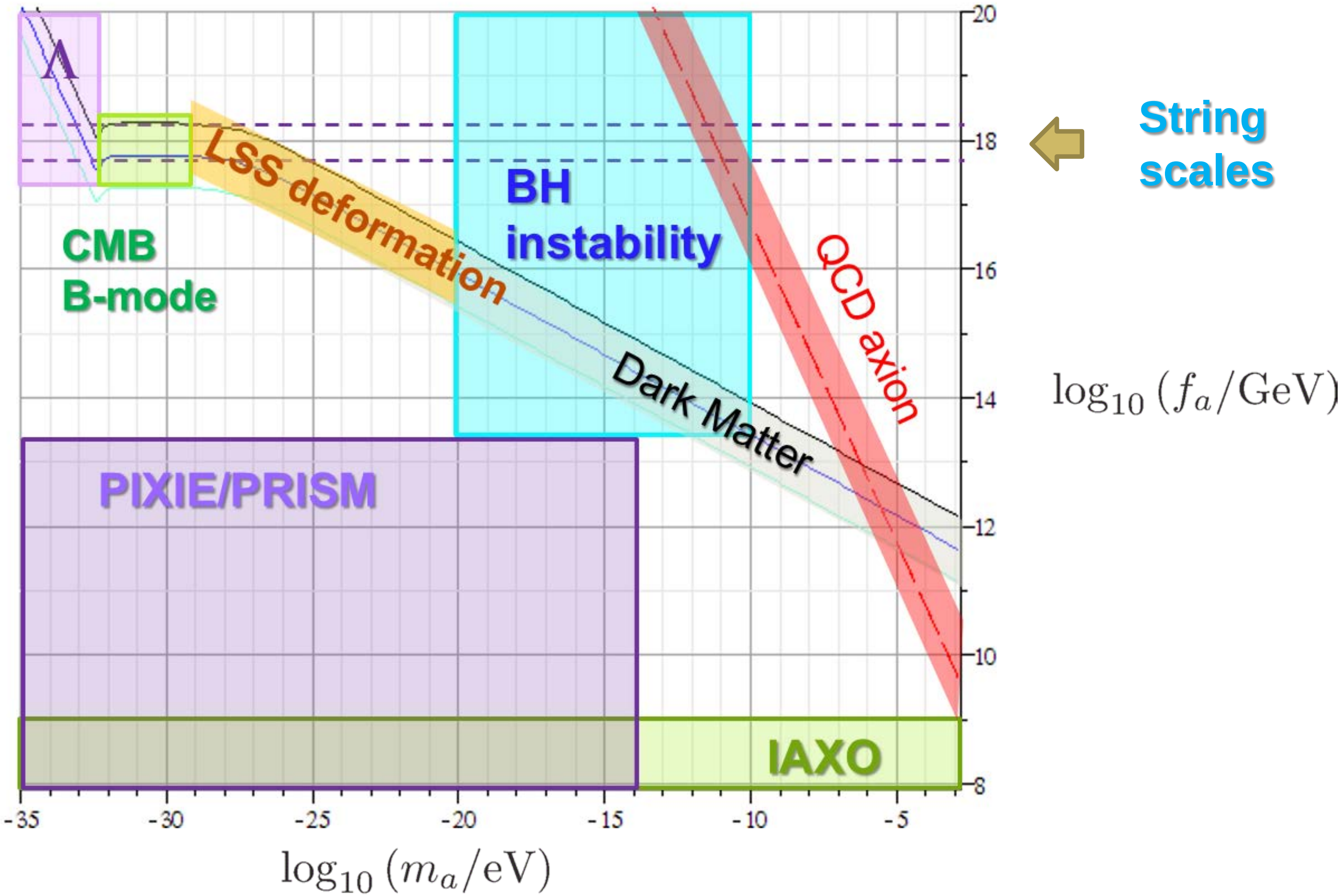

$g_{\alpha\gamma} \approx \frac{\alpha}{\pi f_a}$ is assumed.

Probing the Ultimate Theory by Axion Cosmophysics

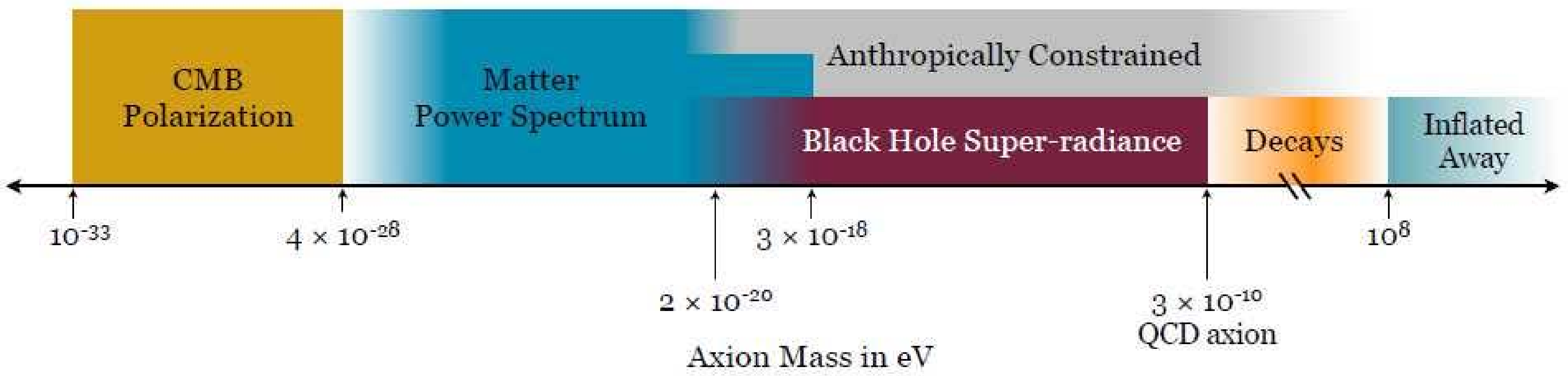

String theories $\Rightarrow$ superlight axionic fields + QCD axion

Superlight axionic moduli $\Rightarrow$ new cosmophysical phenomena.

Arvanitaki A, Dimopoulos S, Dubovsky S, Kaloper N, March-Russell, J: "String Axiverse" arXiv: 0905.4720

4. 5 重力波によるアクシオン探査

Black Hole Instability

Superradiance

Scalar field around a Kerr BH

$$(\Box - \mu^2)\Phi = 0; \quad \Phi \propto e^{-i\omega t + im\phi}$$

KG flux across the future horizon

$$k = \xi + \Omega_h \eta; \quad \xi = \partial_t, \quad \eta = \partial_\phi$$

$$I_{\mathscr{H}^+} = \int_{\mathscr{H}^+} (ik^\mu)\Phi^* \overleftrightarrow{\partial}_\mu \Phi = (\omega - \Omega_h m)\,|C|^2$$

Flux across the horizon can become negative !!

Superradiance

$$\omega |A|^2_{\mathscr{I}^+} + (\omega - \Omega_h m)|C|^2 = \omega |A|^2_{\mathscr{I}^-}$$

$$\omega - m\Omega_h < 0 \Rightarrow \quad I_{\mathscr{I}^+} > I_{\mathscr{I}^-}$$

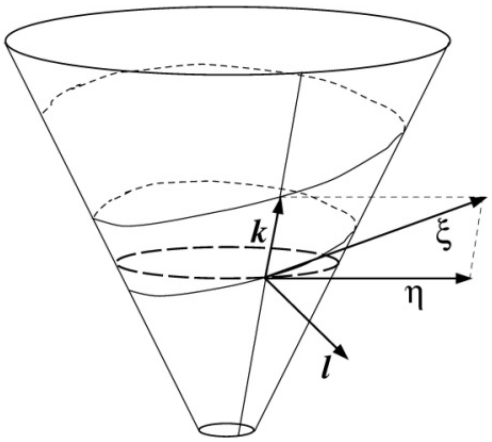

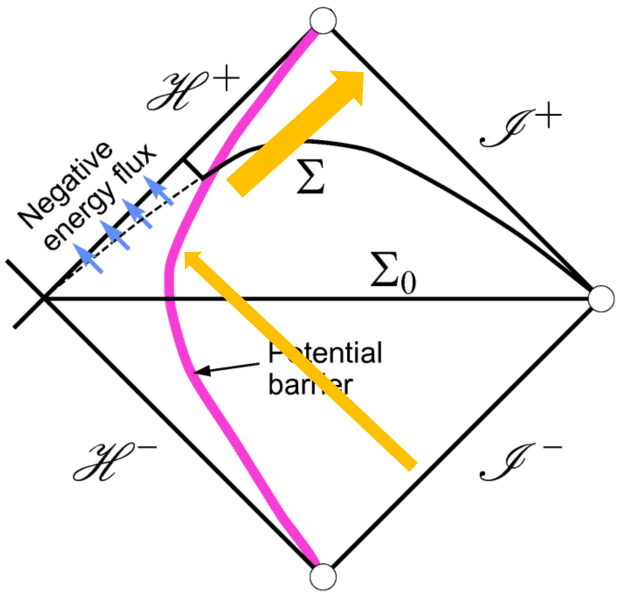

Superradiance Instability

Bound state modes of a massive scalar field around a Kerr BH become unstable due to superradiance.

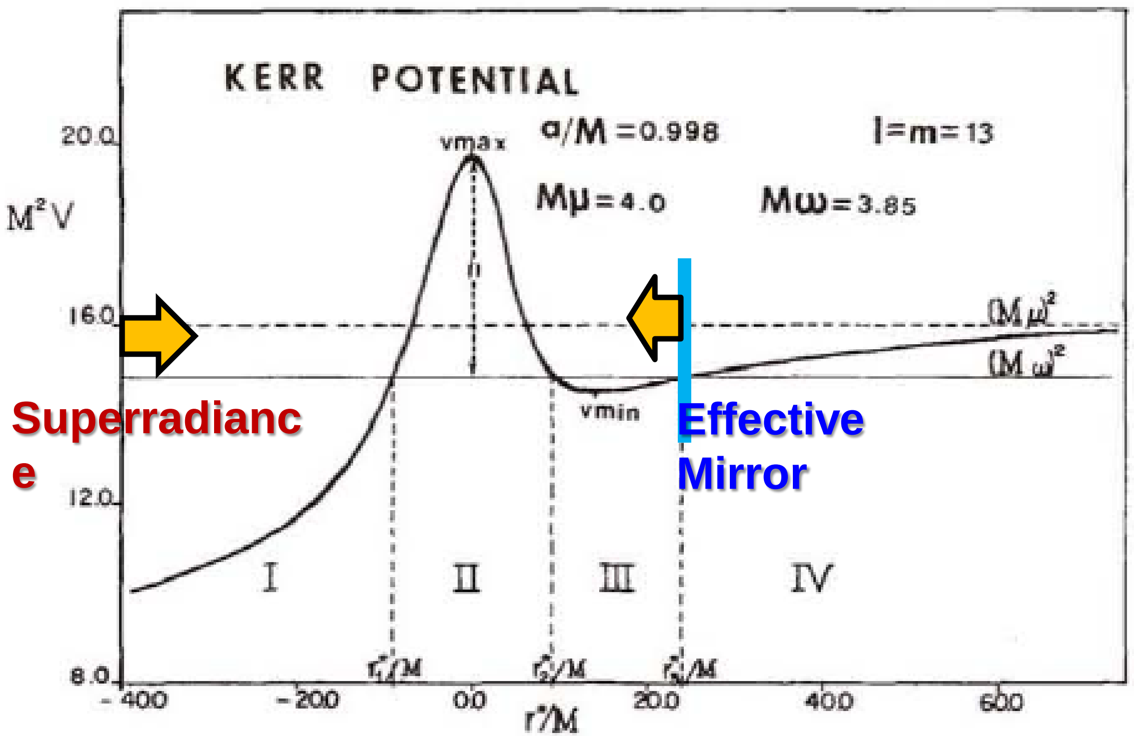

Effective potential for P(r)

Zouros TJM, Eardley DM 1979

[Damour, Deruelle, Ruffini (1976)]

$$\omega < m\Omega_h$$

&

$$\omega < \mu$$

$$\Phi = P(r)S_l^m(\theta)e^{-i\omega t+im\phi} \quad \Rightarrow \quad -\frac{d^2}{dr^{*2}}P + (V-\omega^2)P = 0$$

Instability Growth Rate

- Analytic Estimates [Zouras & Eardley (1979), Detwiler (1980)]

$$\frac{\tau}{M} \approx \begin{cases} 10^7 e^{1.84\alpha_g} & ;\alpha_g \gg 1,\ a/M = 1 \\ 24\left(\frac{a}{M}\right)^{-1}(\alpha_g)^{-9} & ;\alpha_g \ll 1, \end{cases} \qquad (\alpha_g = \mu M)$$

- Growth rate for a massive scalar

The growth timescale becomes minimum $\tau \sim 10^7 M$ at

- $l = m = 1$
- $a_* = \frac{a}{M} \simeq 0.99$
- $\mu M \sim 0.44$

$$M_\odot \Rightarrow \tau \sim 1\text{minute}$$
$$10^6 M_\odot \Rightarrow \tau \sim 2\text{years}$$

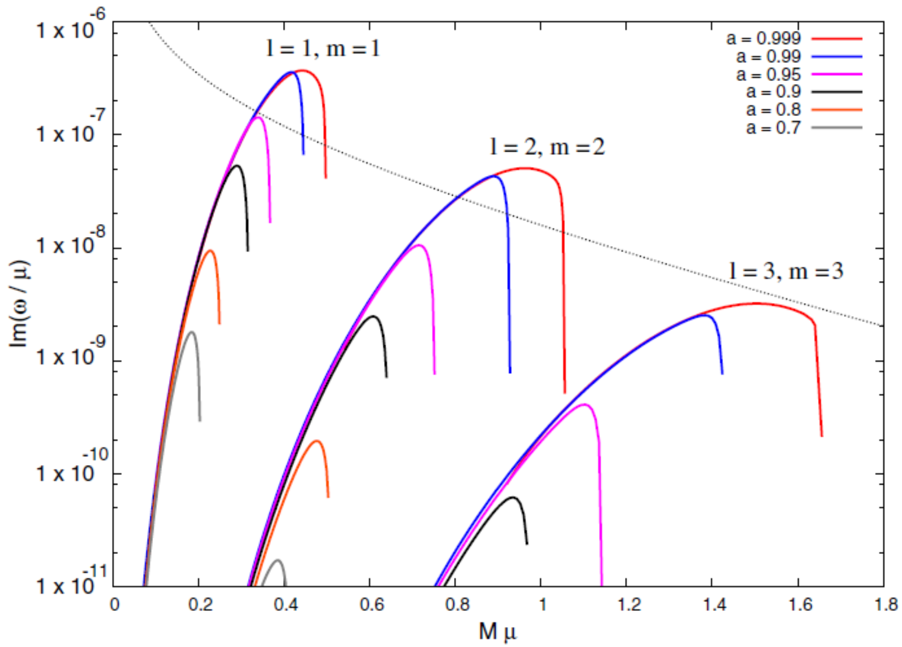

Dolan SR(2007)PRD76,084001

Characteristic Features

Resonant feature of the instability

$$\frac{\tau}{M} \approx \begin{cases} 10^7 e^{1.84\alpha_g} & ;\alpha_g \gg 1,\ a/M = 1 \\ 24\left(\frac{a}{M}\right)^{-1}(\alpha_g)^{-9} & ;\alpha_g \ll 1, \end{cases}$$

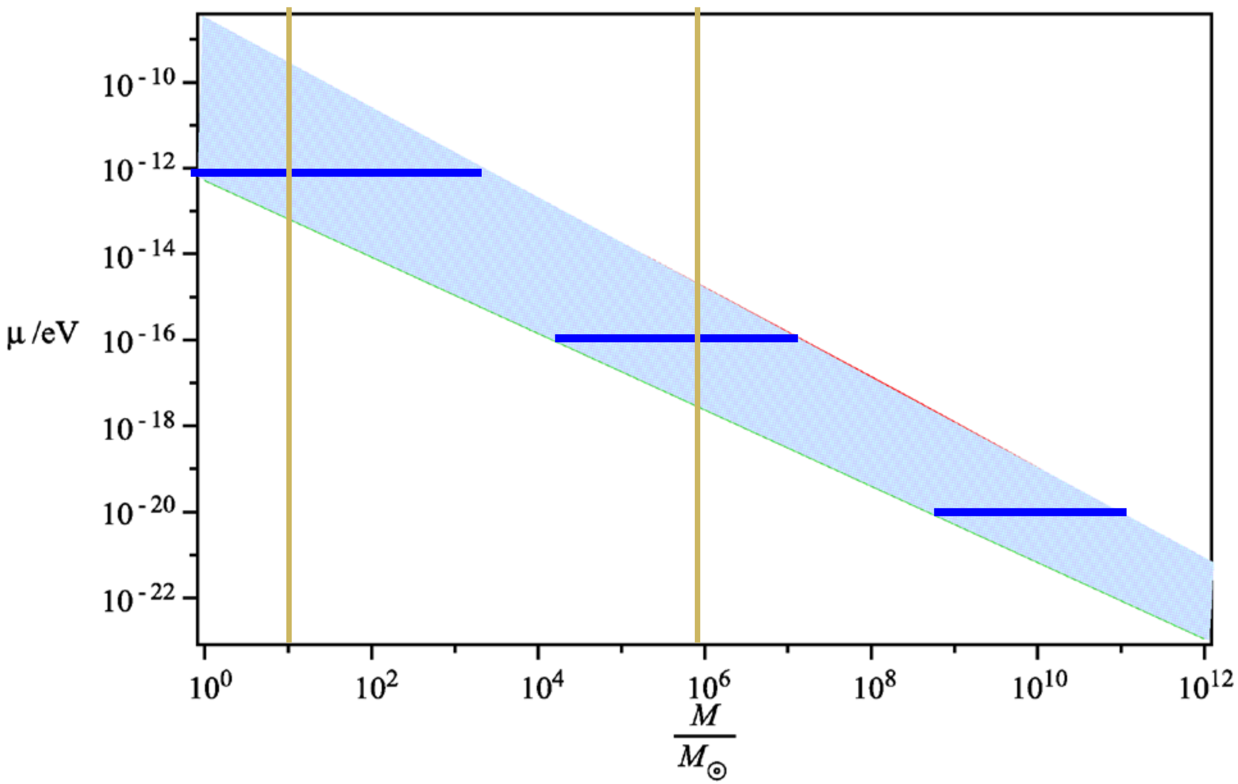

For $M \geq M_\odot$, τ can be shorter than the cosmic age when

$0.003 < \alpha_g = \mu M < 20$

Definite information can be obtained on the field mass if the instability is observed.

G-Atom

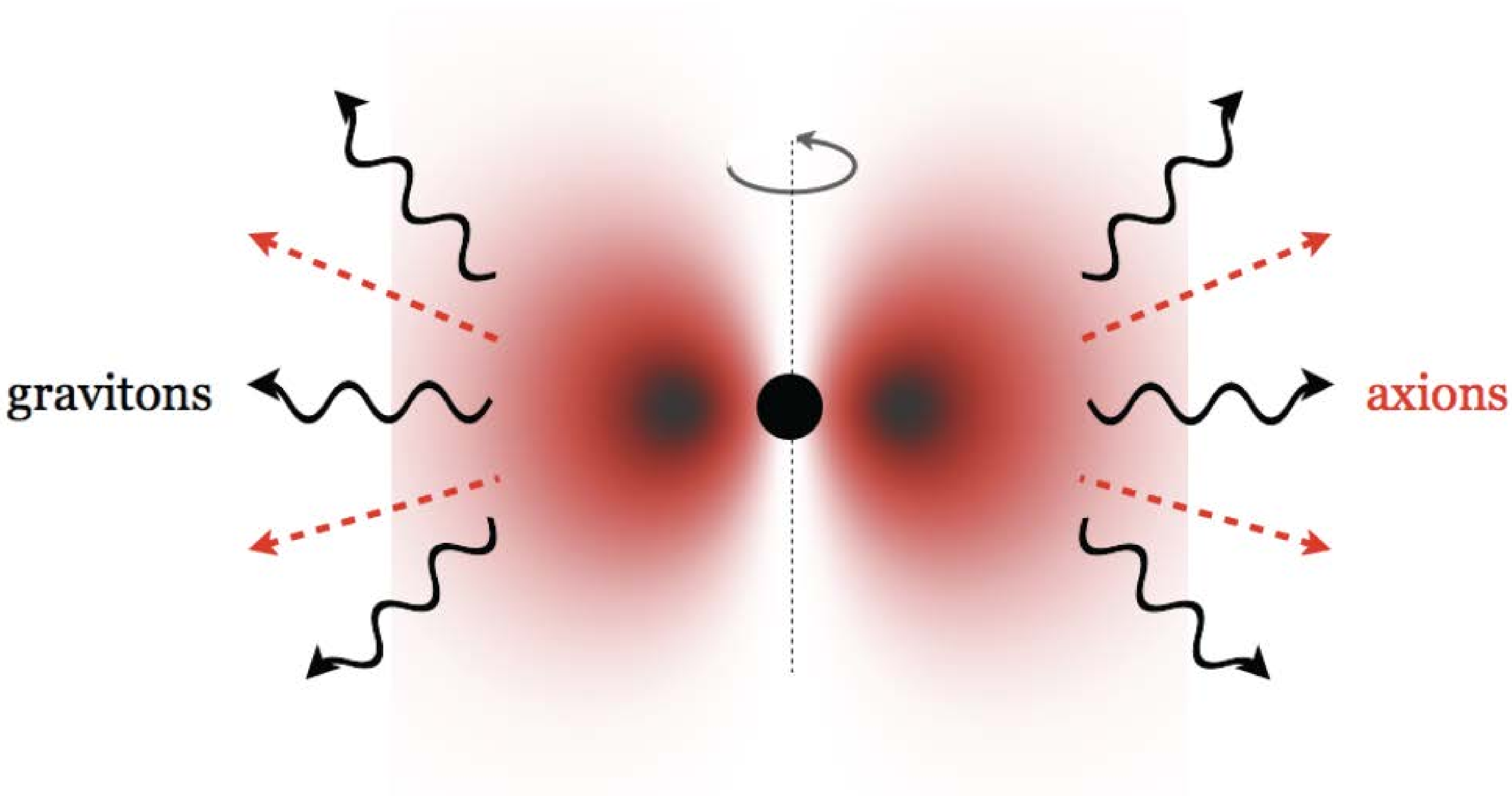

Arvanitaki A, Dubovsky S:
arXiv:1004.3558

Gravitational Atoms

Unstable bound states are classified by the quantum numbers (n, l, m)exactly as in the case of the hydrogen atom.

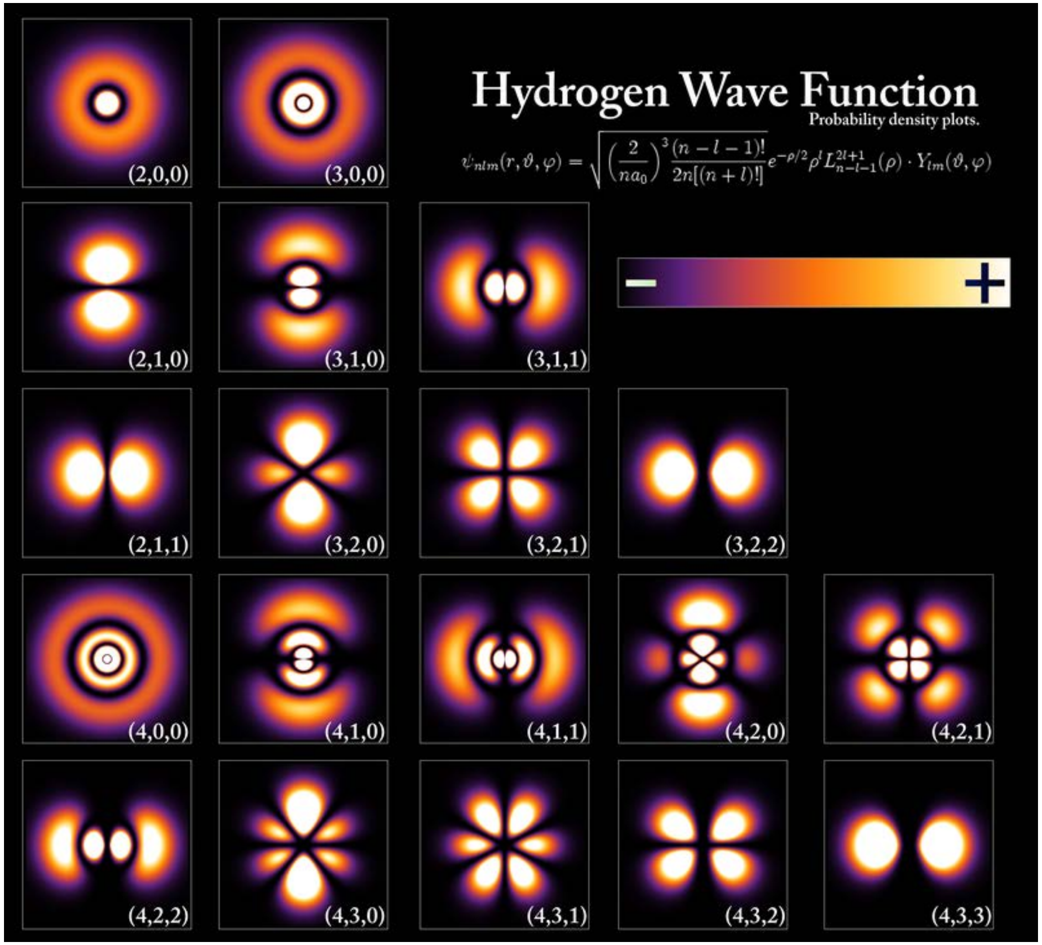

Principal quantum number:

$$n = n_r + \ell + 1 \ (n_r = 0, 1, 2, \cdots)$$

SR Instability for Overtone Modes

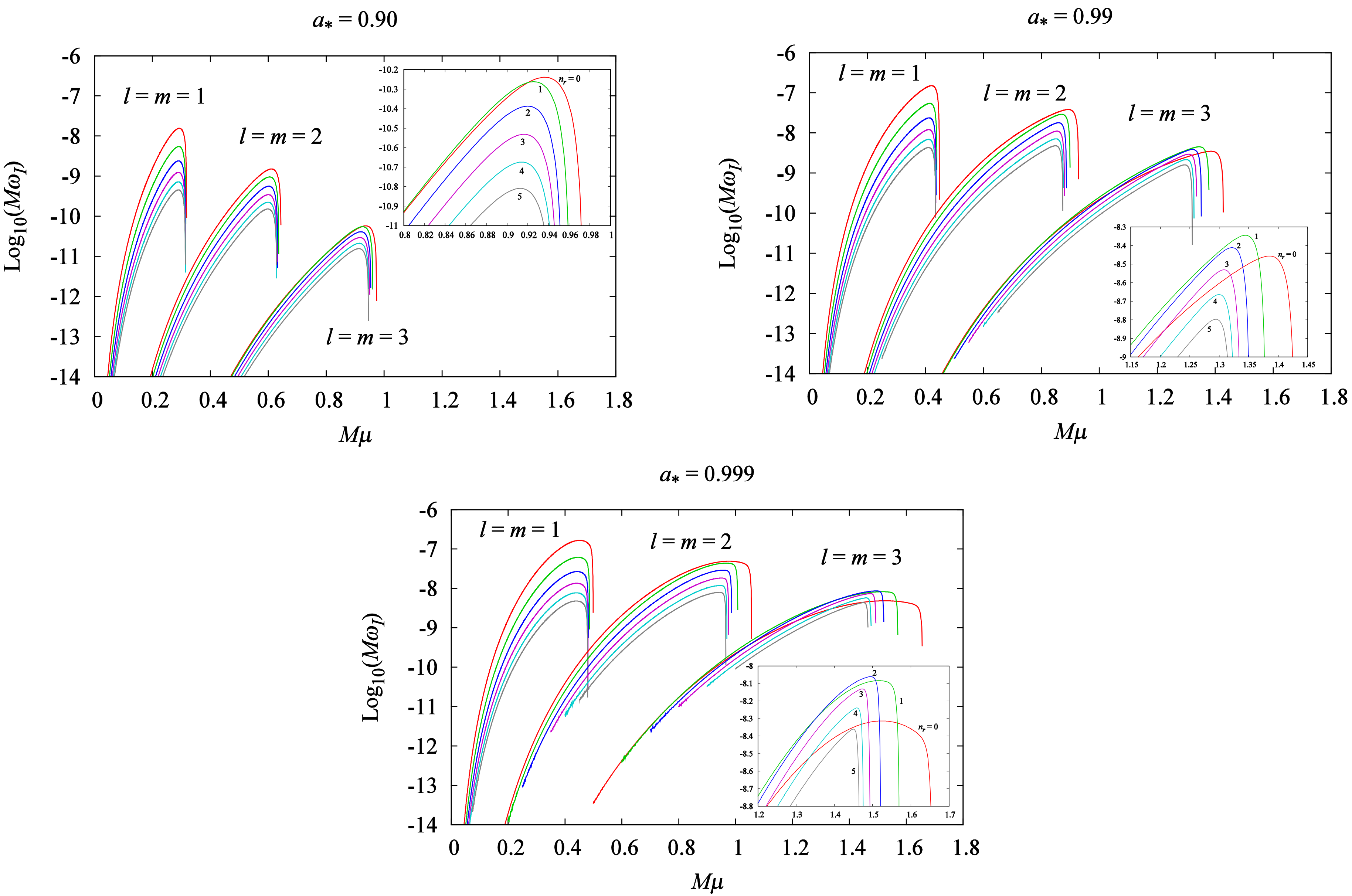

Fate of G-Atom?

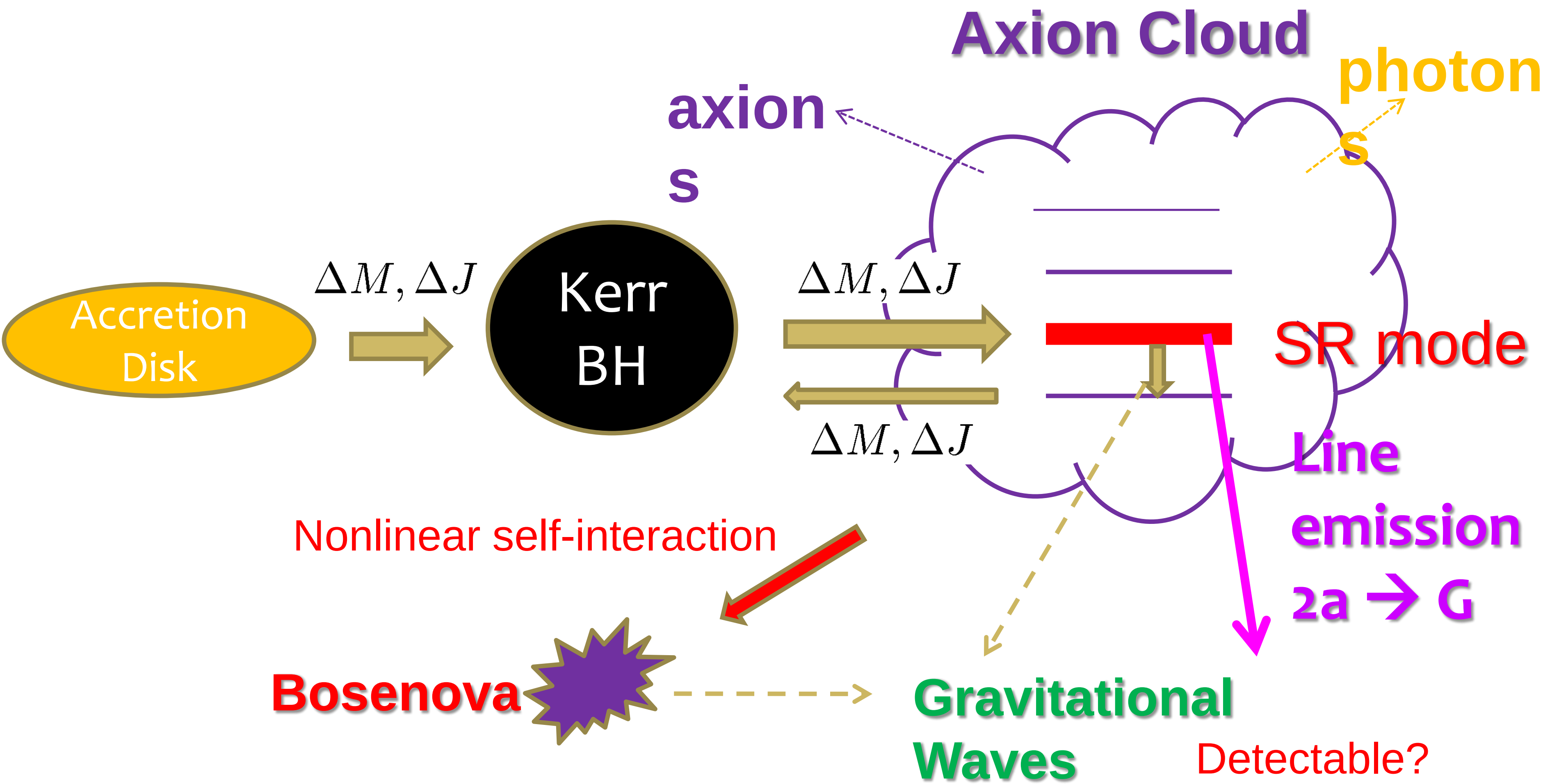

$$\delta g_{\mu\nu} \Leftarrow T_{\mu\nu} \Leftarrow \partial\Phi\partial\Phi \propto (ae^{-i\omega t} + a^* e^{i\omega t})(ae^{-i\omega' t} + a^* e^{i\omega' t})$$

4.5 重力波によるアクシオン探査

Non-linear Dynamics of Axion Clouds and Bose Nova

Non-linear Effects

Action of the axion field

$$S = \int d^4x\sqrt{-g}\left[-\frac{1}{2}(\nabla\Phi)^2 - V\right]$$

$$V = \mu^2 f_a^2\left(1-\cos\frac{\Phi}{f_a}\right)$$

axion decay constant

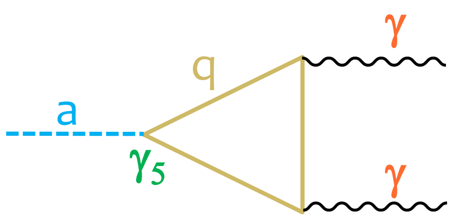

$$g_{a\gamma}\phi\boldsymbol{E}\cdot\boldsymbol{B}; \quad g_{a\gamma}\sim\frac{10^{-3}}{f_a}$$

Small field expansion

$$V = \frac{1}{2}\mu^2\Phi^2 - \frac{\mu^2}{4!f_a^2}\Phi^4 + \frac{\mu^2}{6!f_a^4}\Phi^6 - \cdots$$

Attractive interaction!! $\propto E_a^2$

Semi-analytic Estimation

Non-relativistic Approximation

$$\Phi \simeq \frac{1}{\sqrt{2\mu}} \left(e^{-i\mu t}\psi + e^{i\mu t}\psi^*\right)$$

Averaging S over a time scale $\gg 1/\mu$

$$S_{\rm NR} = \int d^4x \left[i\psi^* \partial_t \psi - \frac{1}{2\mu}\partial_i\psi\partial_i\psi^* - \mu\Phi_g\psi^*\psi - \tilde{U}_{\rm NL}(|\psi|^2/\mu f_a^2)\right]$$

$$\tilde{U}_{\rm NL}(x) = -\mu^2 f_a^2 \sum_{n=2}^{\infty} \frac{(-1)^n}{(n!)^2 2^n} x^n = -\frac{1}{16}\mu^2 f_a^2 x^2 + \cdots$$

Attractive interaction $\propto E_a^2$

- Collective coordinates

$$\psi = A(t,r,\theta)e^{iS(t,r,\theta)+im\phi} \Leftarrow (r_c, p_r),\ (\sigma_r = we^{u}, \pi_r),\ (\sigma_\theta = we^{-u}, \pi_\theta)$$

- Effective potential

Minimising the effective action w.r.t. u and r_c,

$$u = 0, \quad \alpha_g \mu r_c = m^2(1+5w) - \frac{1}{4w}$$

$$\Downarrow$$

$$L = p_w \dot{w} - H; \quad H = k(w)p_w^2 + V_{\text{eff}}(w)$$

$$V_{\text{eff}} = \alpha_g^2 \frac{8w\left\{1 - m^2 w(1+8w)\right\}}{[-1+4m^2w(1+5w)]^2} + V_{\text{NL}}(\beta/[w(\alpha_g \mu r_c)^3]),$$

$$V_{\text{NL}}(x) = -\sum_{n=2}^{\infty} \frac{(-1)^n}{2^n n(n!)^2} x^{n-1}.$$

- Control Parameter
  - $\alpha_g = \mu M$
  - m
  - $\beta = \frac{N}{N_*};\ N_* = (2\pi)^2 \alpha_g^{-3} (f_a/\mu)^2$

Behavior of the $V_{eff}(w)$

The cloud size w suddenly shrinks when β exceed some critical value β_*.

Bose Nova Collapse!!

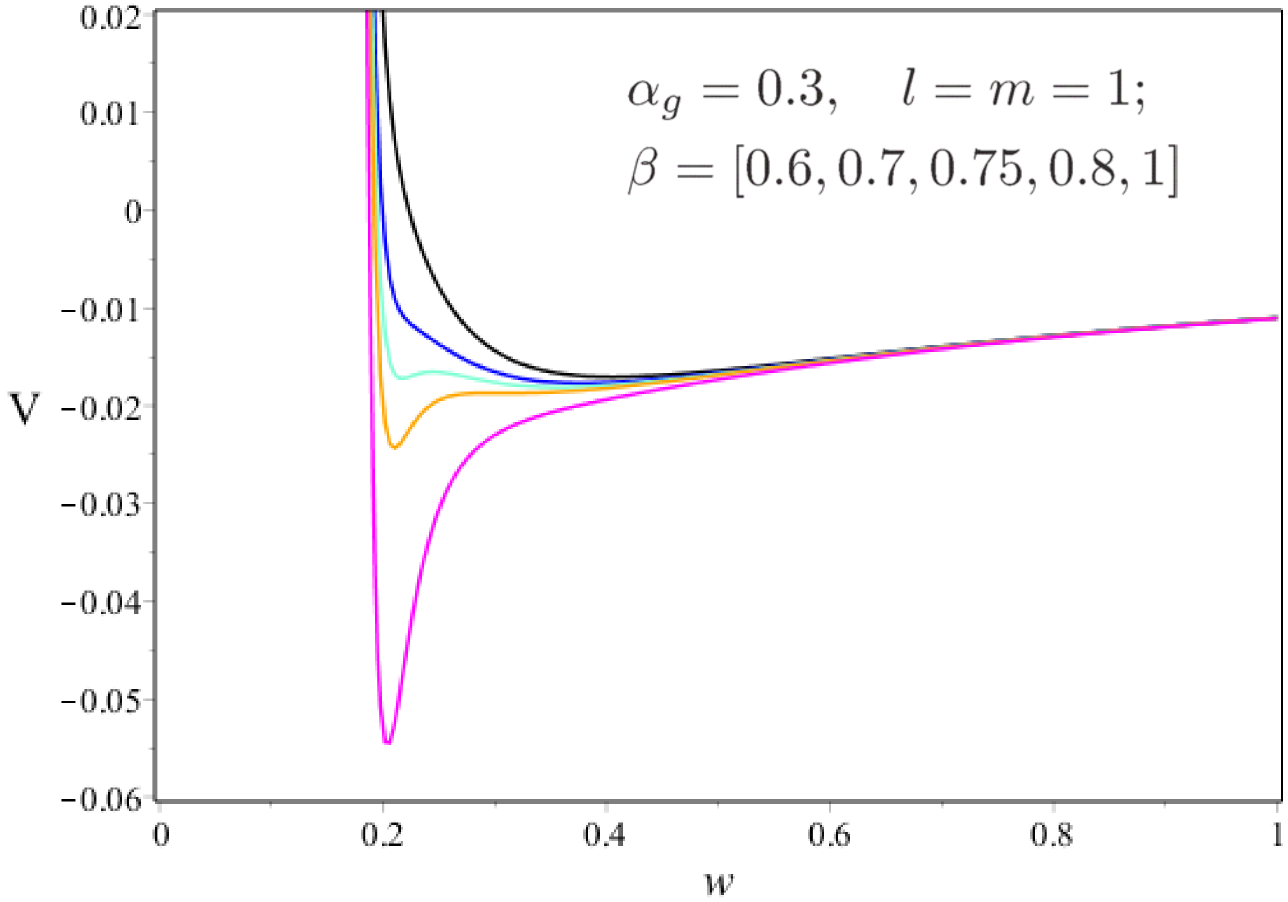

Numerical Methods

- Direct 3D simulation code

$$\Box_{\rm Kerr}\varphi - \mu^2 \sin\varphi = 0$$
$$\text{IC}: \varphi(t=0) = C\varphi_{\rm L},$$
$$\dot\varphi(t=0) = C\dot\varphi_{\rm L}$$

$$\frac{\Phi}{f_a} = \varphi(t,r,\theta,\phi)$$

- Pseudo-spectral code

$$\varphi = \sum_{m\in\mathbb{Z}} f^{(m)}(t,r,\theta)\sin^{|m|}\theta\, e^{im\phi}: \quad f^{(m)}(t,r,\theta) = \sum_{n=0}^{\infty} a_n^{(m)}(t,r_*)\cos^n\theta$$

$$[(r^2+a^2)^2 - a^2\Delta]\ddot a_n^{(m)} + (4imMar)\dot a_n^{(m)}$$
$$= -(a^2\Delta)\ddot a_{n-2}^{(m)} + S(\{a_l^{(m)}\})$$

Behavior of the Energy Flux into BH

Our direct 3D simulations reproduced the SR instability growth rate obtained by the Leaver method with sufficient precisions.

$l = m = 1$
case

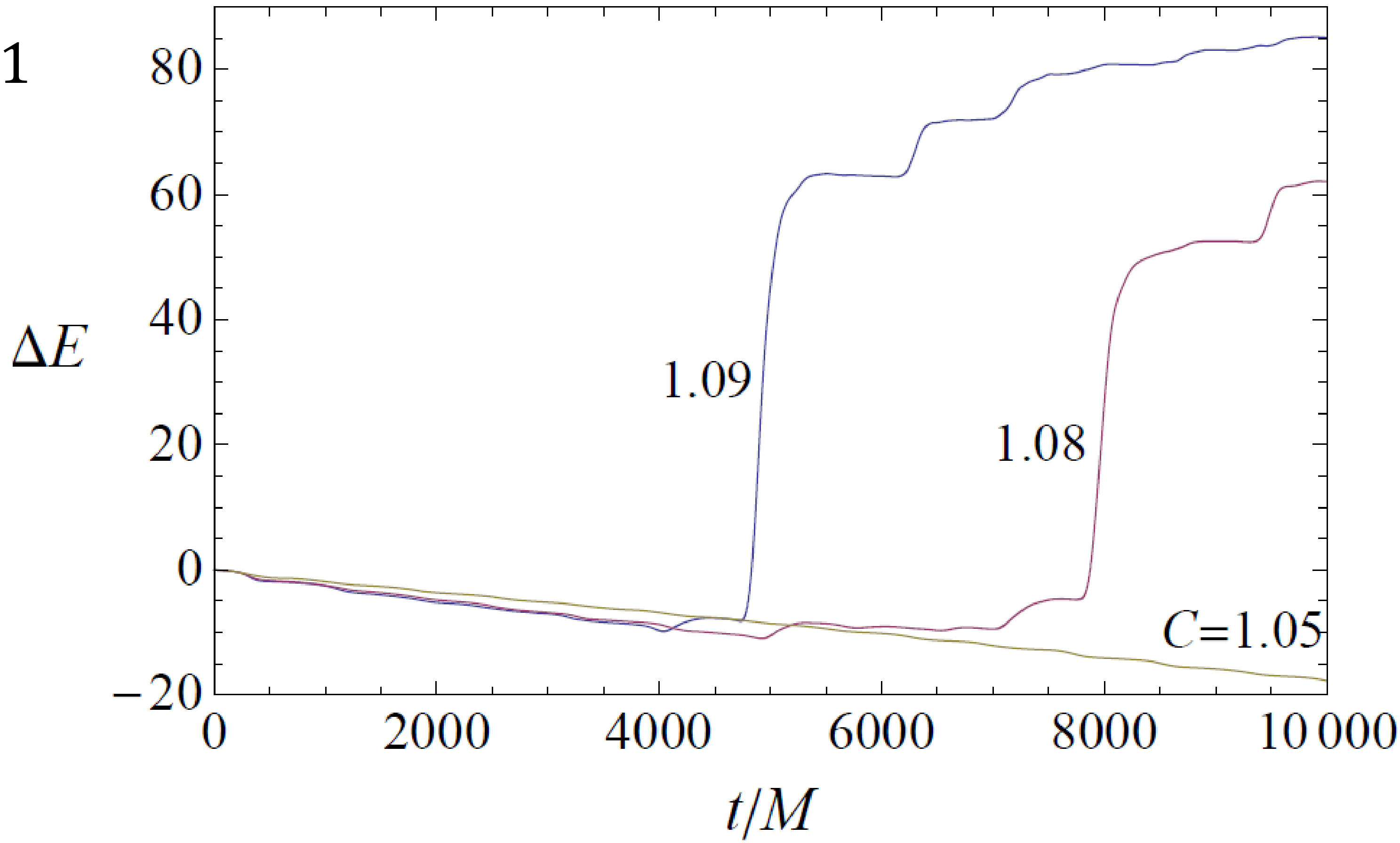

Example of 3D Numerical Simulation: $l = m = 1$

- Parameters: $a_* = 0.99, \ \mu M = 0.30$
- Initial mode: pure $(l, m, nr) = (1,1,0), \Phi/f_a = 0.45$

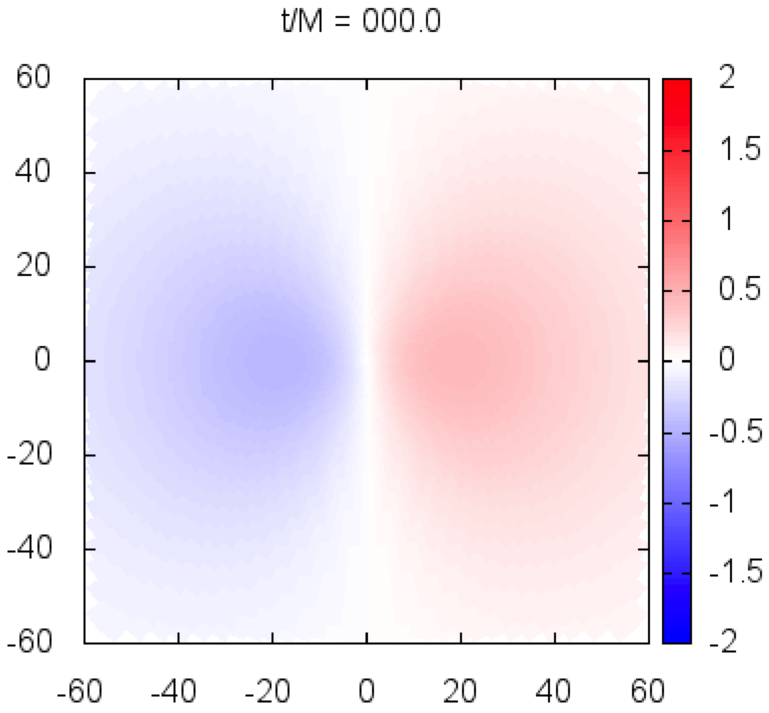

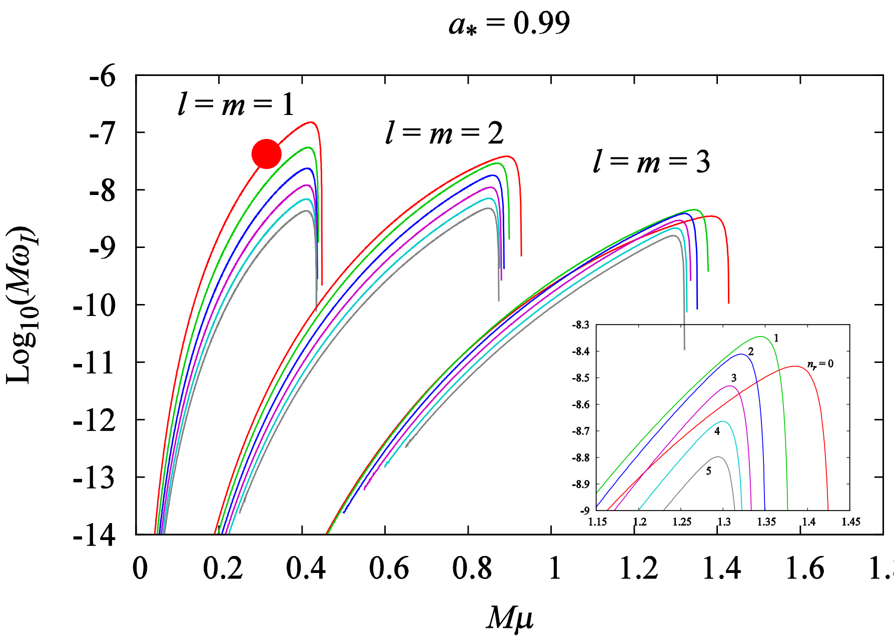

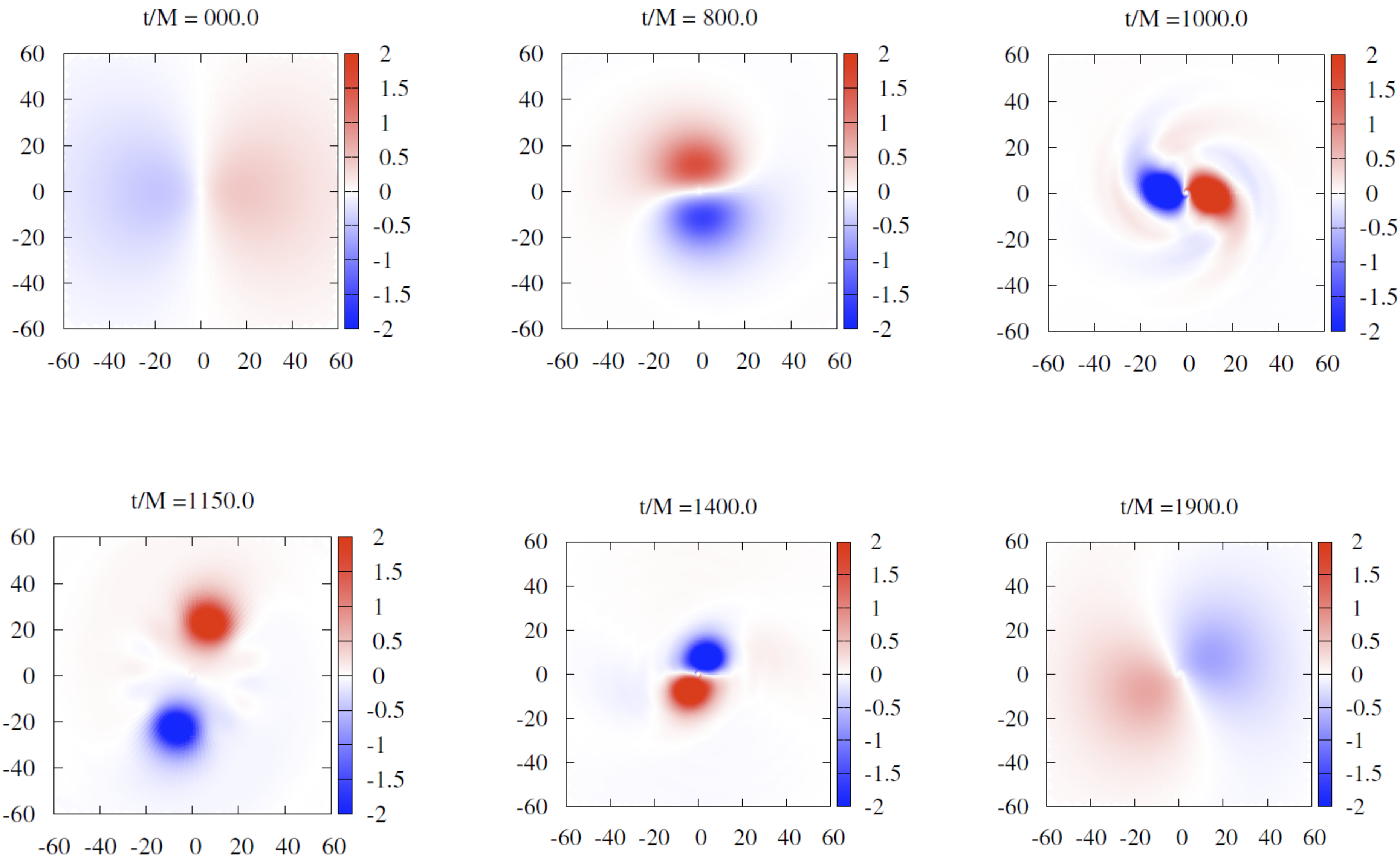
t/M = 000.0
t/M = 800.0
t/M =1000.0
t/M =1150.0
t/M =1400.0
t/M =1900.0

Results

- The energy extraction rate from BH by SR instability increases by a factor around 3 due to nonlinear self-interactions.
- Bose nova happens when

$$|\Phi_{\max}(0)/f_a| \sim 0.7 \quad \Leftrightarrow \quad \frac{E_a}{M} \approx \begin{cases} 2\times 10^{-3}(f_a/10^{16}\mathrm{GeV})^2 & ; M\mu = 0.30 \\ 1\times 10^{-3}(f_a/10^{16}\mathrm{GeV})^2 & ; M\mu = 0.40 \end{cases}$$

- About 5.9% ($\mu M = 0.3$) and 5.3% ($\mu M = 0.4$) of the total axion cloud mass fall into BH by $m = -1$ modes excited by non-linear interations.

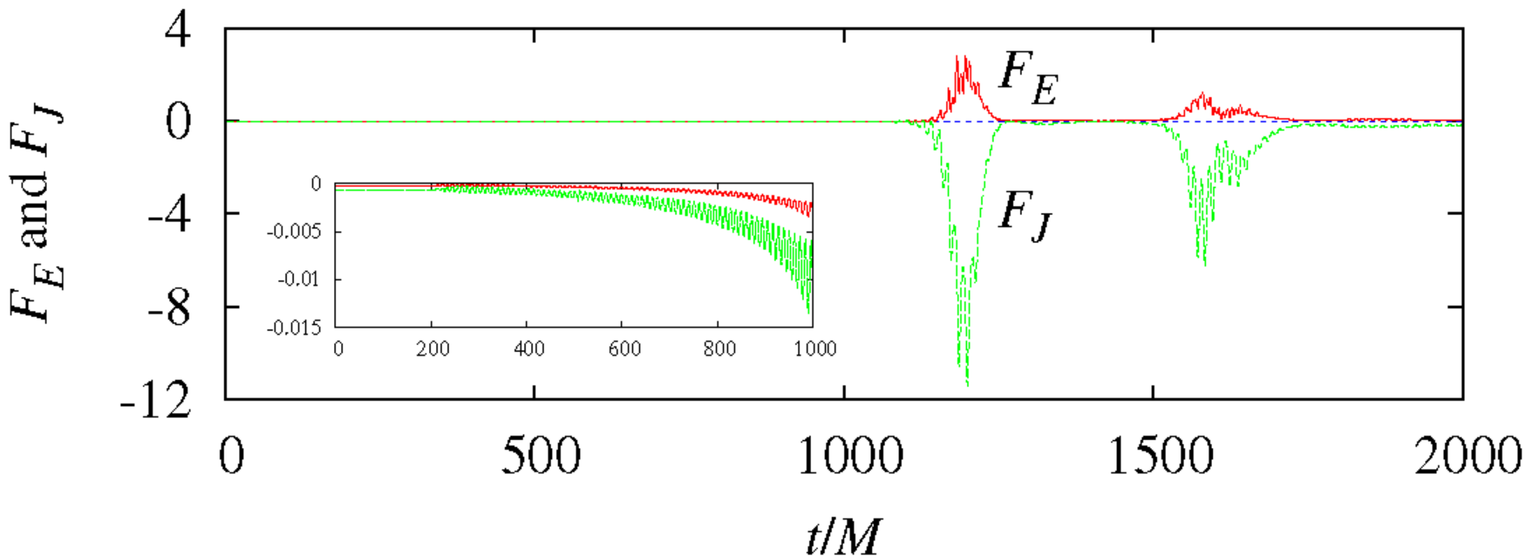

- For $\mu M = 0.3$, about 13.4% of the axion cloud mass is ejected to a far region, while for $\mu M = 0.4$, such an outward ejection is negligible.

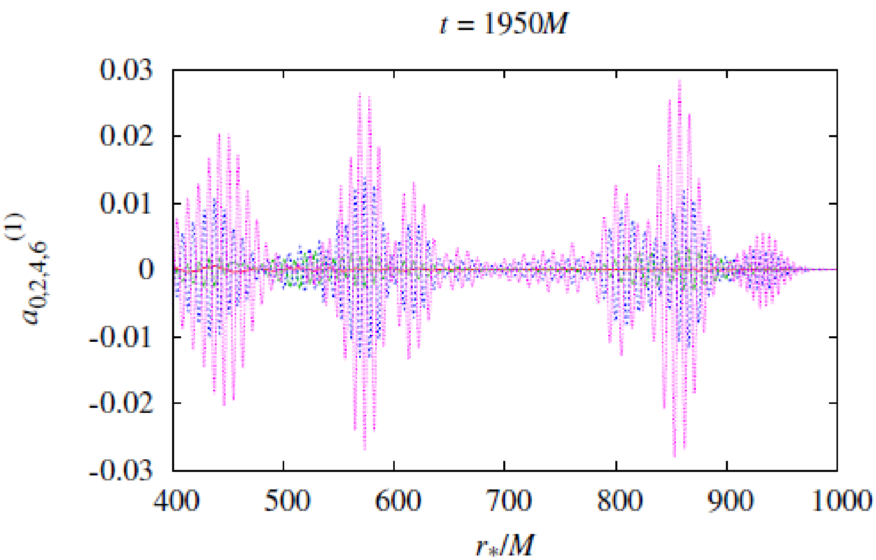

$a_n^{(1)}$: $n = 0, 2, 4, 6$

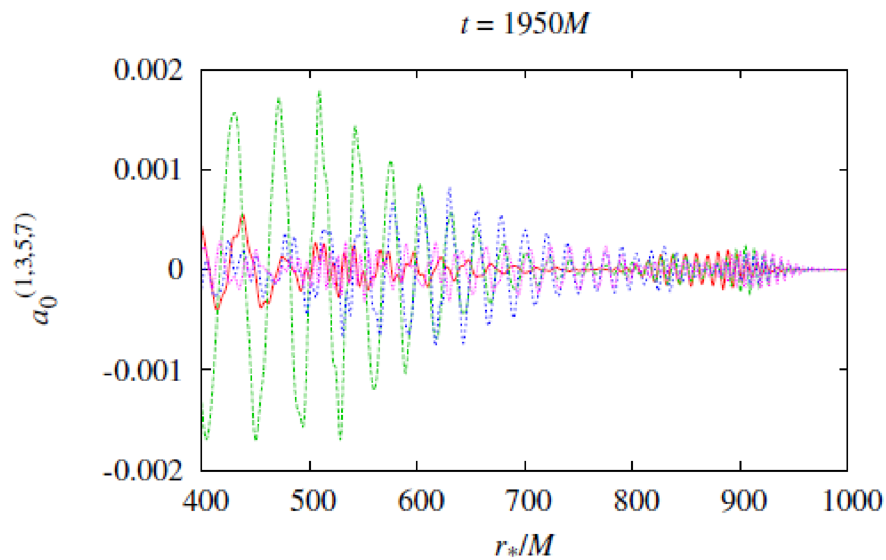

$a_0^{(m)}$: $m = 1, 3, 5, 7$

- After bosenova, the axion cloud soon settle down to a new superradiant phase.

Example of Simulation : $l = m = 2$

- Parameters: $a_* = a/M = 0.99, \quad \mu M$ =0.80
- Initial mode: pure $(l, m, nr) = (1, 1, 0), \Phi/f_a = 1.0$

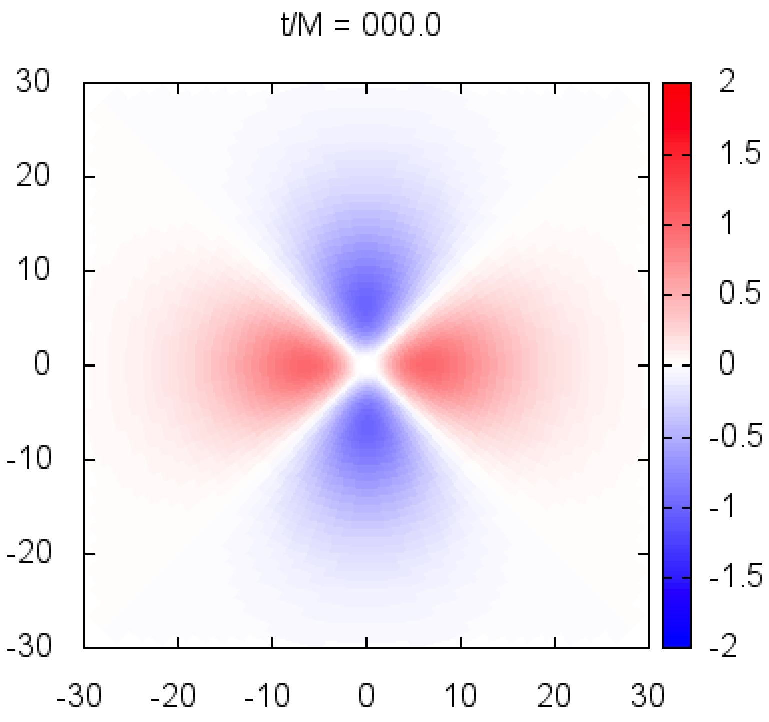

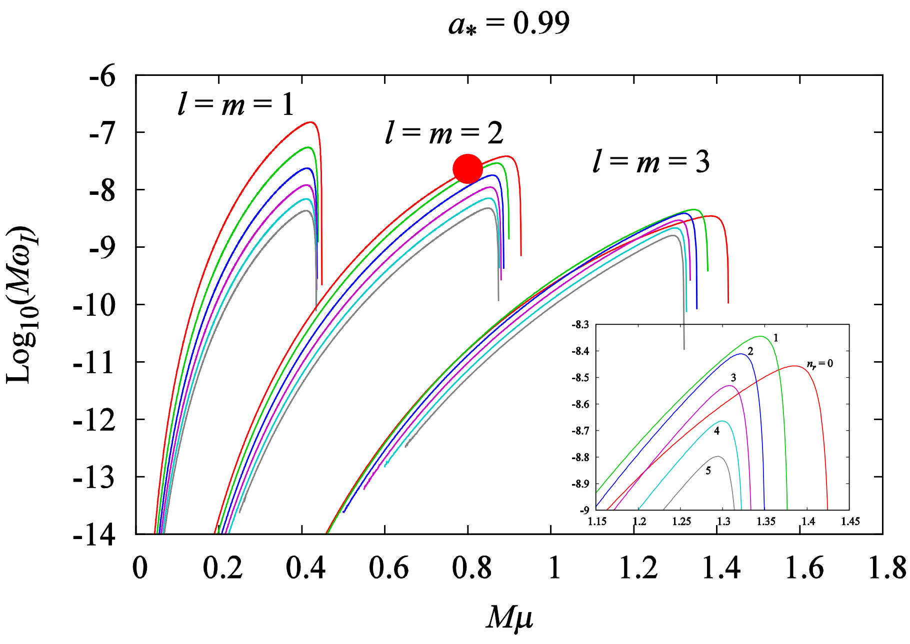

Results

- Due to nonlinear self-interactions, the cloud position and shape show periodic modulations, but no violent phenomenon like bosenova happens.

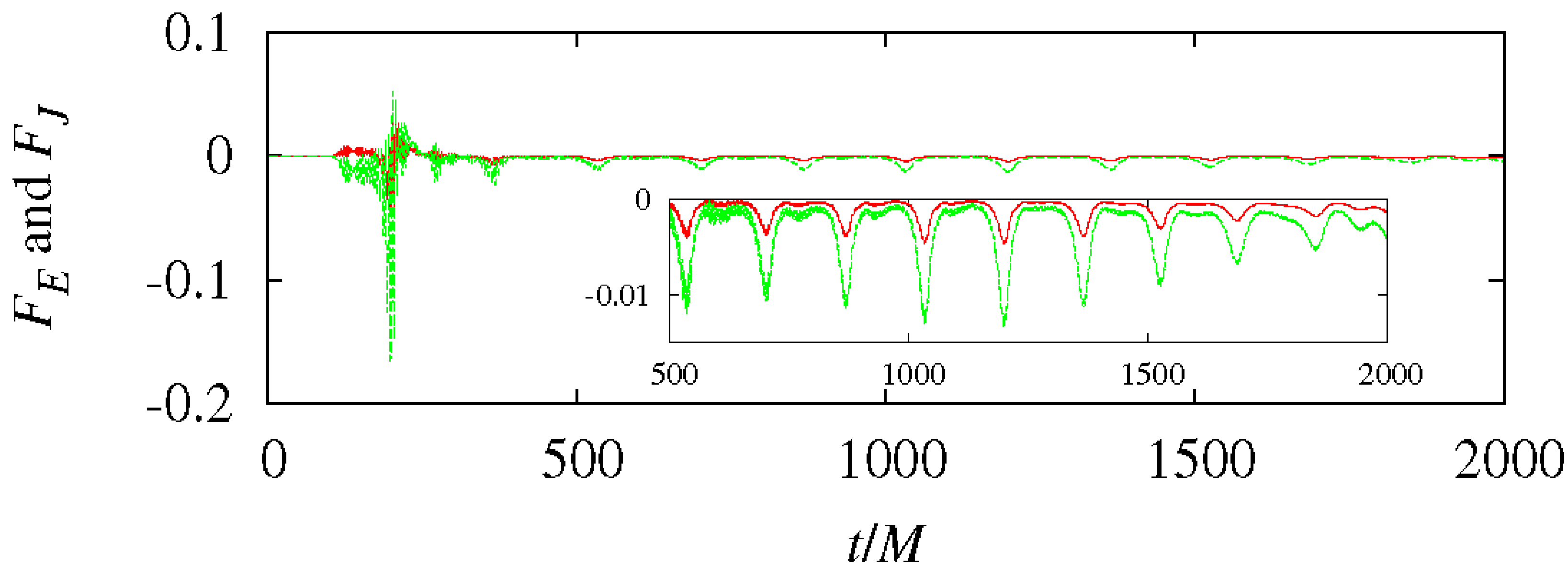

- Instead, the cloud continuously lose energy by shedding. Hence, in the realistic setting, the axion cloud stays in a quasi-stationary state with $\mathrm{E_a}/M \simeq 10^{-3}\left(\frac{f_a}{10^{16}\ \mathrm{GeV}}\right)^2$, for which the SR energy supply and the shedding energy loss (and GW emission) balance.

4.5 重力波によるアクシオン探査

Gravitational Wave Emissions from Axion Cloud

Long-term Behavior of the Axion-BH System

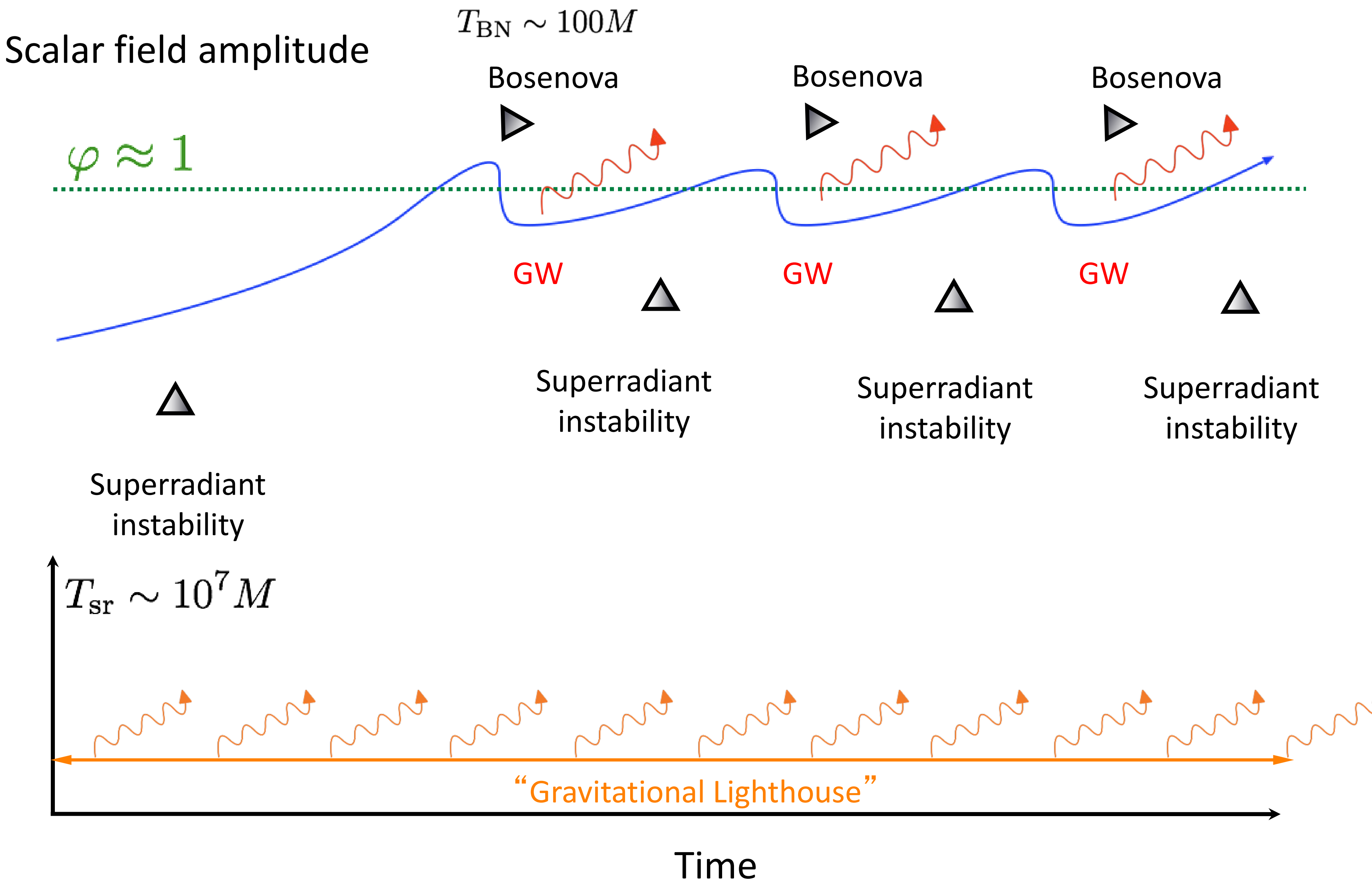

Does GW emissions stop SR instability ?

GW emissions do not hinder the occurrence of the bose nova collapse!!

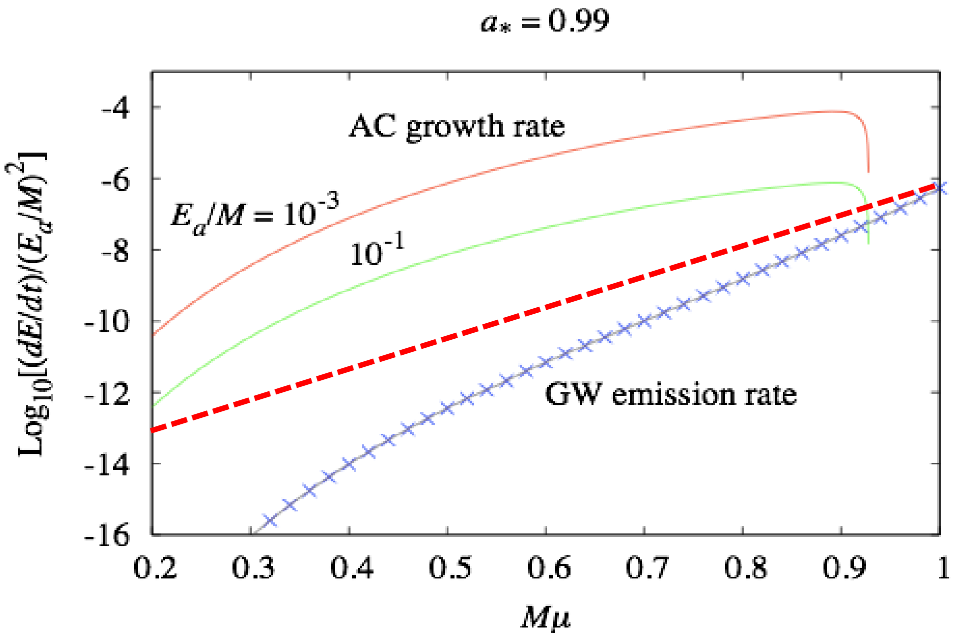

L=m=2 mode

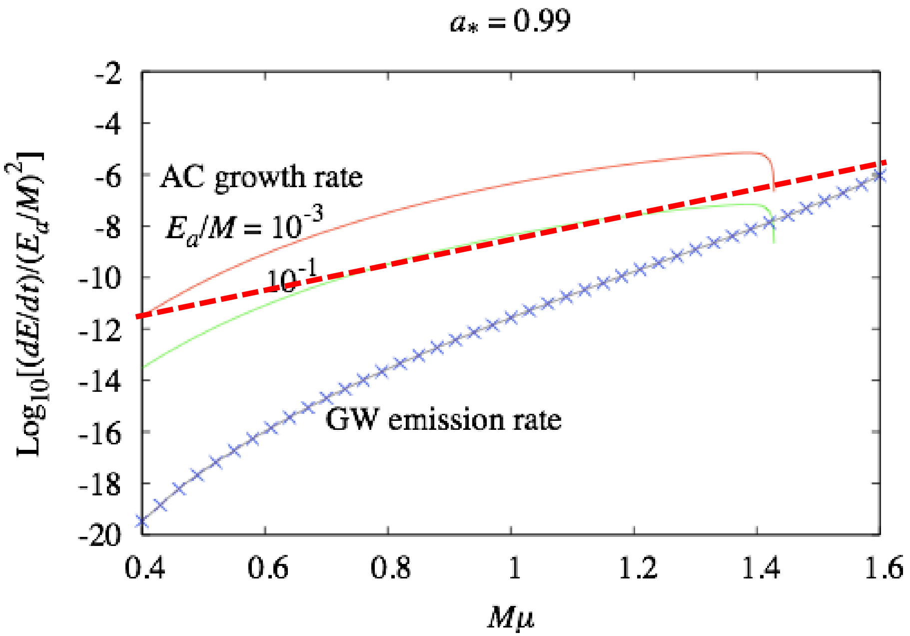

L=m=3 mode

The GW emission rate by the 2 a -> G process of the l=m=1 mode can become 100 times that of the quadrupole formula !!

L=m=1 mode

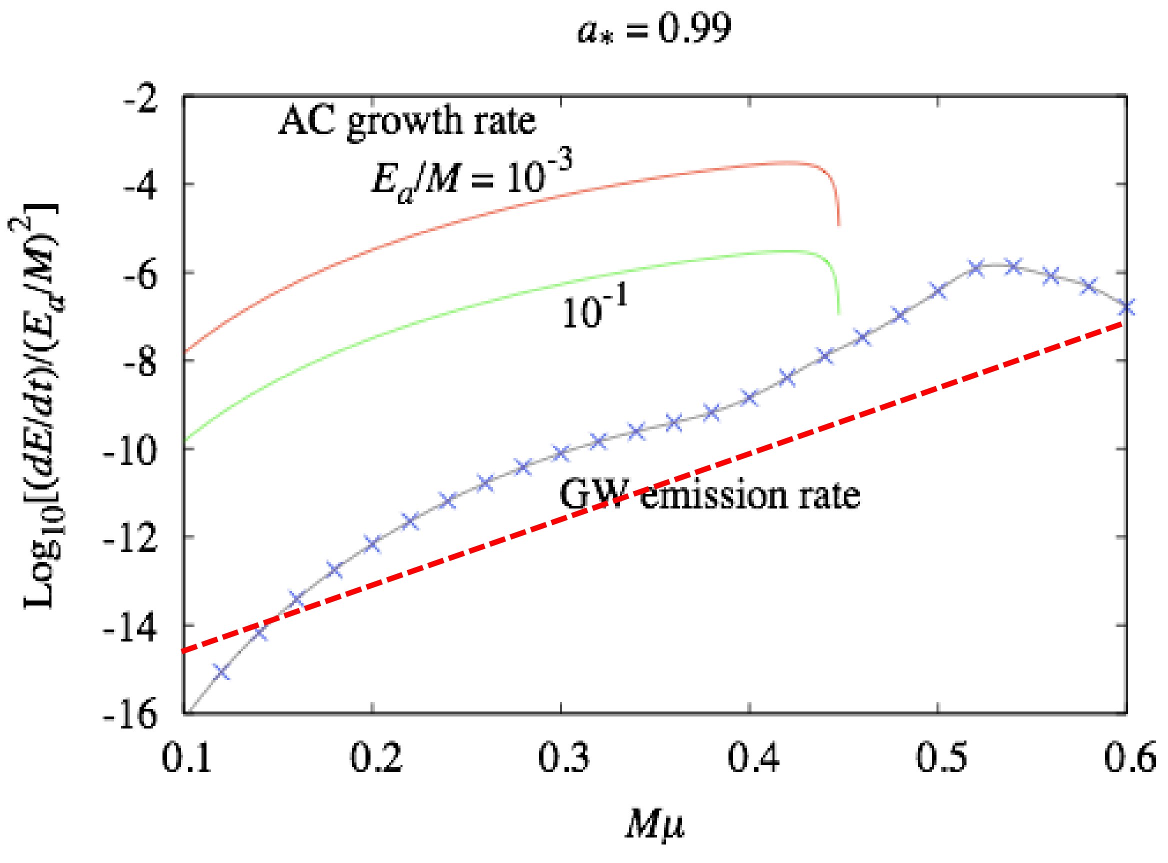

4.5 重力波によるアクシオン探査

Continuous GW Search for Cygnus X-1

Detector Sensitivities

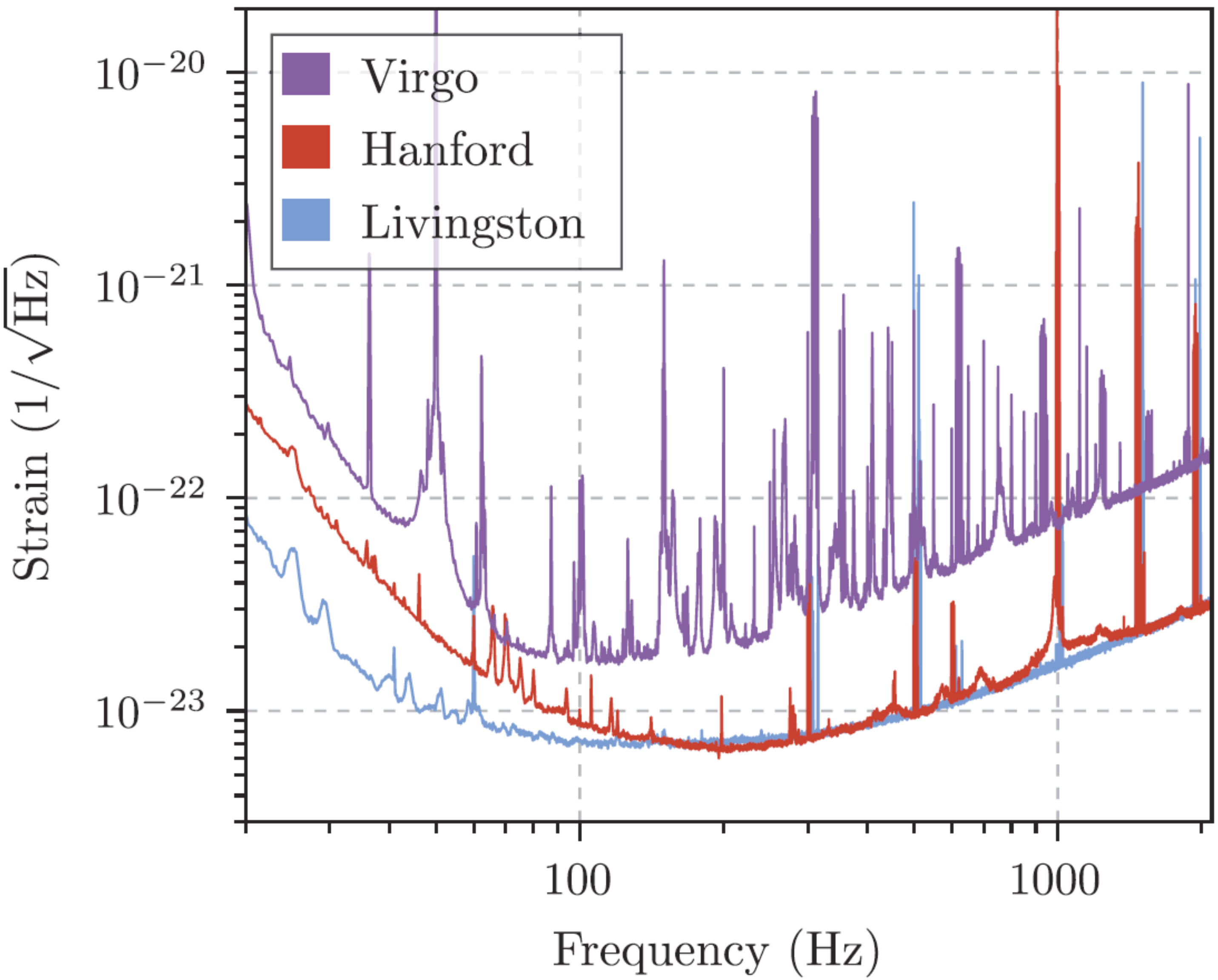

Continuous GW Search by LIGO

PRD87, 042001 (2013)

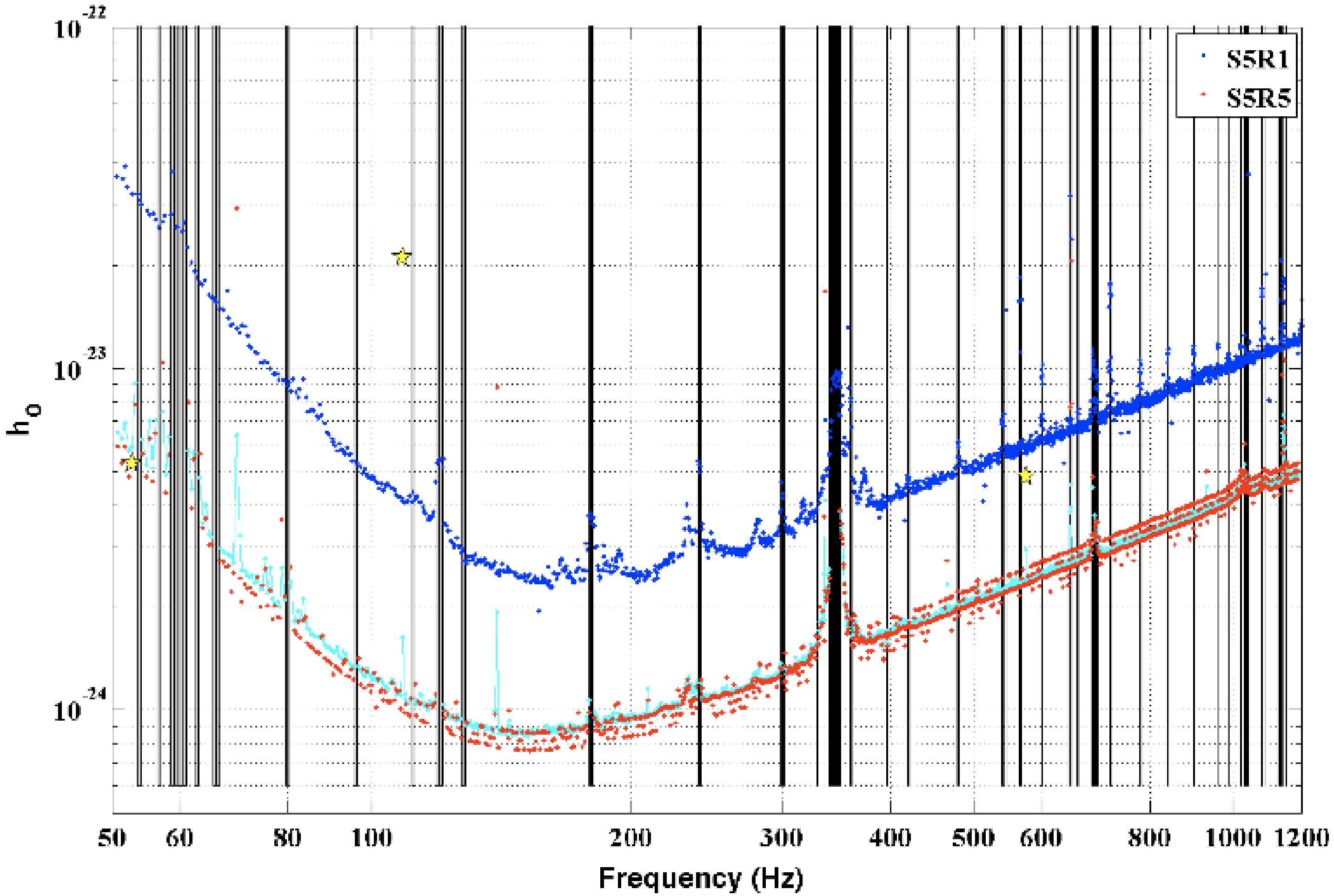

Basic Idea

- Consider continuous waves from BH-axion system

$$50 \text{ Hz} \leq f \leq 1200 \text{ Hz}$$

$$\Leftrightarrow \quad 10^{-13} \text{ eV} \leq \mu \leq 2.4 \times 10^{-12} \text{ eV}$$

- If we assume $M \approx 15 M_\odot$, $0.0125 \leq M\mu \leq 0.3$

$\Rightarrow$ We consider an axion cloud in the $l = m = 1$ mode.
We use the approximate formula for small $M\mu$

$\Rightarrow$ The wave form is the same as the distorted pulsar case

Amplitude: $h_0 \approx \left(\frac{E_a}{M}\right) (\mu M)^6 \left(\frac{M}{d}\right)$

- As E_a, we adopt the value when the nonlinear self-interaction becomes important:

$$\varphi_{\rm max} = \frac{\Phi_{\rm max}}{f_a} \approx \frac{1}{\sqrt{8\pi e^2}} \sqrt{\frac{E_a}{M}} \left(\frac{f_a}{M_p}\right)^{-1} (\mu M)^2 \approx 1$$

$$\Rightarrow \boxed{10^{-22} \left(\frac{f_a}{10^{16}\mathrm{GeV}}\right)^2 \left(\frac{M}{15 M_\odot}\right)^3 \left(\frac{\mu}{10^{-12}\mathrm{eV}}\right)^2 \left(\frac{d}{1\mathrm{kpc}}\right)^{-1} < h_{\rm UL}}$$

- In order to exclude the situation where gravitational backreaction is significant, we require

$$\frac{E_a}{M} < 0.05 \quad \Rightarrow \quad \boxed{\frac{f_a}{10^{16}\mathrm{GeV}} < 0.1 \times \left(\frac{M}{15 M_\odot}\right)^2 \left(\frac{\mu}{10^{-12}\mathrm{eV}}\right)^2}$$

Cygnus X-1

$$M \approx 15 M_{\odot}$$

$$a_* \gtrsim 0.9$$

$$d \approx 1.86 \text{ kpc}$$

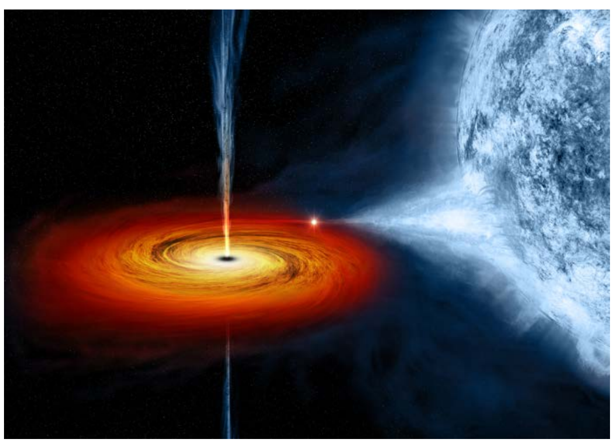

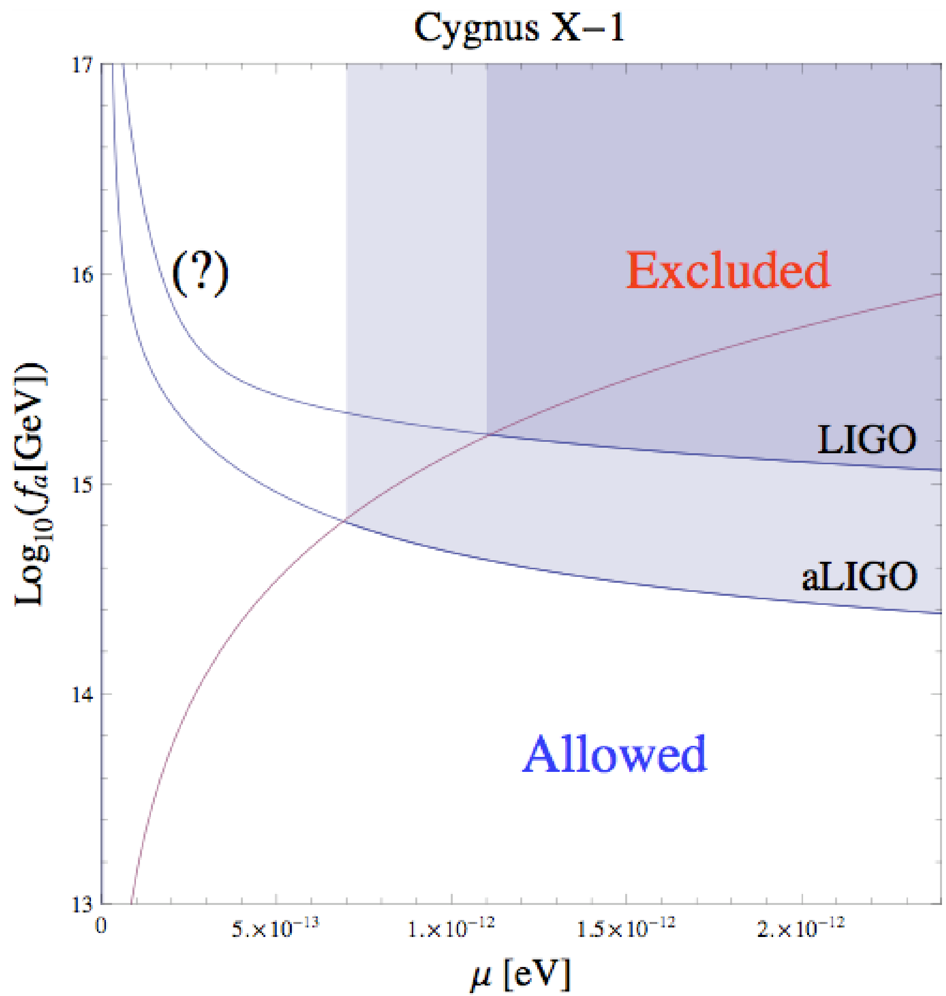

McClintock, et al., arXiv:1106.3688-3690{astro-ph}

Subtleties in Matched Filtering

The method of continuous GW search from deformed pulsars by LIGO cannot be directly applied to our case because isolated pulsars are assumed in their analysis:

- **Modulation due to the orbital motion of Cygnus X-1**
- **Modulation due to non-linearity of the axion cloud.**

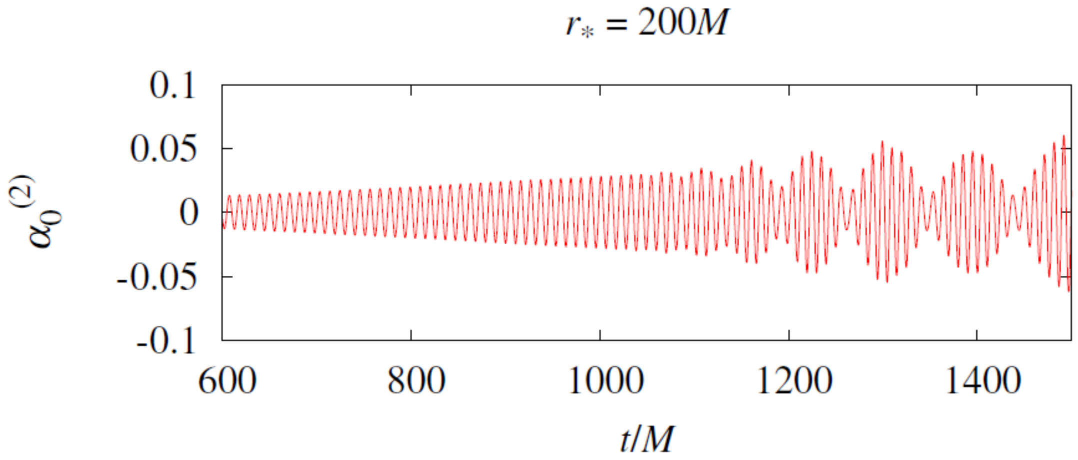

The time variation of a GW amplitude for the l=m=1 simulation

These modulations can be precisely determined by using the results of our direct numerical simulations, and at the same time, they can be smoking gun features to discriminate GWs from the Cygnus X-1 from GWs from deformed pulsars.

Anomaly in the spin statistic of BHs

Black holes satisfying the resonance condition $\mu M \sim 1$ lose spin up to the point at which the SRI time scale is longer than its age.

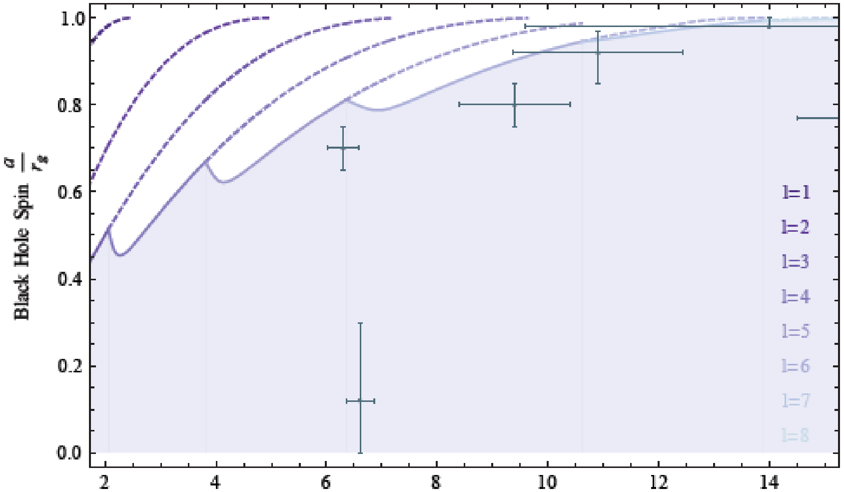

Caveats:

- Matter accretion onto BHs may compensate the loss of the angular momentum of BHs by SRI.
- Self-interactions of the axion field changes the evolution of the axion cloud and the angular momentum loss rate of the BH.

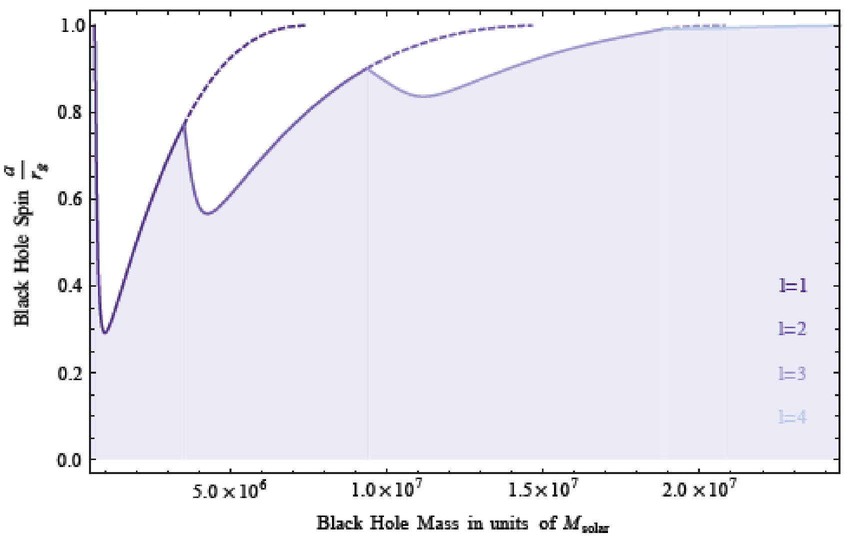

Arvanitaki A, Dubovsky S: PRD83, 044026 (2011)

Spin Limit by Arvanitaki et al

- BHs with spin satisfying the following condition are excluded:

$$\Gamma_{\rm st}\tau_{\rm bh} \geq \log N_{\rm max} \quad \text{or} \quad \Gamma_{\rm sr}\tau_{\rm bh}(N_{\rm BN}/N_{\rm max}) \geq \log N_{\rm BN}$$

  - BH-XRB: τ_{bh} = min(the age, Eddington accretion time).
  - SMBH: τ_{bh} = compact object infalling time

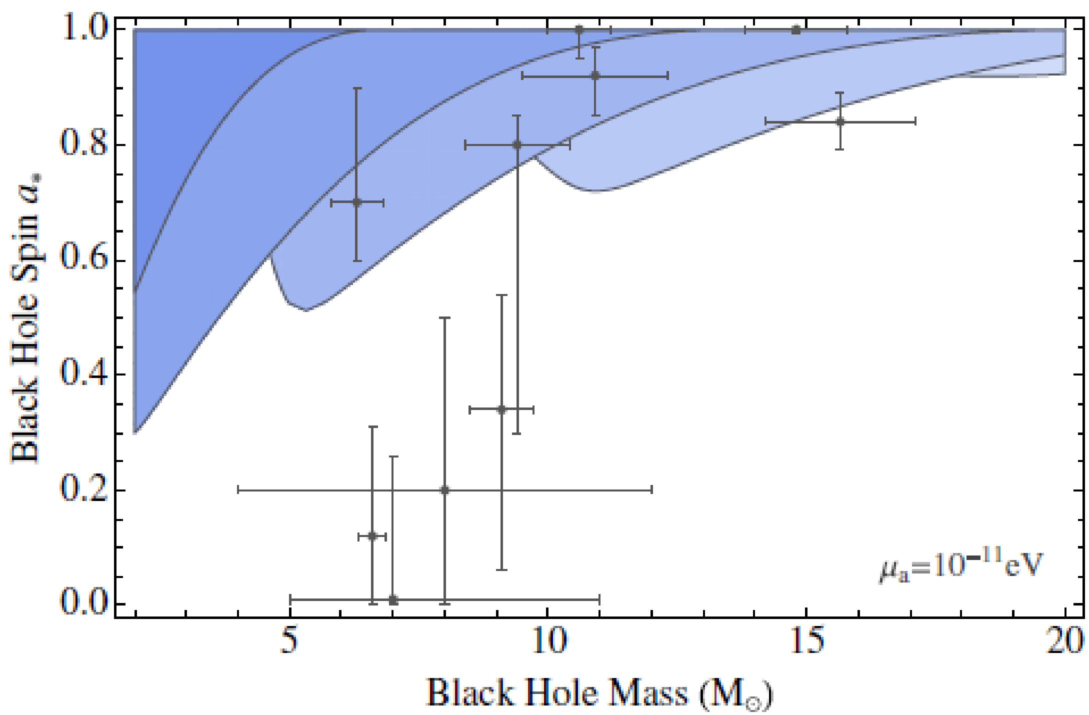

No self-interaction case

Arvanitaki, Baryakhtar, Huang: PRD91, 084011 (2015)

BH data

X-ray Binary BHs

No.	Object	Mass ($M_\odot$)	Spin	Age (yrs)	Period (days)	$M_{\text{comp star}}$ ($M_\odot$)	$\dot{M}/\dot{M}_E$
1	M33 X-7	15.65 ± 1.45	$0.84^{+0.10}_{-0.10}$ [53]	3×10^6 [54]	3.4530 [55]	$\gtrsim 20$ [55]	$\gtrsim 0.1$ [55]
2	LMC X-1	10.91 ± 1.4	$0.92^{+0.06}_{-0.18}$ [56]	5×10^6 [54]	3.9092 [57]	31.79 ± 3.48 [57]	0.16 [57]
3	GRO J1655 − 40	6.3 ± 0.5	$0.72^{+0.16}_{-0.24}$ [53]	3.4×10^8 [58]	2.622 [58]	2.3–4 [58]	$\lesssim 0.25$ [59]
4	Cyg X-1	14.8 ± 1.0	> 0.99 [60]	4.8×10^6 [61]	5.599829 [54]	17.8 [54]	0.02 [54]
5	GRS1915 + 105	10.1 ± 0.6	> 0.95 [53,62]	4×10^9 [63]	33.85 [64]	0.47 ± 0.27 [64]	$\gtrsim 1$ [64].

[a]We thank J. Steiner and J. McClintock for providing the latest 2σ errors on the spin measurements.

SMBHs

No.	Object	Mass ($10^6 M_\odot$)	Spin
1	NGC 3783	29.8 ± 5.4	> 0.88
2	Mrk 110	25.1 ± 6.1	> 0.89
3	MCG-6-30-15	$2.9^{+0.18}_{-0.16}$	> 0.98
4	NGC 4051	1.91 ± 0.78	> 0.99

X-ray Binary BHs

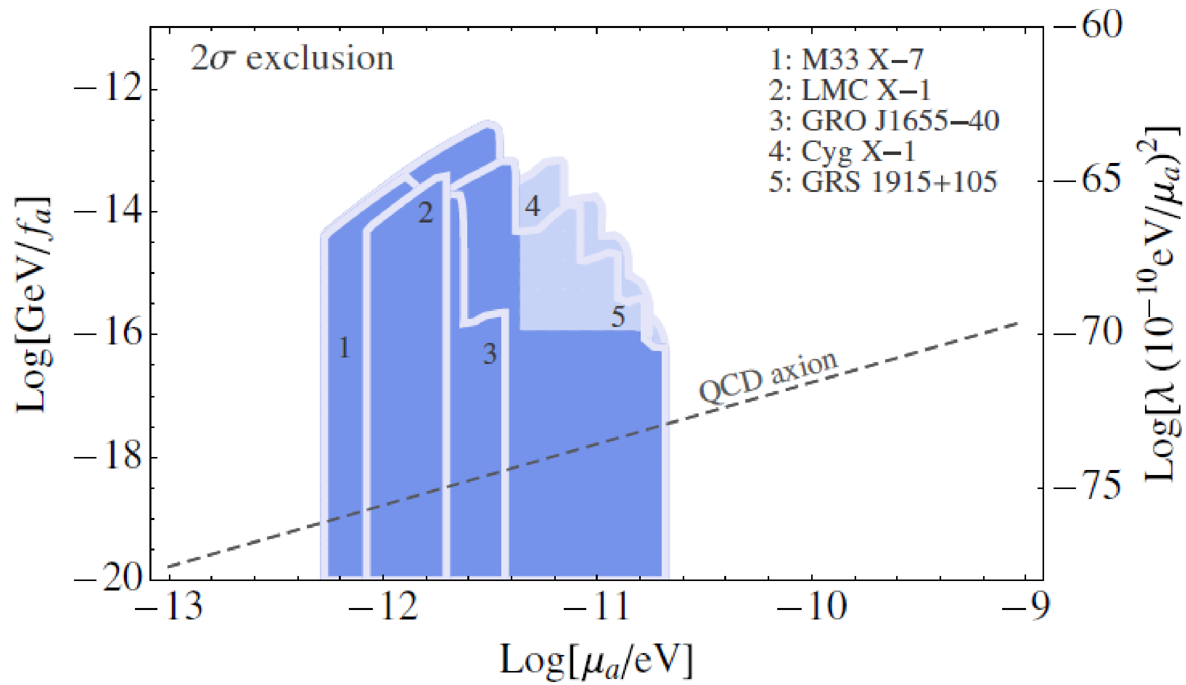

SMBHs

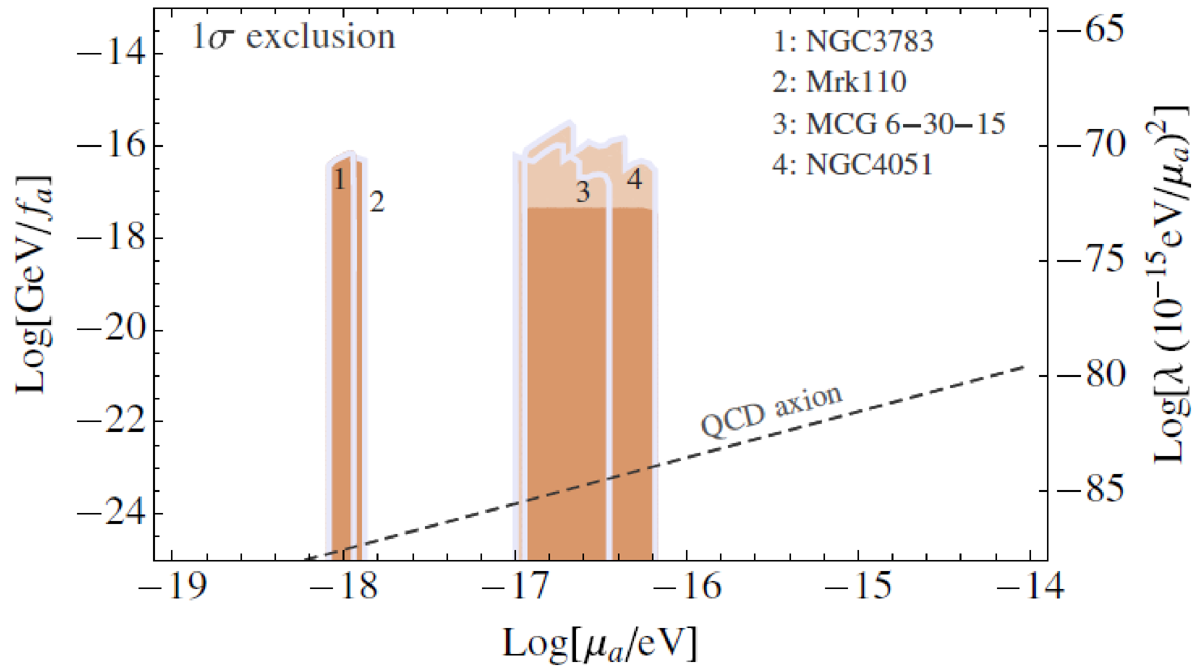

GW Constraint by Cygnus X-1

[Yoshino H, Kodama H: PTEP 2015, 061E01

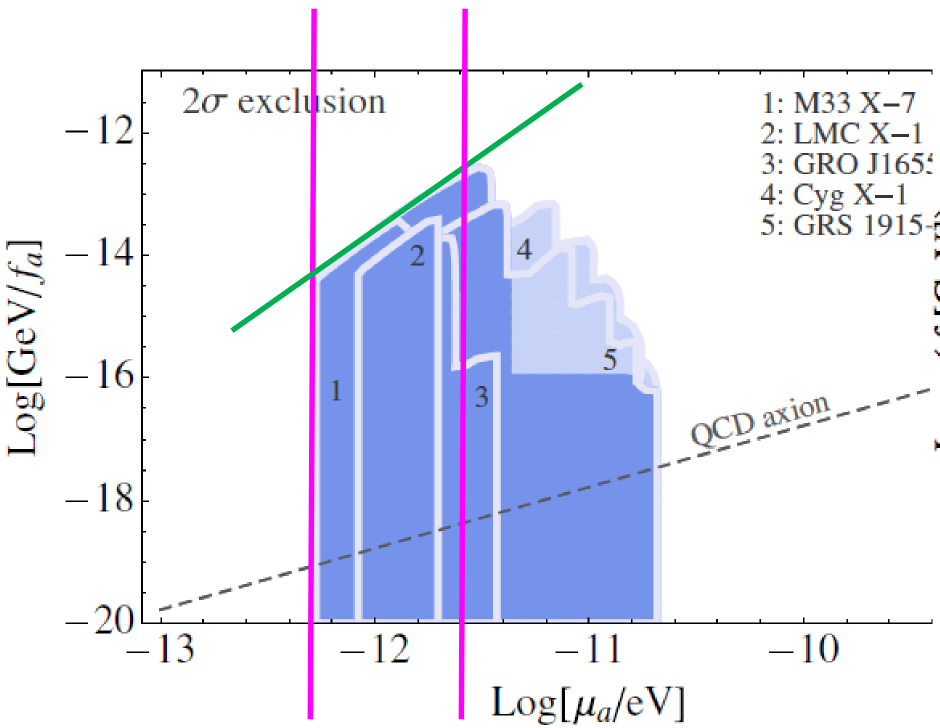

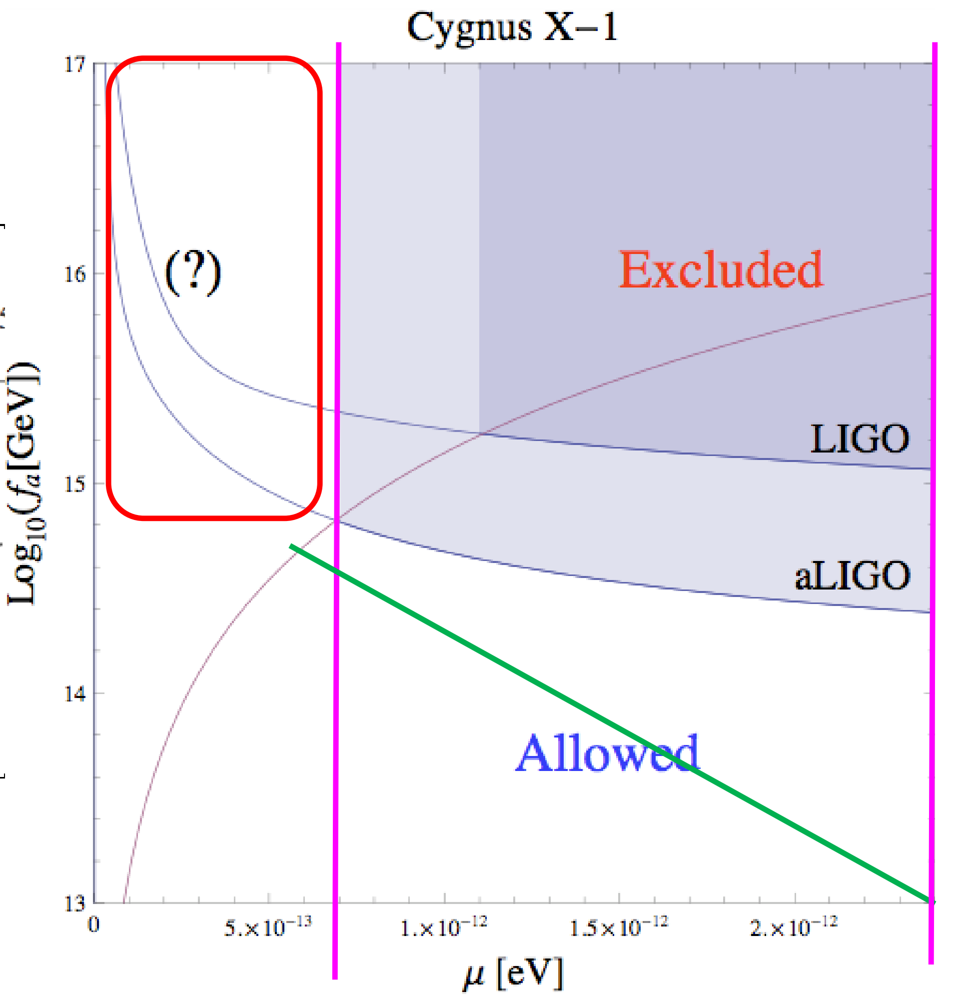

様々な時間スケール

- スピンパラメータ: $a_* = \frac{a}{M} = \frac{J}{M^2} = \frac{2X}{X^2+1}$
- SRIが起きる条件($\mu M \ll 1$)

$$t > \tau_{\rm SR} = \frac{GM}{c^3} \frac{\gamma_{nl} \alpha_g^{-(4l+5)}}{mX - 2\alpha_g} \quad \Leftrightarrow \quad mX \geq 2\alpha_g + \frac{10^{-23}}{t/t_0} \left(\frac{M}{M_\odot} \right) \frac{\gamma_{nl}}{\alpha^{4l+5}}$$

- Bosenovaが起きる条件

$$\frac{E_a(BN)}{M} = \frac{\epsilon_0}{\alpha_g^4}; \quad \epsilon_0 = 5.59 \times 10^{-5} \left(\frac{0.67}{\Phi_{\rm max}/f_a} \right)^2 f_{a,16}^2, \quad f_{a,16} = \frac{f_a}{10^{16}{\rm GeV}}$$

$$t > t_{\rm BN} = \frac{\tau_{\rm SR}}{2} \ln \frac{E_a(BN)}{\mu} \quad \Leftrightarrow \quad mX \gtrsim 2\alpha_g + \frac{10^{-21}}{t/t_0} \left(\frac{M}{M_\odot} \right) \frac{\gamma_{n\ell}}{\alpha_g^{4\ell+5}} \times \left\{ 1 + \frac{1}{165} \log \frac{f_{a,16}^2}{\alpha_g^5} \left(\frac{M}{M_\odot} \right)^2 \right\}$$

- スピンパラメータが大きく変化しない条件
  - 非線形効果を無視した場合

$$\dot{J} = \frac{m}{\omega}\dot{M} \quad \Leftrightarrow \quad \frac{\dot{a}_*}{a_*} = -\frac{E_a/M}{\tau_{\rm SR}/2}\left(\frac{m}{\alpha_g}\frac{X^2+1}{2X} - 2\right)$$

➡ $$mX \lesssim 2\alpha_g + \frac{8.7\cdot 10^{-22}}{t/t_0}\left(\frac{M}{M_\odot}\right)\frac{\gamma_{n\ell}}{\alpha_g^{4\ell+5}}\left\{1 + \frac{1}{175}\log\frac{(M/M_\odot)^2}{m/a_* - 2\alpha_g}\right\}$$

  - Bose novaが起きる場合　（複雑なので省略）

- スピンパラメータの減少を降着円盤により補給できる条件

$$L_{\rm Edd} \geq L = \eta_e \dot{E}, \quad \dot{E} = \eta_{\rm disk}\frac{c^3}{GM}\dot{J}_{\rm SR}$$

➡ $$\ell X \leq 2\alpha_g + 1.70\times 10^{-22}\frac{\gamma_{n\ell}}{\eta\ell\epsilon_0}\frac{1}{\alpha_g^{4\ell}}\frac{M}{M_\odot}.$$

$$\eta = \eta_{\rm e}\eta_{\rm disk} f_{\rm NL} \approx 0.01\times 0.1\times 1 = 10^{-3}$$

Constraints in the a_*-α plain: Cyg X-1

$f_a = 10^{16}$ GeV: $M = 15\, M_\odot$, $t = 5 \times 106$ yrs

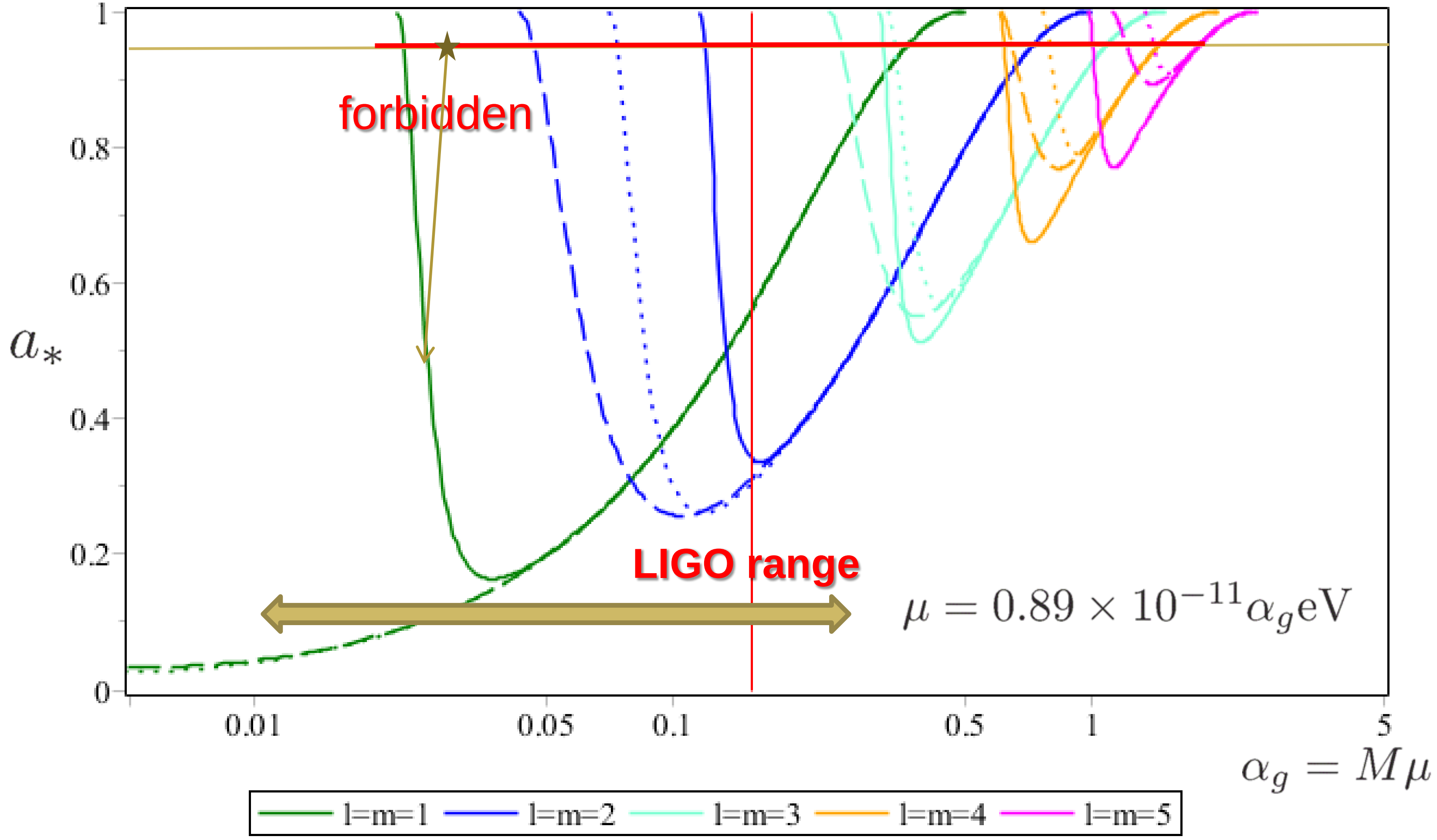

Solid line: $t = t_{BN}$, Dashed line: $t = ta_{*}$, Dotted line: $L_{disk} > L_{Edd}$

$f_a = 10^{13}$GeV: $M = 15\, M_\odot$, $t = 5 \times 106$ yrs

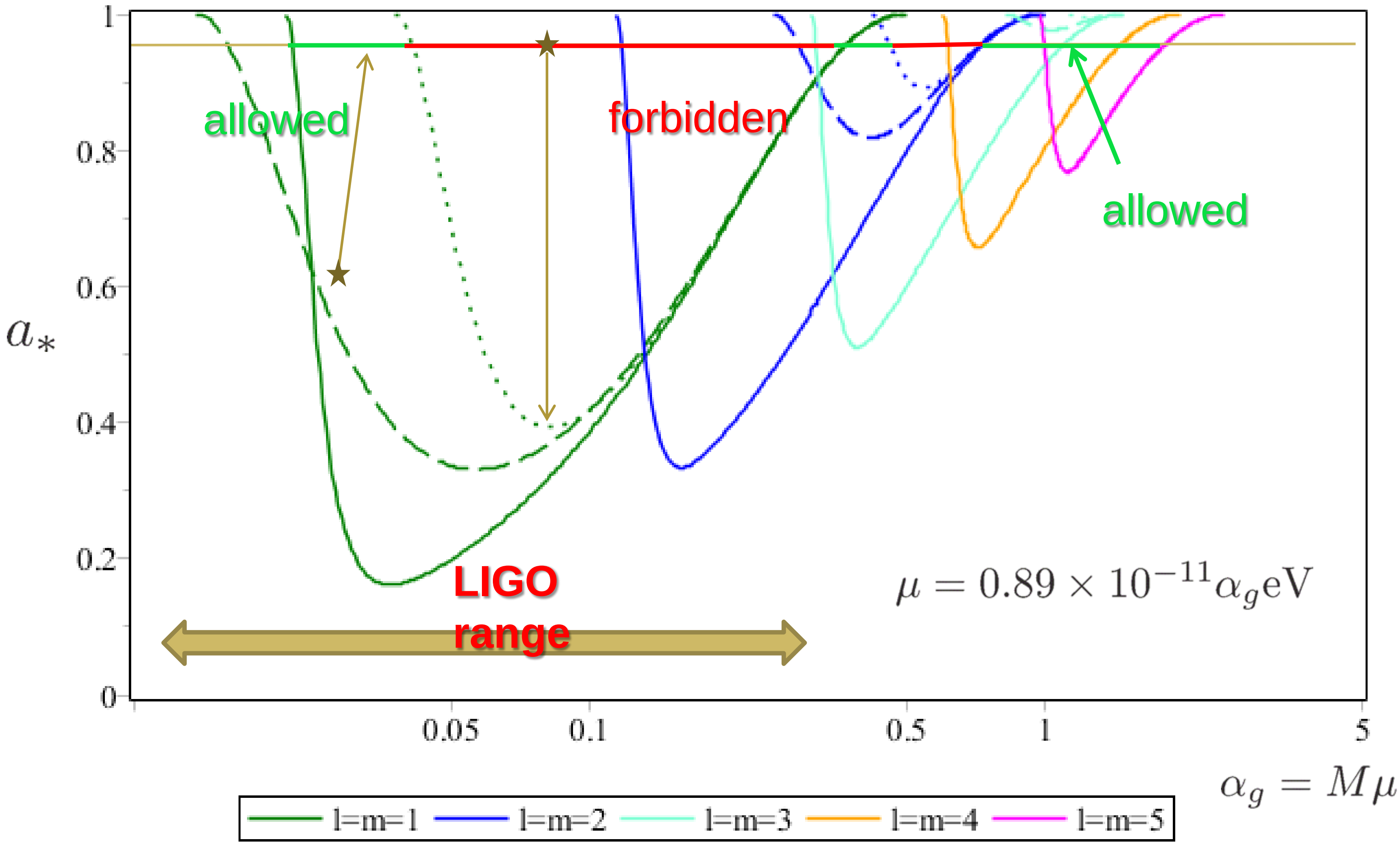

Solid line: $t = t_{BN}$, Dashed line: $t = ta_*$, Dotted line: $L_{disk} > L_{Edd}$

GW Bursts from Bosenova – preliminary calculation –

GWs from a Strongly Nonlinear Cloud

Schwarzschild Background: $l = m = 1, n_r = 0, \ \Phi_{peak}/fa = 0.5$

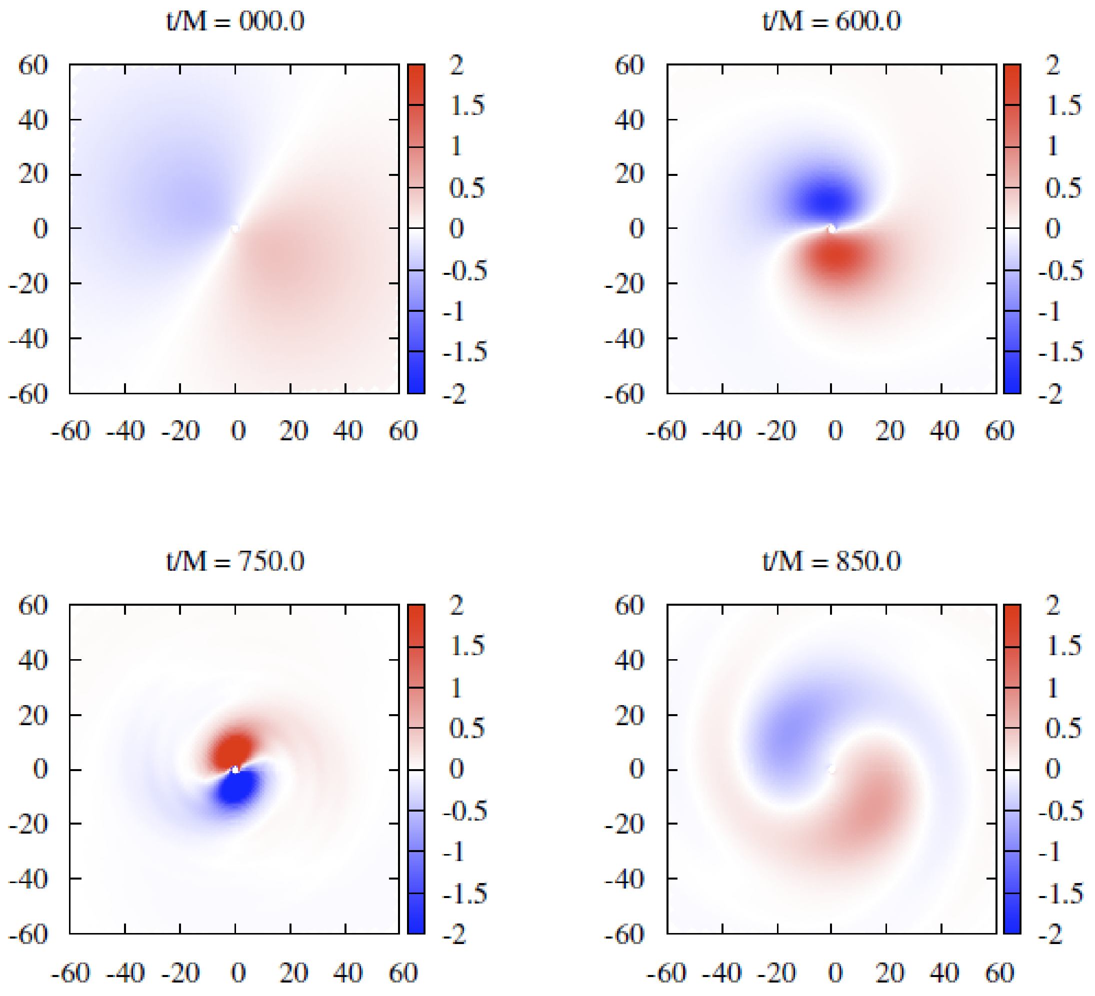

Bosenova happens around t=800M as in the Kerr BG case.

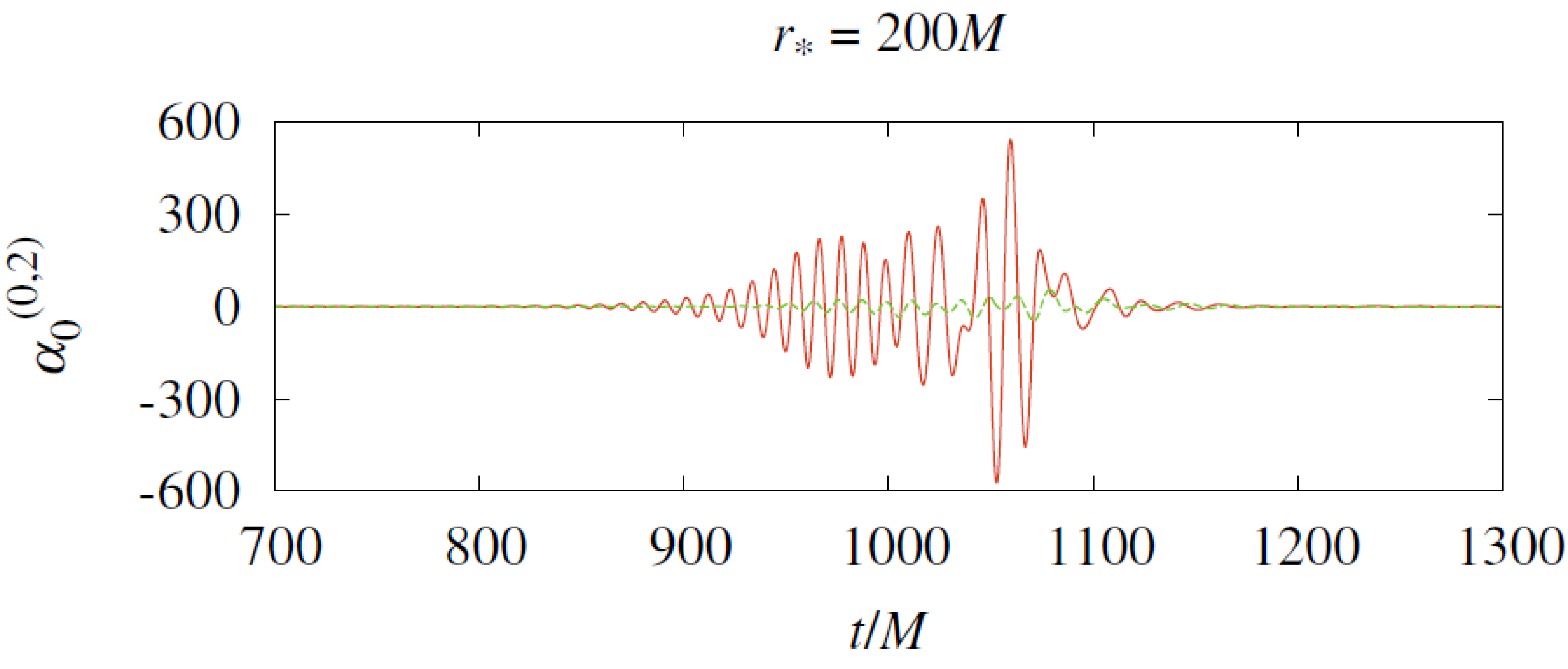

The amplitude of GW grows exponentially around the bosenova collapse and reaches 10^4 times the initial amplitude.

Constraints in the a_*-α plain: Massive BH

$f_a = 10^{15}\text{GeV}$: $M = 10^6\, M_\odot$, t = cosmic age

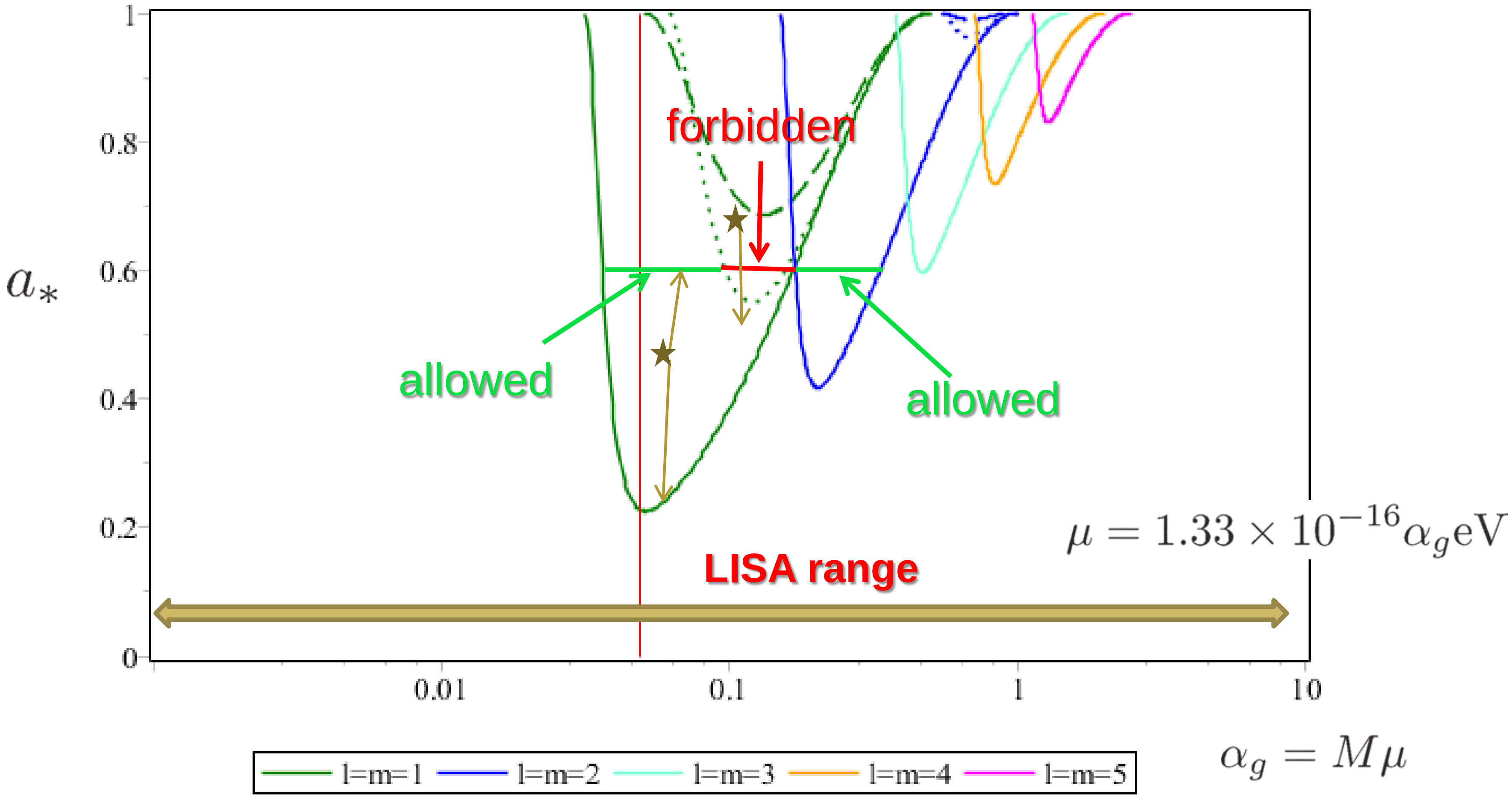

Solid line: $t = t_{BN}$,   Dashed line: $t = ta_{*}$, Dotted line: $L_{disk} > L_{Edd}$

Bosenova GWs from Sgr A*

Sagittairus A*

$$M \approx 10^6 M_\odot, \quad d \approx 8\text{kpc}$$

$$\Delta t \approx 100M \approx 500 \text{ s}$$

$$\Rightarrow \quad h\Delta t^{1/2} \approx 10^{-17}\text{Hz}^{-1/2}$$

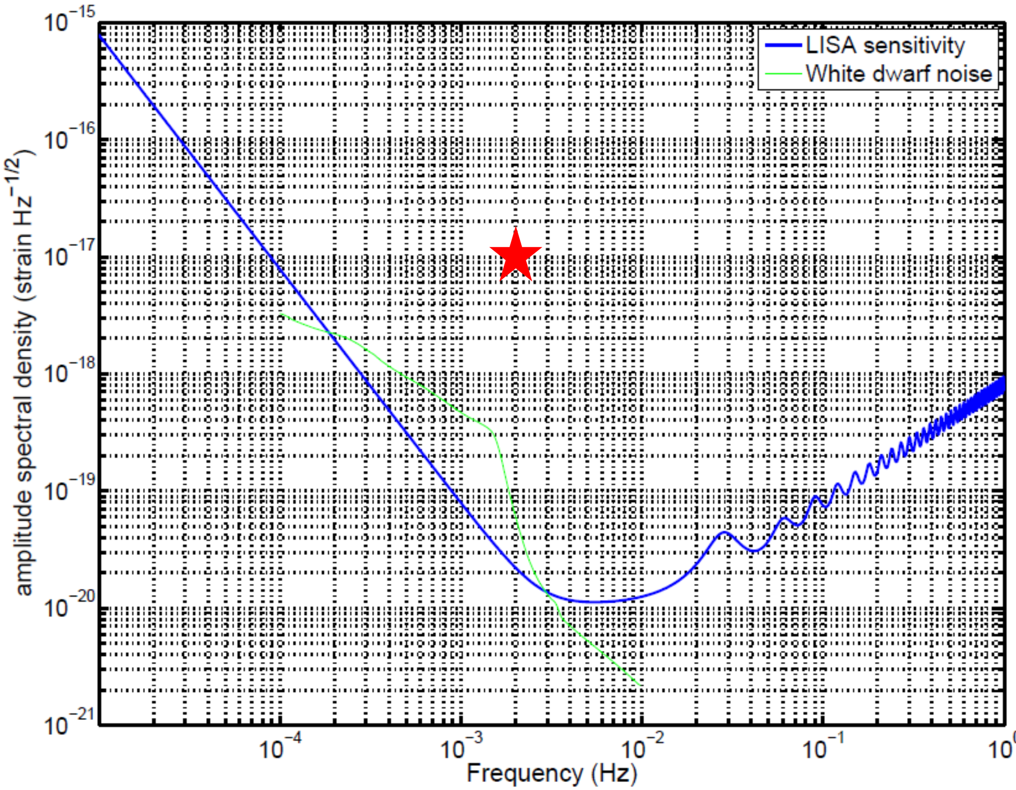

LISA sensitivity curve

$$\mu = 1.33 \times 10^{-16}\text{eV} \left(\frac{\alpha_g}{M/10^6 M_\odot} \right),$$

$$f = \frac{\mu}{2 \times 10^{-15}\text{eV}}\text{Hz} = 6.65 \times 10^{-2}\text{Hz} \left(\frac{\alpha_g}{M/10^6 M_\odot} \right)$$

4. 6 ガンマ線天文学によるアクシオン探査

ガンマ線ホライズン

Gamma-Ray Horizon

Optical depth against CBR

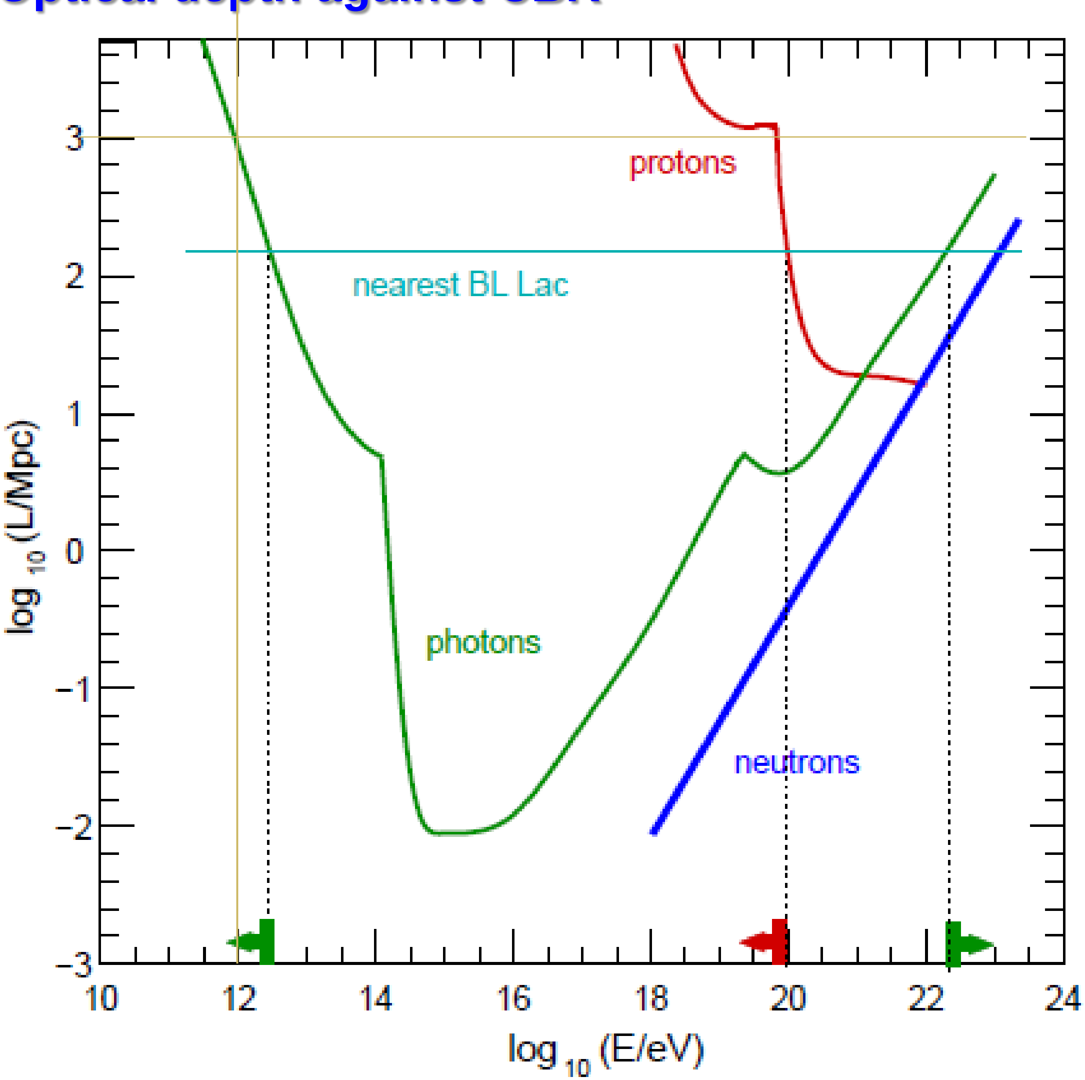

GZK cut-off

$$p + \gamma \to p + \pi^0, \; n + \pi^+$$

$$E_p \gtrsim 10^{20}\mathrm{eV}$$

γ–γ opacity

$$\gamma + \gamma \to e^+ + e^-$$

$$\omega_{\mathrm{HE}\gamma} \geq \frac{2.5\times10^{11}\mathrm{eV}^2}{\omega_{\mathrm{BG}\gamma}}$$

Fairbairn, Rashba, Troitsky: PRD84, 25019 (2011); Roncadelli, de Angelis, Mansutti 2009

Deformation of the Gamma Ray Spectrum

L

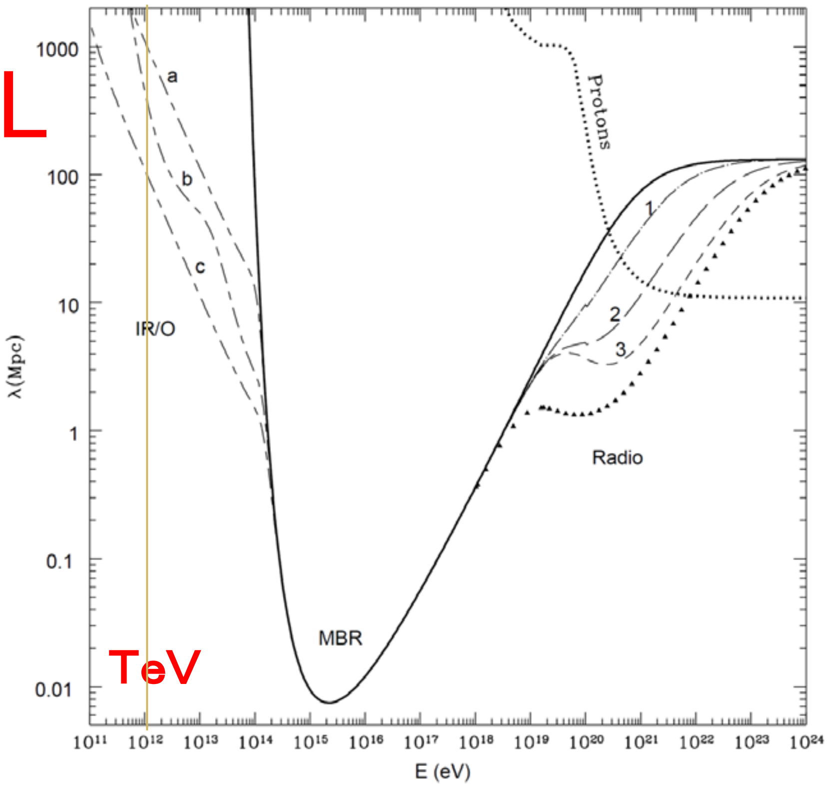

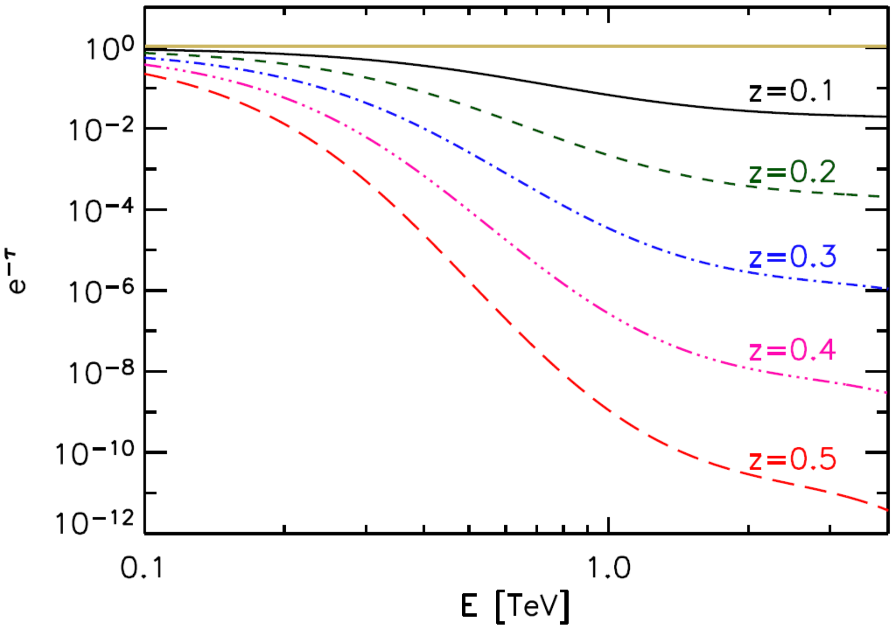

M Simet, D Hooper, PD Serpico: PRD 77, 063001 (2008)

PS Coppi and AF Aharonian: ApJ 487, L9 (1997).

$$z = 0.1 \Leftrightarrow L \simeq 430\ Mpc$$

$$a \quad : \quad \epsilon^2 n(\epsilon, 0) = 10^{-3} \mathrm{eV/cm^3}$$

$$c \quad : \quad \epsilon^2 n(\epsilon, 0) = 10^{-2} \mathrm{eV/cm^3}$$

$$\text{Cf.} \quad \rho_{\mathrm{CMB}} = 0.26\, \mathrm{eV/cm^3}$$

Observation of EBL absorption in the spectra of AGNs

- HESS observation: power-law fitting
  - Two blazars with strong absorption were observed.
- Fermi-LAT observation: power-law fitting

  [Ackermann at al (Fermi Coll): Science 338, 1190 (2012)]

  The spectral deformation due to absorption has been observed for 150 blazars of BL Lac type.

  (z=0.03 -1.6, E= 40GeV – 100 GeV)
- Multi-frequency observation: synchrotron/SSC model

  [Dominguez et al: apj770, 88 (2013)]

  Opacity around a TeV range is determined by observations of 15 blazars from radio to Gamma-ray (Fermi-LAT & IACTs).

  The opacity is consistent with the minimum EBL model.

  (z=0.031 – 0.5, E=200 GeV – 10 TeV)

Detection of the Absorption by Fermi

Sample: 150 blazers of BL Lac type (z=0.03 -1.6, E= 40GeV – 100 GeV)

Fig. 1. Measurement, at the 68 and 95% confidence levels (including systematic uncertainties added in quadrature), of the opacity $\tau_{\gamma\gamma}$ from the best fits to the Fermi data compared with predictions of EBL models. The plot shows the measurement at $z \approx 1$, which is the average redshift of the most constraining redshift interval (i.e., $0.5 \leq z < 1.6$). The Fermi-LAT measurement was derived combining the limits on the best-fit EBL models. The downward arrow represents the 95% upper limit on the opacity at $z = 1.05$ derived in (*13*). For clarity, this figure shows only a selection of the models we tested; the full list is reported in table S1. The EBL models of (*49*), which are not defined for $E \geq 250/(1 + z)$ GeV and thus could not be used, are reported here for completeness.

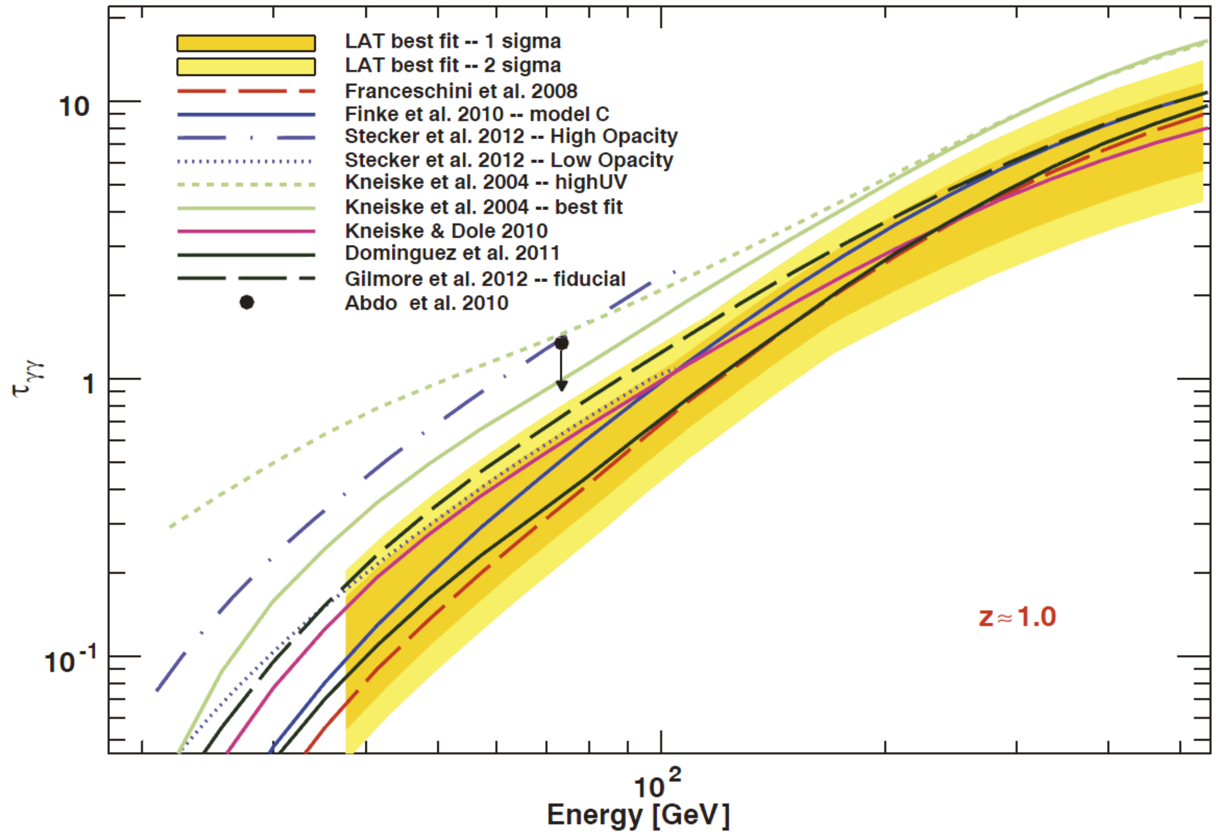

Ackermann at al (Fermi Coll): Science 338, 1190 (2012)

Observed CGRH : Eo(z)

Dominguez et al: apj770, 88 (2013)

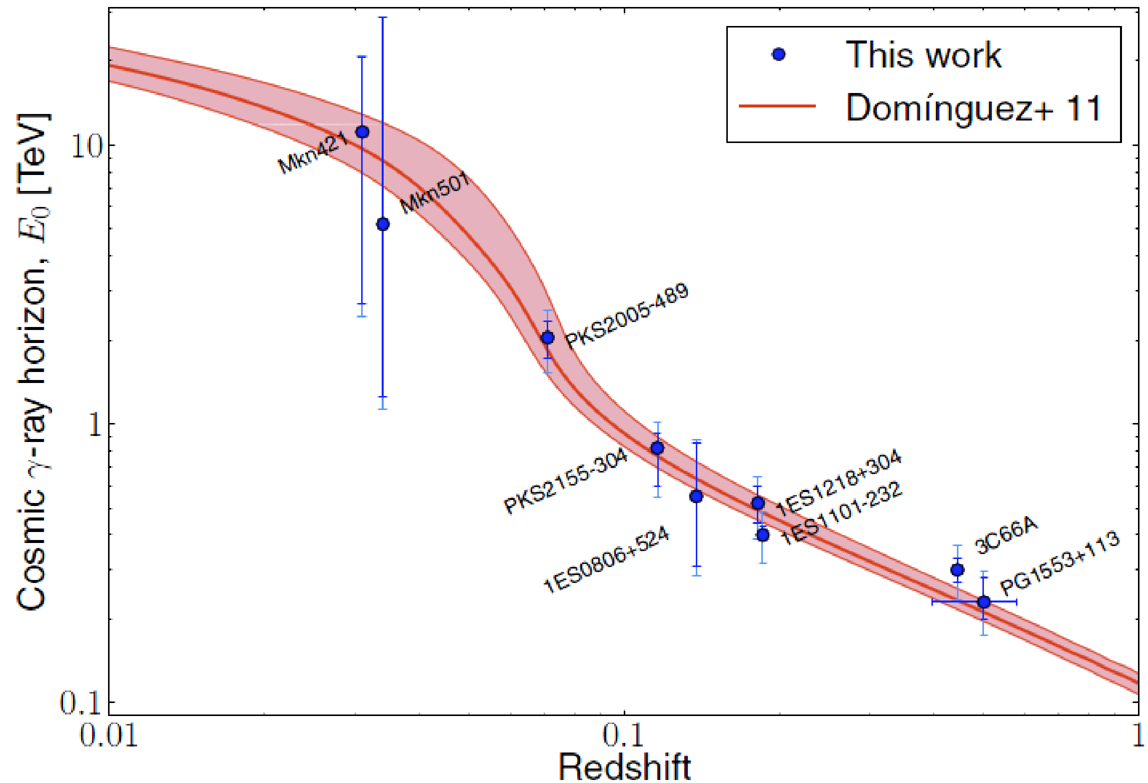

Figure 2. Estimation of the CGRH from every blazar in our sample plotted with blue circles. The statistical uncertainties are shown with darker blue lines and the statistical plus 20% of systematic uncertainties are shown with lighter blue lines. The CGRH calculated from the EBL model described in Domínguez et al. (2011a) is plotted with a red thick line. The shaded regions show the uncertainties from the EBL modeling, which were derived from observed data.

宇宙赤外線背景放射

EBL models and measurements

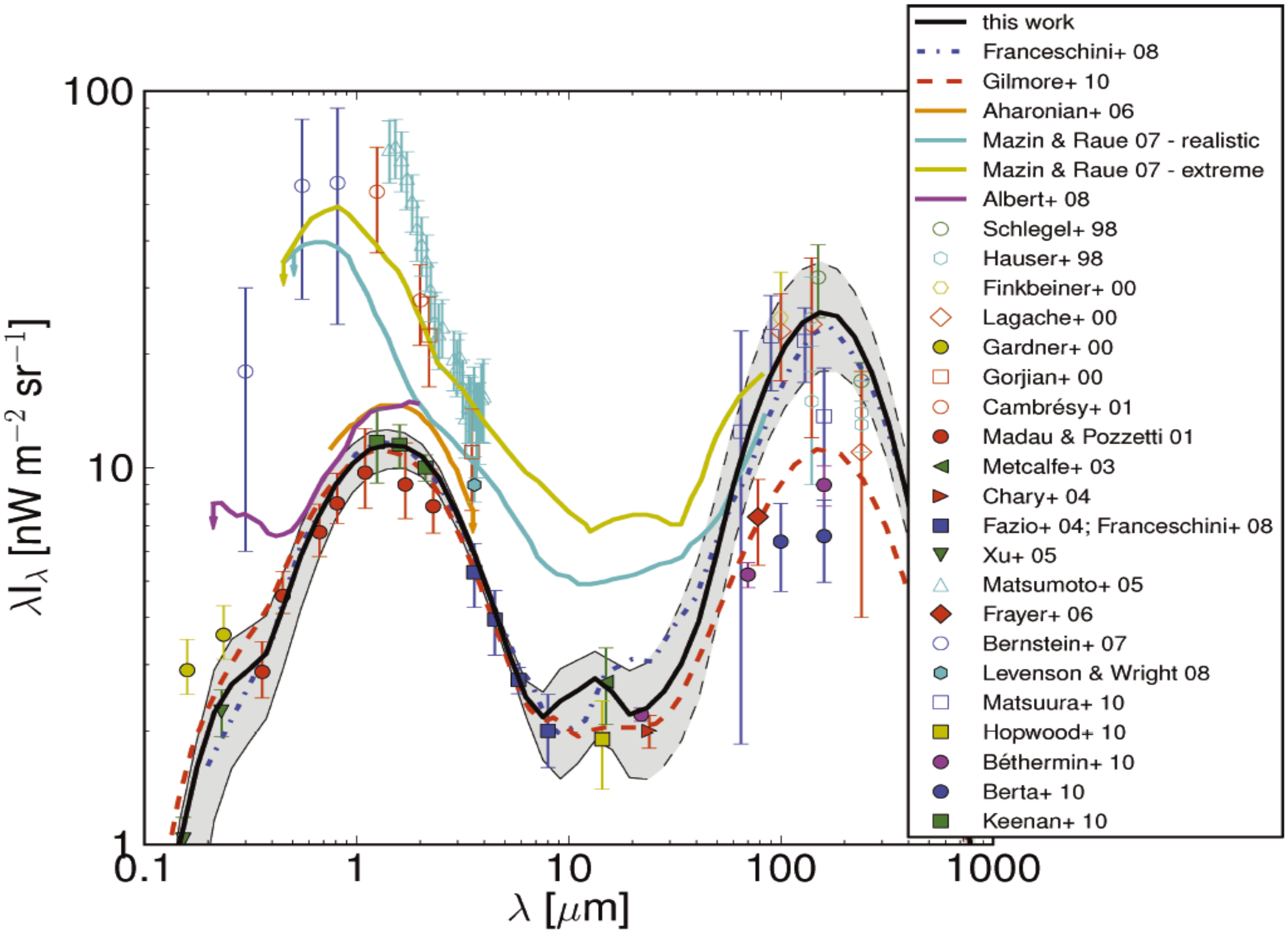

Dominguez A et al: mnras 410, 2556 (2011)

CIBER

JAXA ISAS

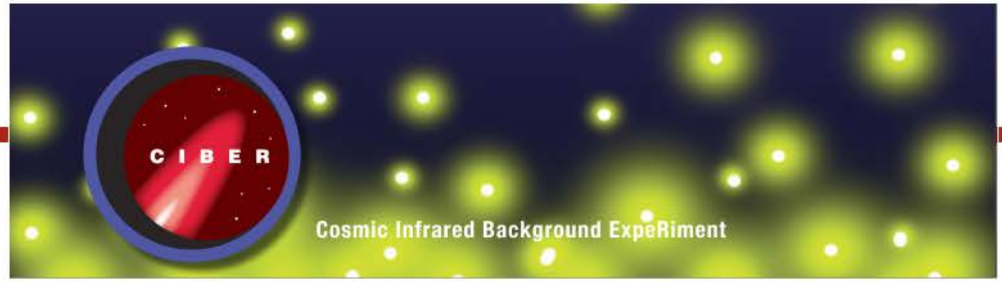

The CIBER Collaboration

Jet Propulsion Laboratory
California Institute of Technology

John Battle
Jamie Bock
Viktor Hristov
Anson Lam
Phil Korngut
Peter Mason
Michael Zemcov

Asantha Cooray
Joseph Smidt
Matt Weiss

Brian Keating
Tom Renbarger

JAXA Japan Aerospace Exploration Agency

Shuji Matsuura
Toshiaki Arai
Kohji Tsumura
Mai Shirahata
Takehiko Wada

SEOUL NATIONAL UNIVERSITY

Min Gyu Kim

Korea Astronomy and Space Science Institute

Dae Hee Lee
Uk Won Nam

ASIAA

Toshio Matsumoto

Axion Cosmophysics AIU2012, KEK, Nov 6-9, 2012

[From the slides of the talk by S Matsuura at AIU2012]

Observational limits on the NIR background

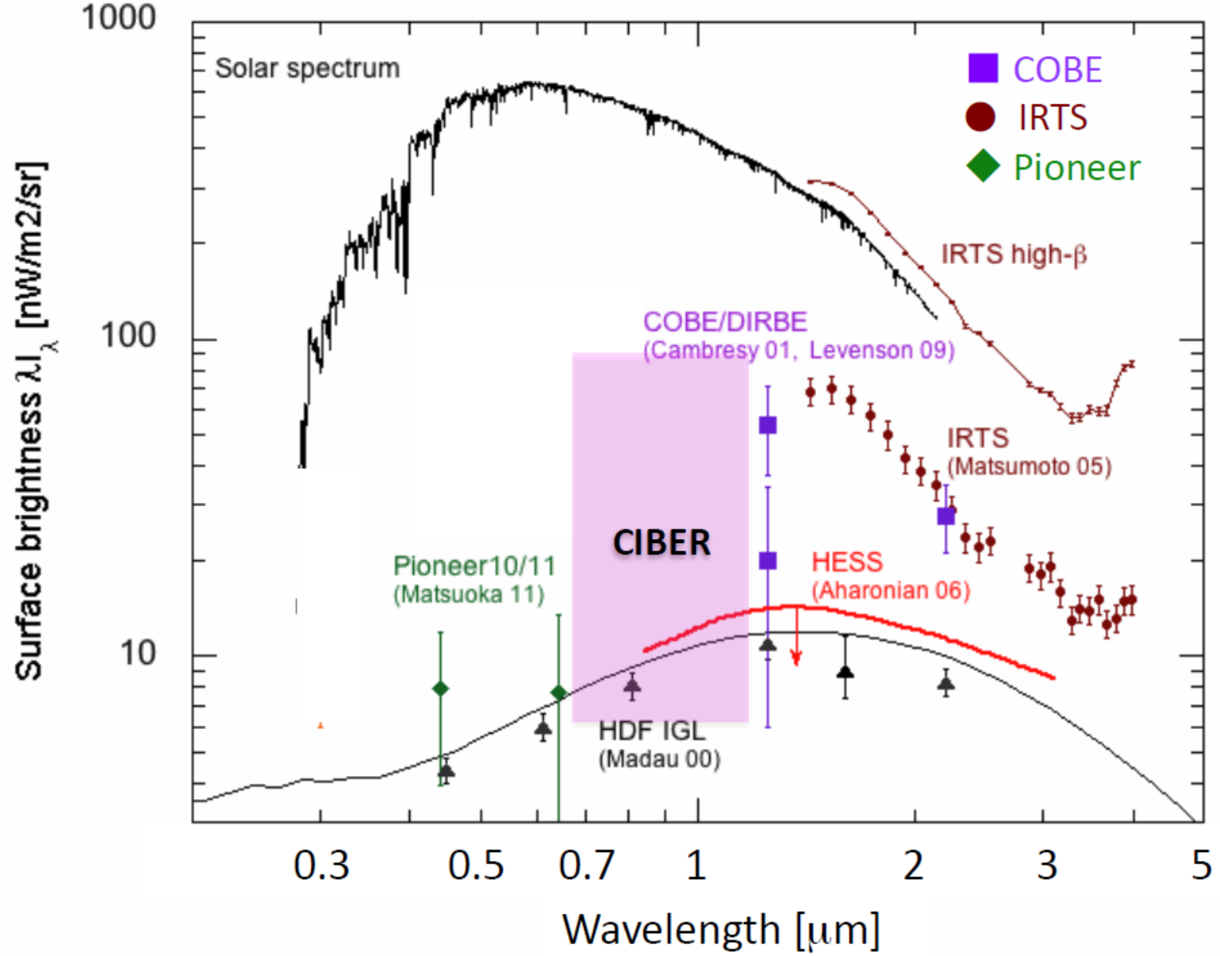

[From the slides of the talk by S Matsuura at AIU2012]

Zodiacal Light

- Scattered sun light by interplanetary dust
- Strong ecliptic latitude dependence

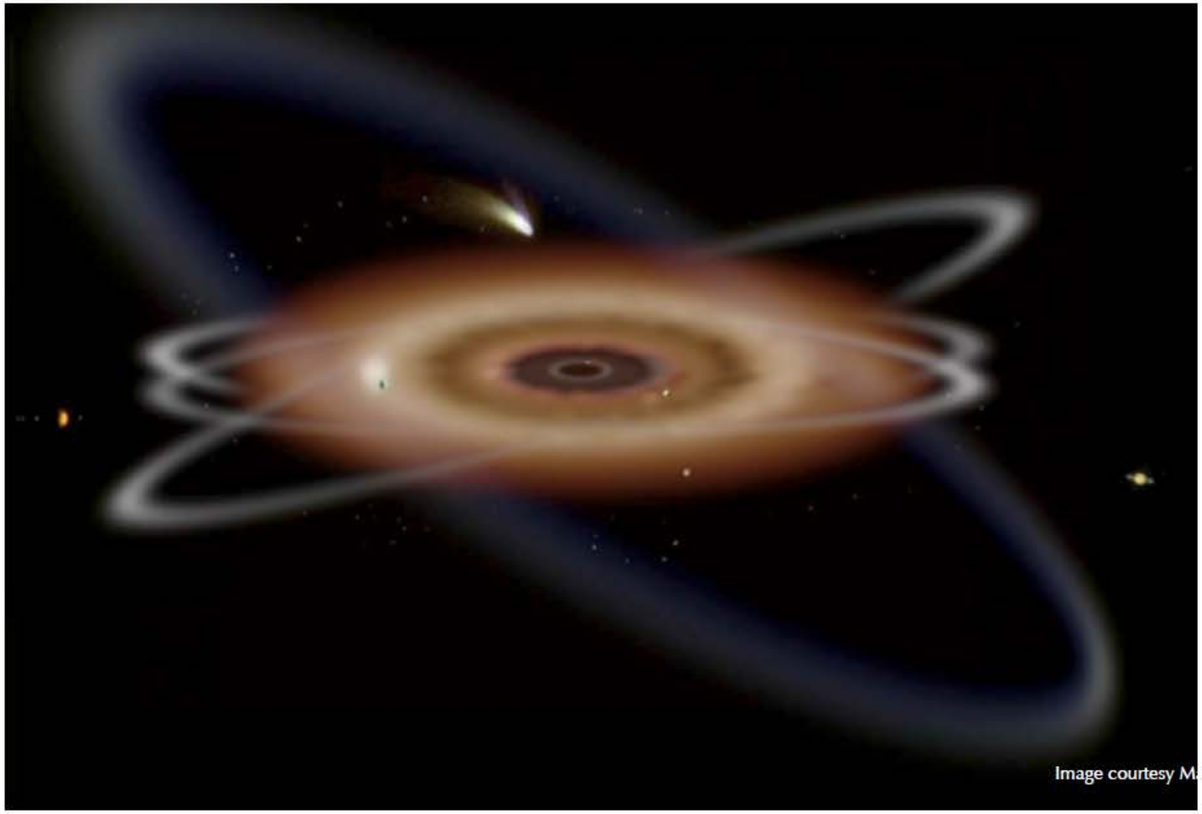

[From the slides of the talk by S Matsuura at AIU2012]

The Cosmic Infrared Background ExpeRiment (CIBER)

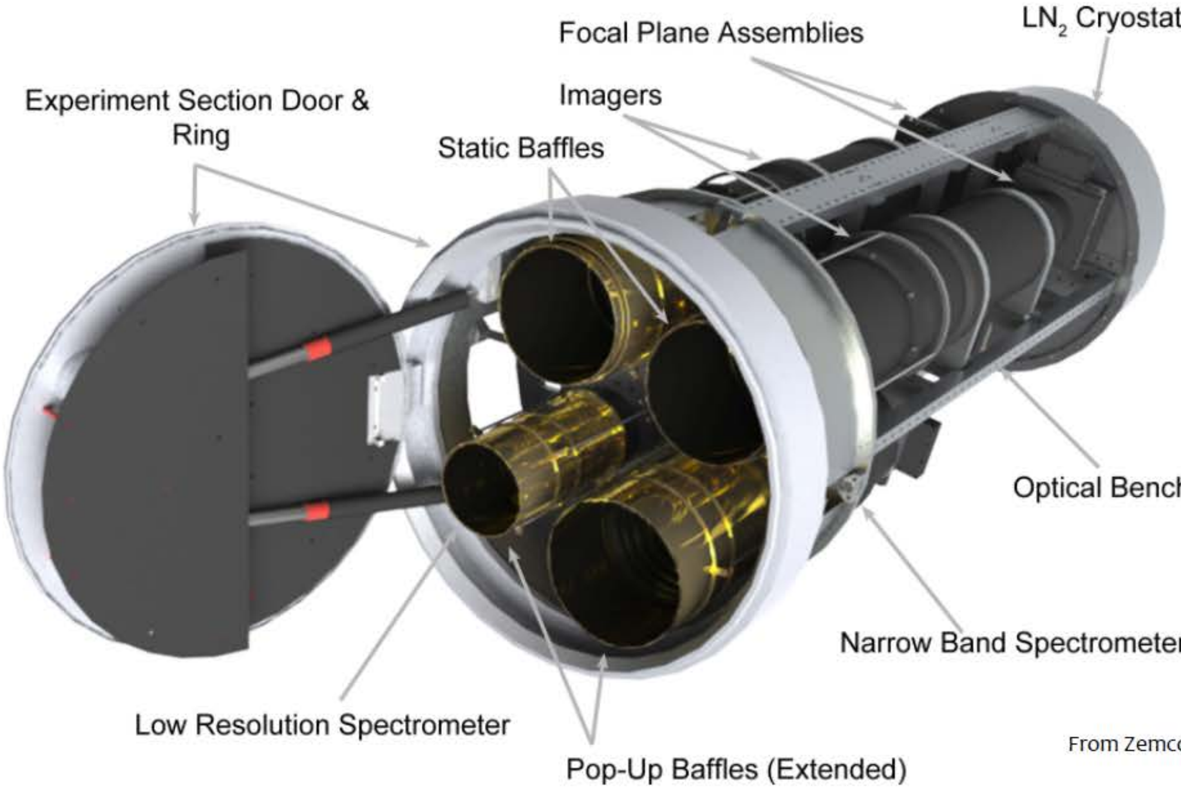

From Zemcov et al. (2012)

[From the slides of the talk by S Matsuura at AIU2012]

Launch vehicle & orbit

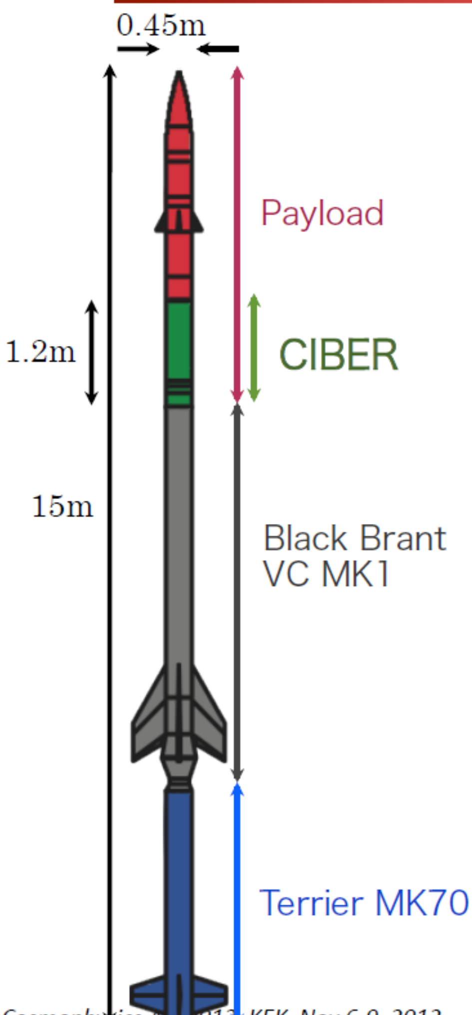

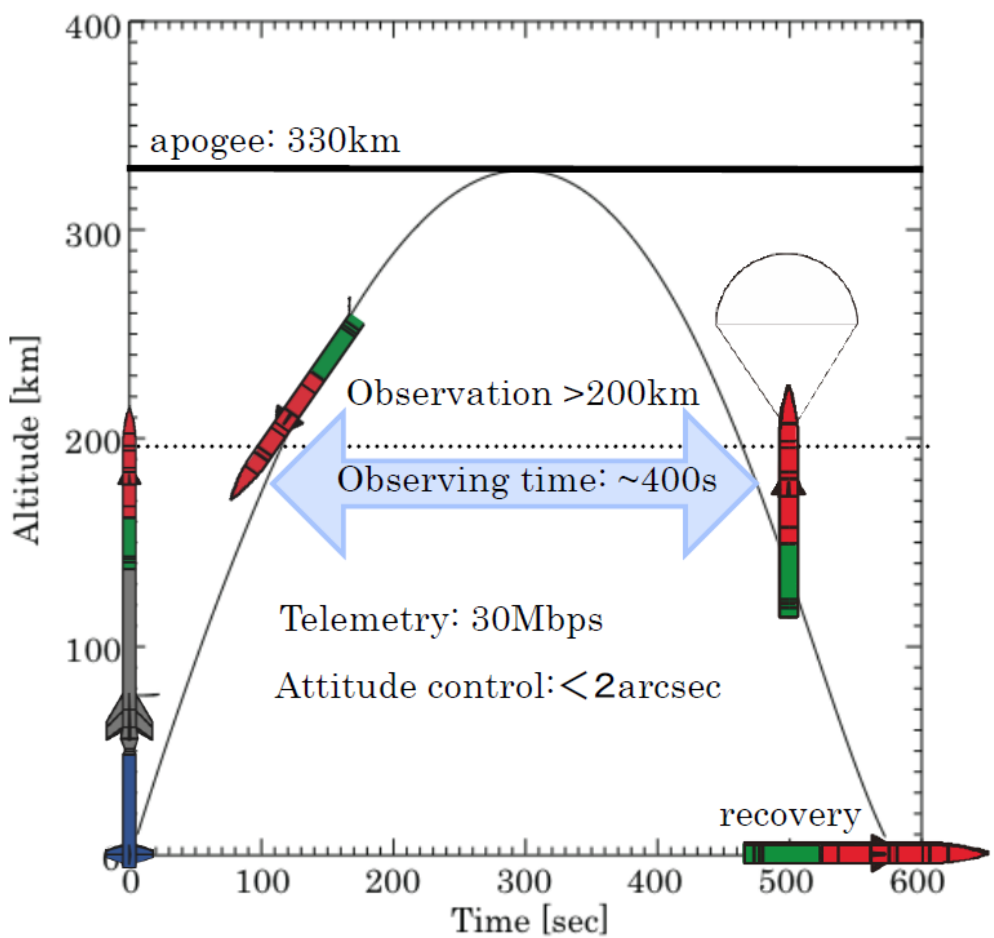

[From the slides of the talk by S Matsuura at AIU2012]

Rocket experiment CIBER

- We have already flown CIBER three times.
  (Feb 2009, Jul 2010 and Mar 2012)
- All flights were successful.
- Analyzing the data.

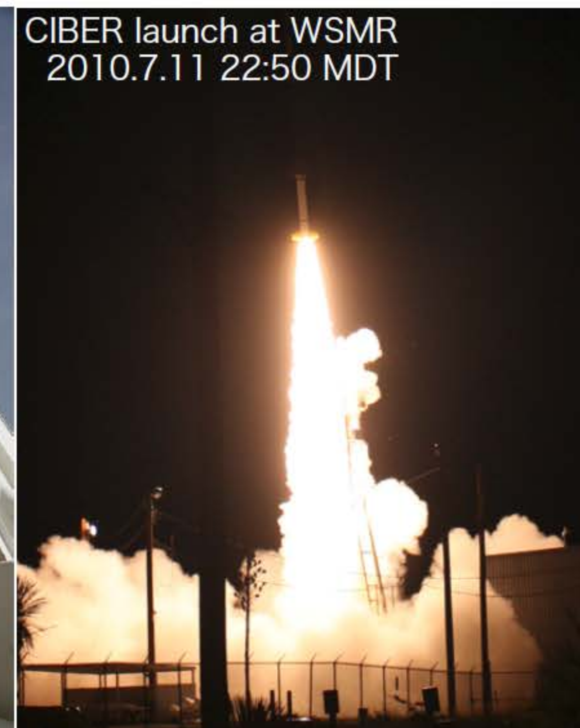

[From the slides of the talk by S Matsuura at AIU2012]

CIBER result

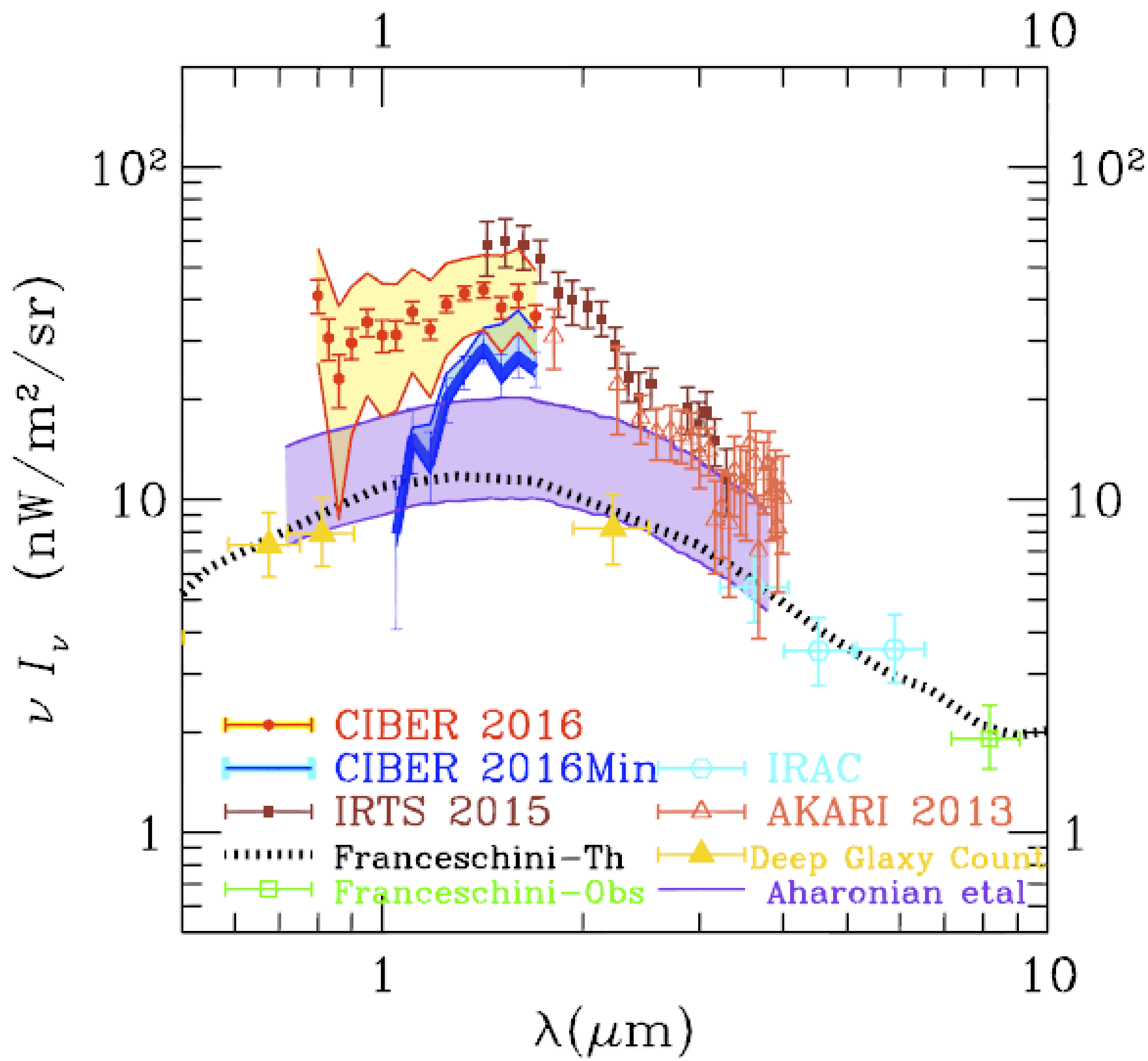

Matsuura S et al: ApJ 839, 7 (2017)

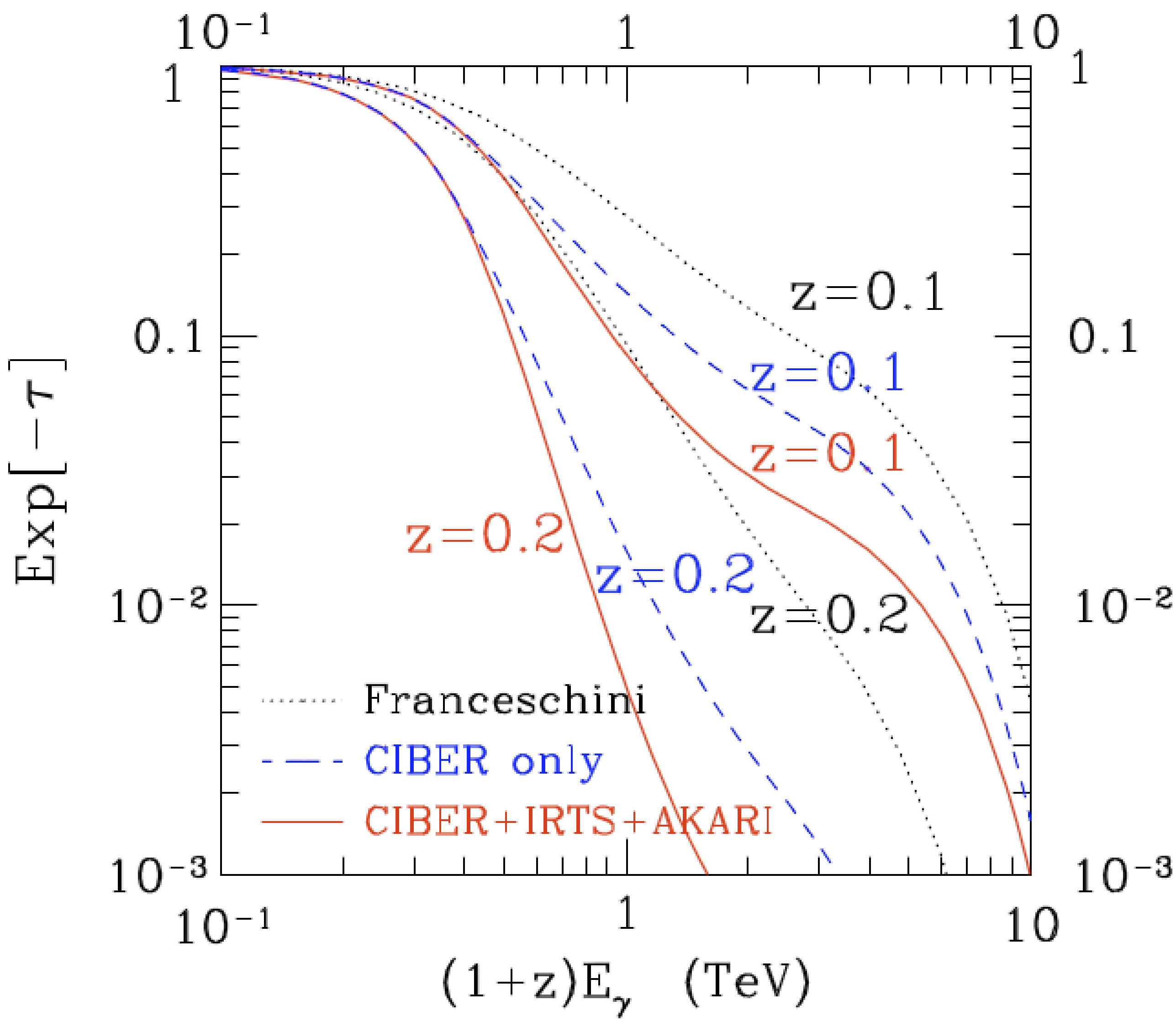

10⁻¹
1
10
1
0.1
10⁻²
10⁻³
Exp[−τ]
z=0.1
z=0.1
z=0.1
z=0.2
z=0.2
z=0.2
Franceschini
CIBER only
CIBER+IRTS+AKARI
(1+z)Eγ (TeV)

アクシオンによる宇宙の透明化

Axion-Photon Conversion

- Chern-Simons coupling of axion with EM fields

$$\mathscr{L} = -\frac{1}{2}(\partial a)^2 - \frac{1}{2}m_a^2 a^2 - \frac{1}{2}F\cdot F - \frac{1}{2}g_{a\gamma} a F\cdot *F$$

$$\Downarrow$$

$$\mathscr{L} = \frac{1}{2}|\dot{a}|^2 - \frac{1}{2}\omega_a^2|a|^2 + \frac{1}{2}|\dot{\boldsymbol{A}}|^2 - \frac{1}{2}|\boldsymbol{k}\times\boldsymbol{A}|^2 - g_{a\gamma} a \boldsymbol{B}_0\cdot\dot{\boldsymbol{A}}$$

- Wave equations in plasma

$$\begin{aligned}
\epsilon\partial_t^2\boldsymbol{E} &= c^2\boldsymbol{k}\times(\mu^{-1}\boldsymbol{k}\times\boldsymbol{E}) - \frac{\omega_p^2\omega^2}{\omega^2-\omega_g^2}\boldsymbol{E} - g_{a\gamma}\omega^2 a\boldsymbol{B}_0 \\
&\quad + \frac{\omega_p^2}{\omega^2-\omega_g^2}\left\{i\omega\omega_g\boldsymbol{E}\times\boldsymbol{b} + \omega_g^2(\boldsymbol{E}\cdot\boldsymbol{b})\boldsymbol{b}\right\}, \\
\partial_t^2 a &= -\omega_a^2 a + g_{a\gamma}\boldsymbol{E}\cdot\boldsymbol{B}_0.
\end{aligned}$$

where

$$\omega_g = \frac{eB_0}{cm_e}, \quad \omega_p^2 = \frac{4\pi n_e e^2}{m_e}.$$

- High frequency limit

When a wave propagates nearly at the speed of light, we have

$$\partial_t X \approx -\partial_z X \approx -ikX$$

⇓

$$(\partial_t^2 - \partial_z^2)X(t,z) = (\partial_t - \partial_z)(\partial_t + \partial_z)X \simeq -2ik(\partial_t + \partial_z)X = -2ik\frac{dX}{dz}$$

Hence, the wave equations can be approximated by a first-order system of ODEs as

$$\left(-i\frac{d}{dz} + \mathscr{M}\right)\begin{pmatrix} A_\perp \\ iA_{//} \\ a \end{pmatrix} = 0; \quad \mathscr{M} = \begin{pmatrix} \Delta_\perp & \Delta_R & 0 \\ \Delta_R & \Delta_{//} & \Delta_B \\ 0 & \Delta_B & \Delta_a \end{pmatrix}$$

where

$$\Delta_\perp = \Delta_{\rm pl} + \Delta_{\rm CM}^{\perp}, \quad \Delta_{//} = \Delta_{\rm pl} + \Delta_{\rm CM}^{//}, \quad \Delta_{\rm pl} = \omega_{\rm pl}^2/(2E)$$

$$\Delta_B = g_{a\gamma}B/2, \quad \Delta_a \simeq m_a^2/(2E), \quad \Delta_R = \omega_p^2 e B_z/(2cm_e E^2)$$

Mass eigenvalues

Neglecting the Faraday rotation, the mass matrix can be diagonalised as

$$\begin{pmatrix} \Delta_\gamma & \Delta_B \\ \Delta_B & \Delta_a \end{pmatrix} = R(\theta)[\lambda_1, \lambda_2]R(-\theta) :$$

$$\lambda_1 + \lambda_2 = \Delta_\gamma + \Delta_a,$$
$$(\lambda_1 - \lambda_2)\cos(2\theta) = \Delta_\gamma - \Delta_a,$$
$$(\lambda_1 - \lambda_2)\sin(2\theta) = 2\Delta_B.$$

$$\Rightarrow \quad \lambda = \frac{1}{2}\{\Delta_\gamma + \Delta_a \pm \Delta_{\rm osc}\}; \quad \Delta_{\rm osc}^2 = (\Delta_\gamma - \Delta_a)^2 + 4\Delta_B^2$$

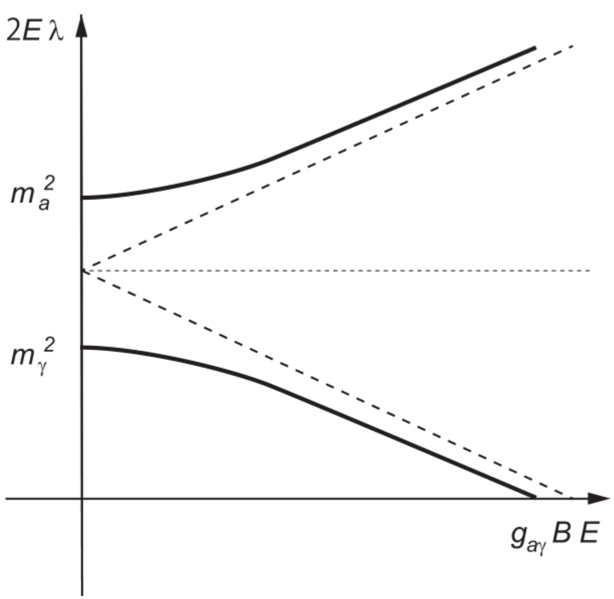

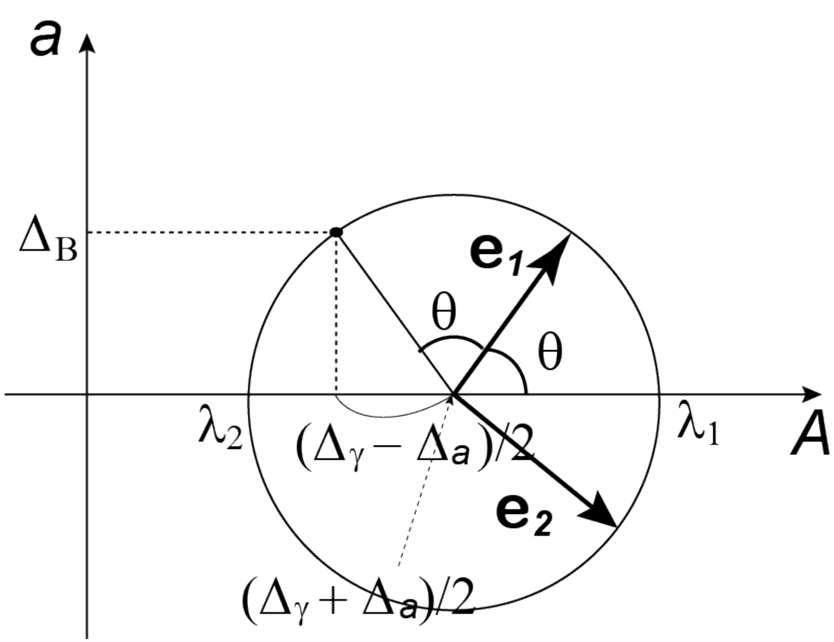

- Non-resonant transition

Neglecting the change of $\theta, \lambda_1, \lambda_2$, the solution is

$$\begin{pmatrix} iA_{//}(z) \\ a(z) \end{pmatrix} = R(\theta) \begin{pmatrix} e^{i\lambda_1 z} & 0 \\ 0 & e^{i\lambda_2 z} \end{pmatrix} R(-\theta) \begin{pmatrix} iA_{//}(0) \\ a(0) \end{pmatrix}.$$

Hence, the conversion rate is

$$P_{\gamma\to a} = P_0 := \sin^2(2\theta)\sin^2\frac{s\,\Delta_{\rm osc}}{2} = \frac{4\Delta_B^2}{\Delta_{\rm osc}^2}\sin^2\frac{s\,\Delta_{\rm osc}}{2}$$

where

$$\Delta_{\rm osc}^2 = (\Delta_{\rm CM} + \Delta_{\rm pl} - \Delta_a)^2 + 4\Delta_B^2.$$

- Resonant transition (non-uniform case)

$$2\pi|\Delta'_{\rm pl} + \Delta'_{\rm CM}| \lesssim \Delta_B^2 \Rightarrow \quad P_{\gamma\to a} = {\rm O}(1)$$

Axion makes the Universe transparent!

Chern-Simons coupling of axion and EM

$$\frac{1}{2} g_{a\gamma}\, aF\cdot *F = g_{a\gamma}\, a\boldsymbol{E}\cdot\boldsymbol{B}$$

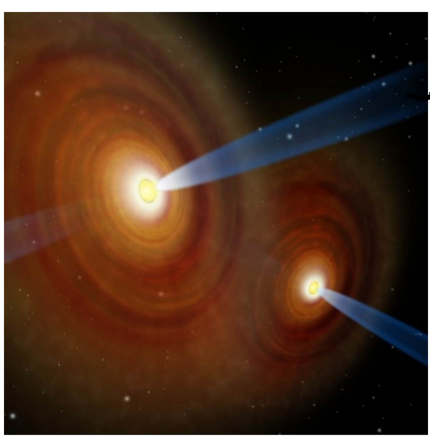

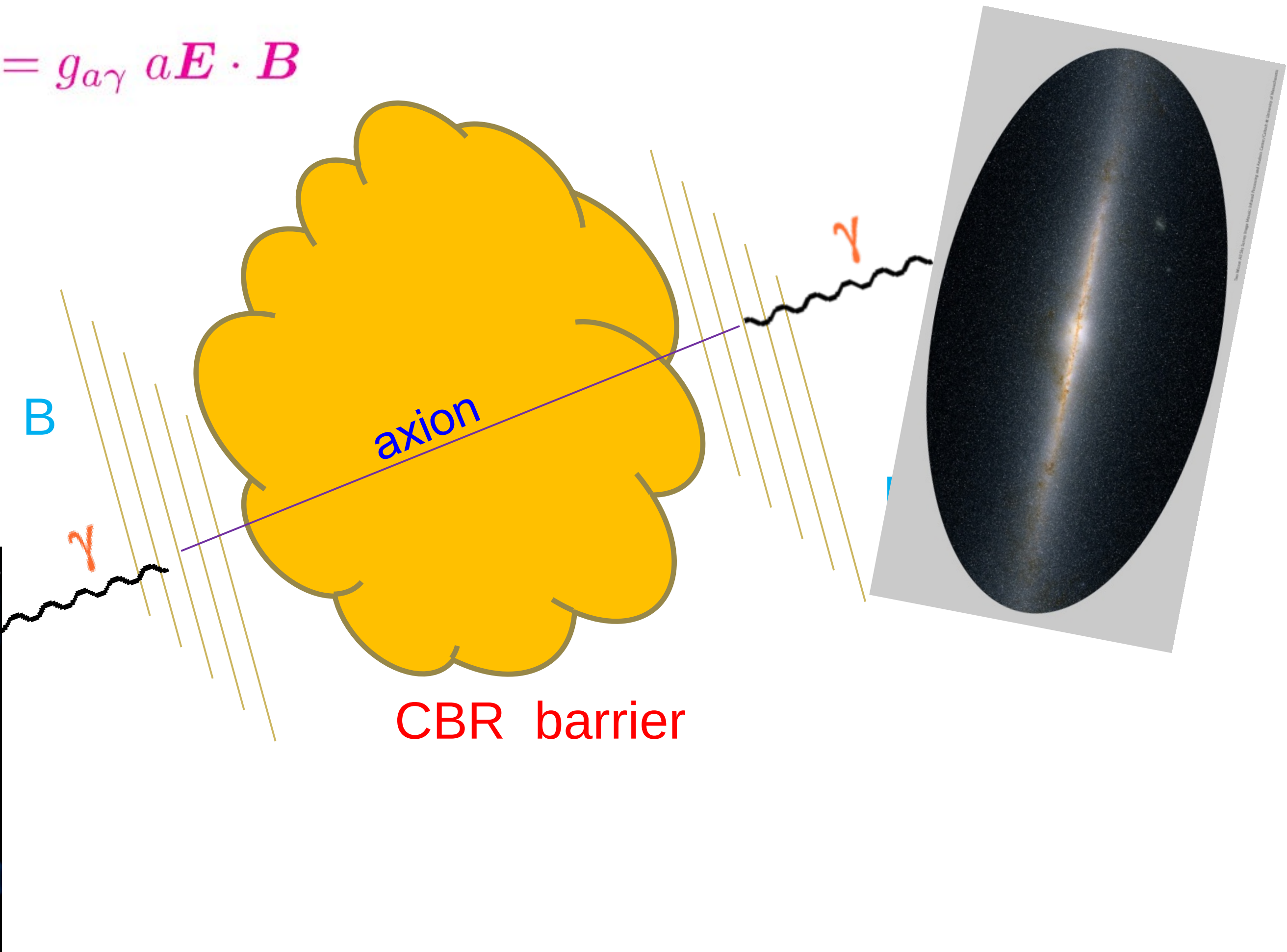

Conditions for Strong Conversion

- Conversion rate

$$P_0 = \frac{1}{1+(E_*/E)^2}\sin^2\left(g_{a\gamma}B\left[1+(E_*/E)^2\right]^{1/2}\frac{L}{2}\right),$$

$$E_* := \frac{|m_a^2 - m_\gamma^2|}{2g_{a\gamma}B} \simeq 0.7\frac{|m_a^2 - m_\gamma^2|}{(10^{-7}\text{eV})^2}\left(\frac{10\mu\text{G}}{B}\right)\left(\frac{g_{a\gamma}^{-1}}{10^{11}\text{GeV}}\right)\text{TeV}$$

- Condition 1: Near resonance

$$E \gtrsim E_* \Rightarrow \quad g_{a\gamma}\cdot 10^{11}\text{GeV} \gtrsim 0.7\left(\frac{m_a}{10^{-7}\text{eV}}\right)^2\frac{1}{B_{10\mu\text{G}}E_{\text{TeV}}}$$

- Consition 2: Sufficient oscillations

$$g_{a\gamma}BL \gtrsim \pi \Rightarrow \quad g_{a\gamma}\cdot 10^{11}\text{GeV} \gtrsim 0.3\frac{1}{B_{10\mu\text{G}}L_{10\text{kpc}}}$$

Axion solution

Kohri K, Kodama H: PRD96, 051701(R) (2017)
[arXiv: 1704.05189

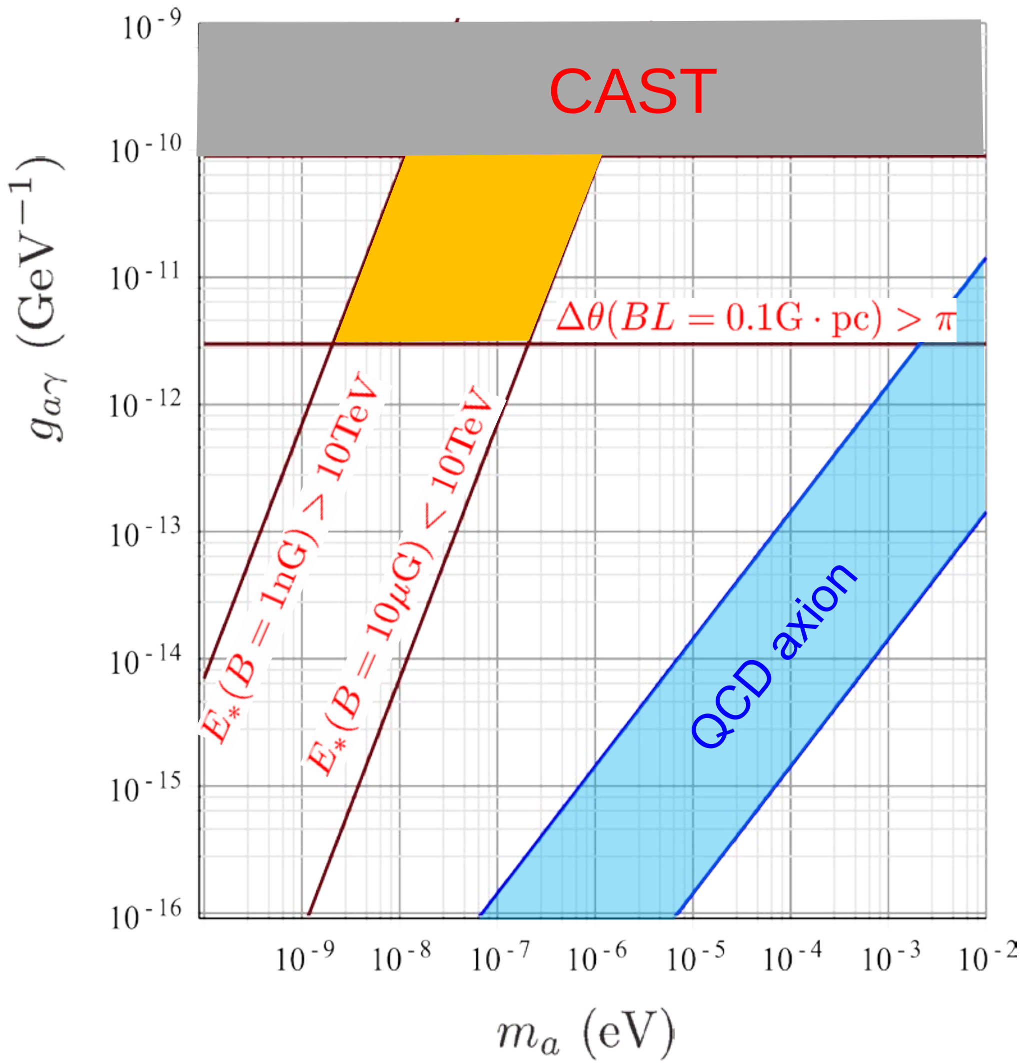

$$g_{a\gamma} = \frac{\xi}{16\pi^2} \times \frac{1}{f_a}$$

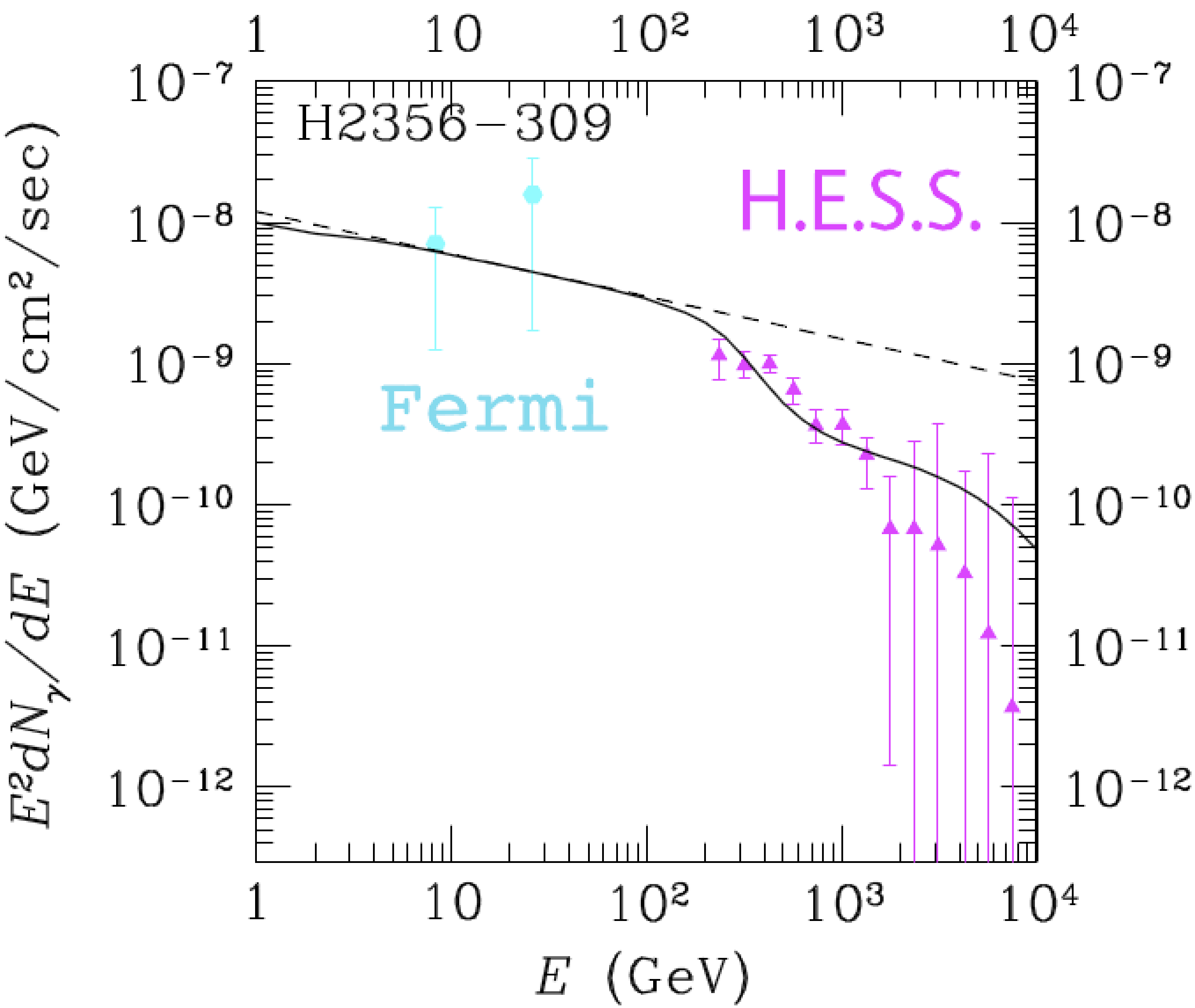

H2356−309
H.E.S.S.
Fermi
$E^2 dN_\gamma/dE$ (GeV/cm²/sec)
E (GeV)
1
10
10^2
10^3
10^4
10^{-7}
10^{-8}
10^{-9}
10^{-10}
10^{-11}
10^{-12}

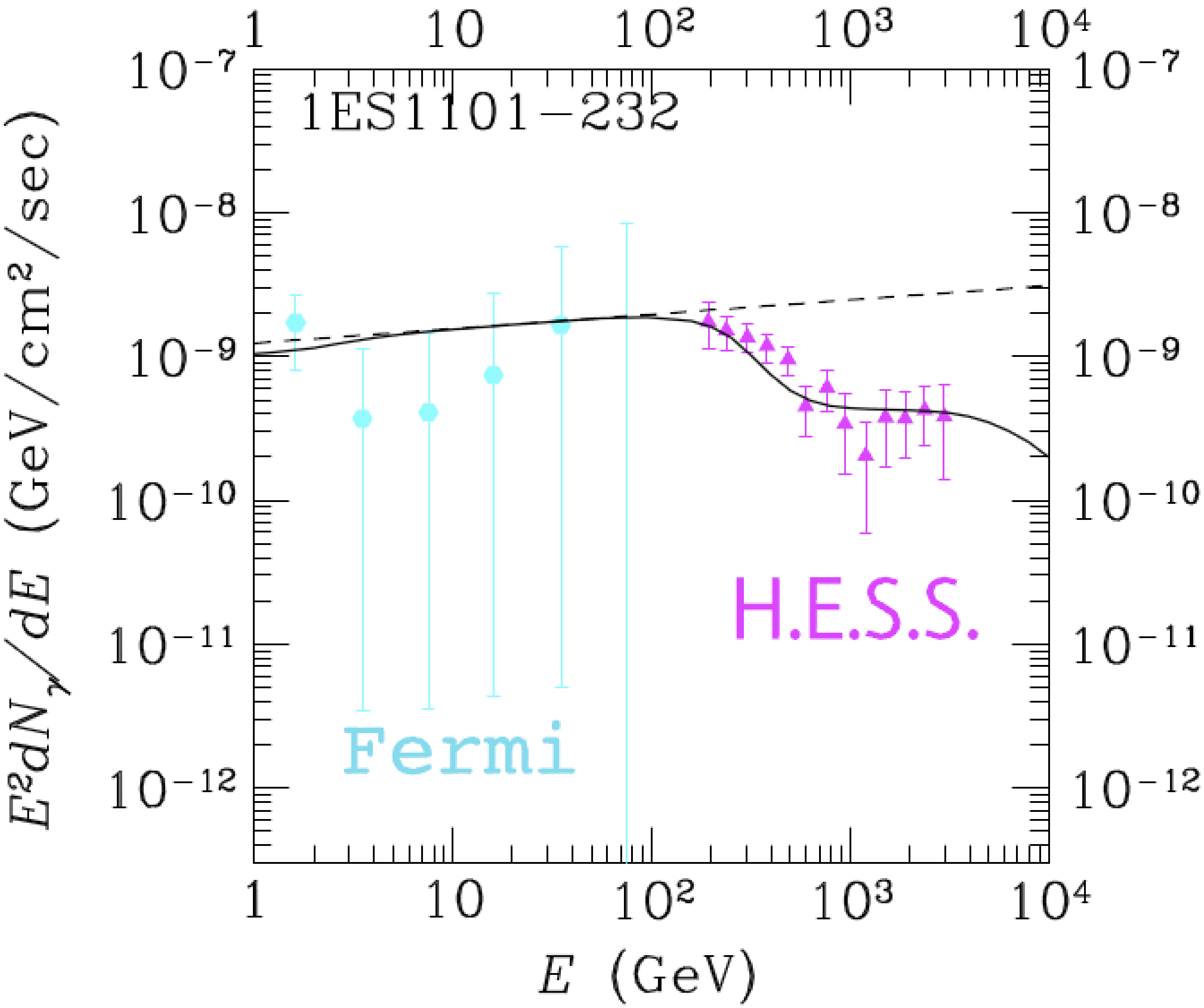

1ES1101−232
Fermi
H.E.S.S.
$E^2 dN_\gamma/dE$ (GeV/cm^2/sec)
E (GeV)
1
10
10^2
10^3
10^4
10^{-7}
10^{-8}
10^{-9}
10^{-10}
10^{-11}
10^{-12}

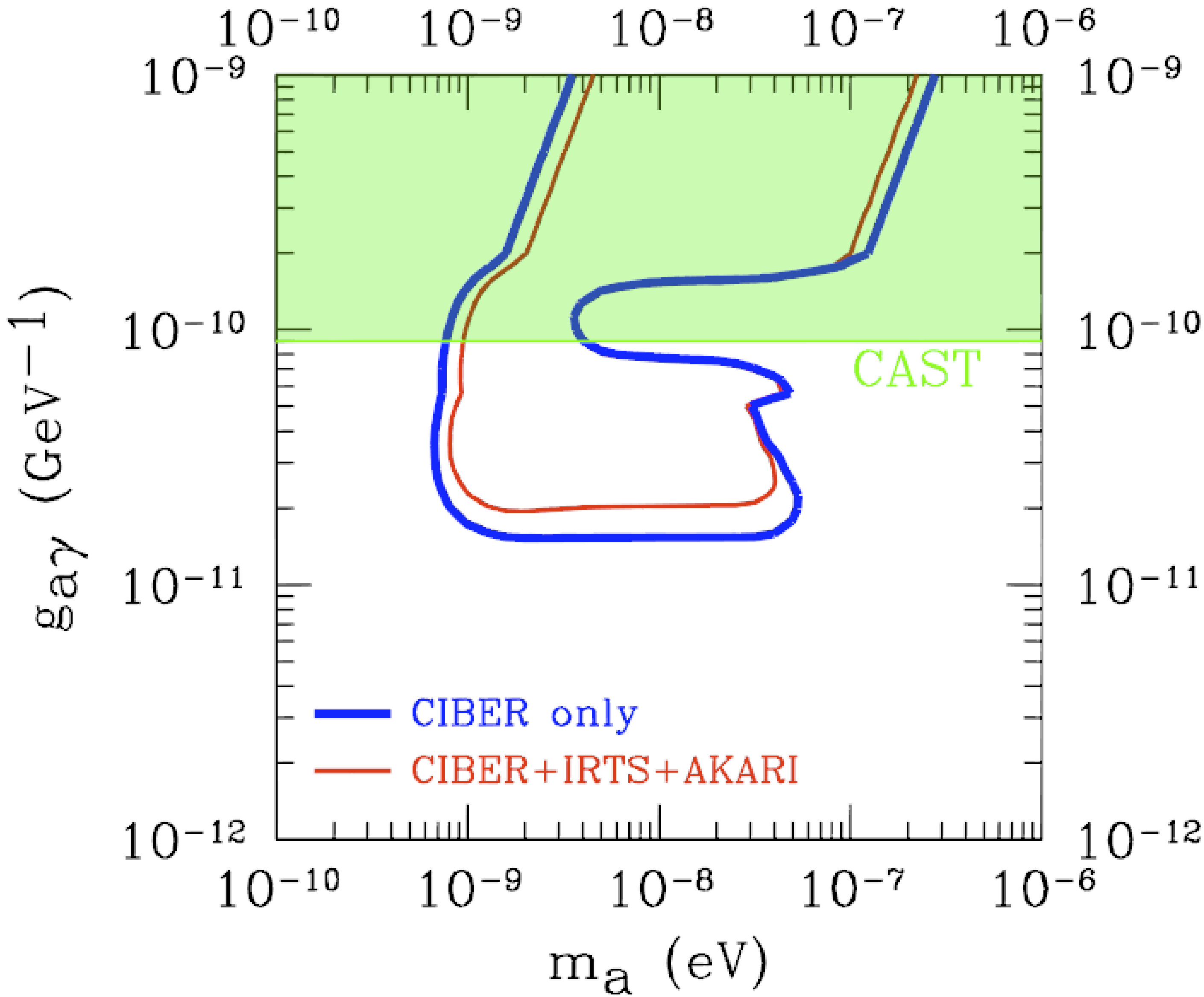

10^{-10} 10^{-9} 10^{-8} 10^{-7} 10^{-6}
10^{-9}
10^{-10}
10^{-11}
10^{-12}
CAST
CIBER only
CIBER+IRTS+AKARI
$g_{a\gamma}$ (GeV^{-1})
m_a (eV)

Backup Slides

Mode Mixture: l=m=1 + l=m=2

- Parameters: a_*=a/M=0.99,   Mμ = 0.40
- Initial mode: (l, m, n_r) = (1, 1, 0)+(2,2,0), Φ/f_a =0.7 + 0.01

$$\Phi/f_a = \sum_{l,m} b_{lm}(t, r_*) Y_l^m(\theta, \phi)$$

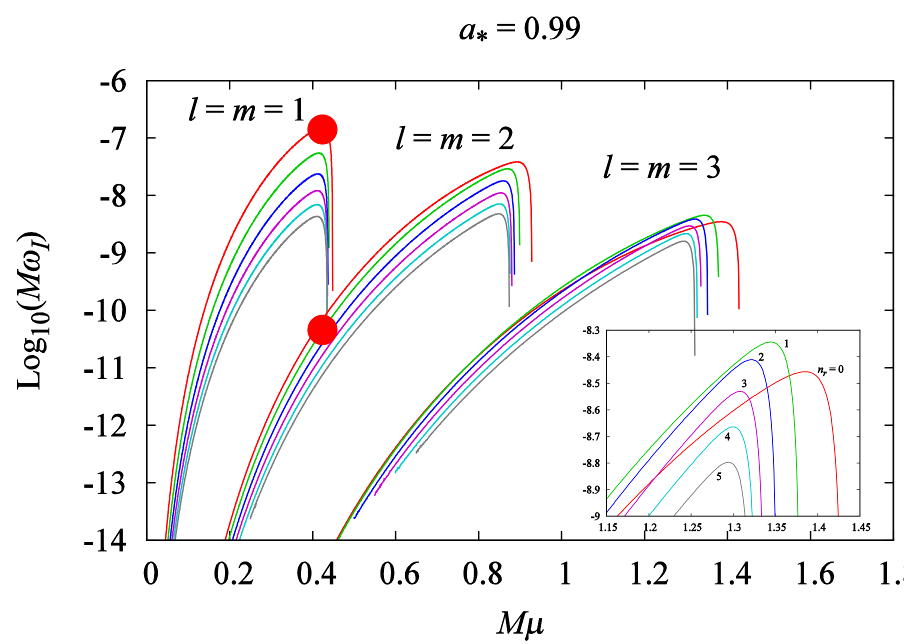

Results

- Bose nova happens as in the pure l=m=1 case.
- The l=m=2 mode, which is tiny initially, rapidly grows during bosenova due to resonant interactions.
- After the bosenova, the l=m=2 components settle down to stationary states but a large fraction of them are unbounded modes.

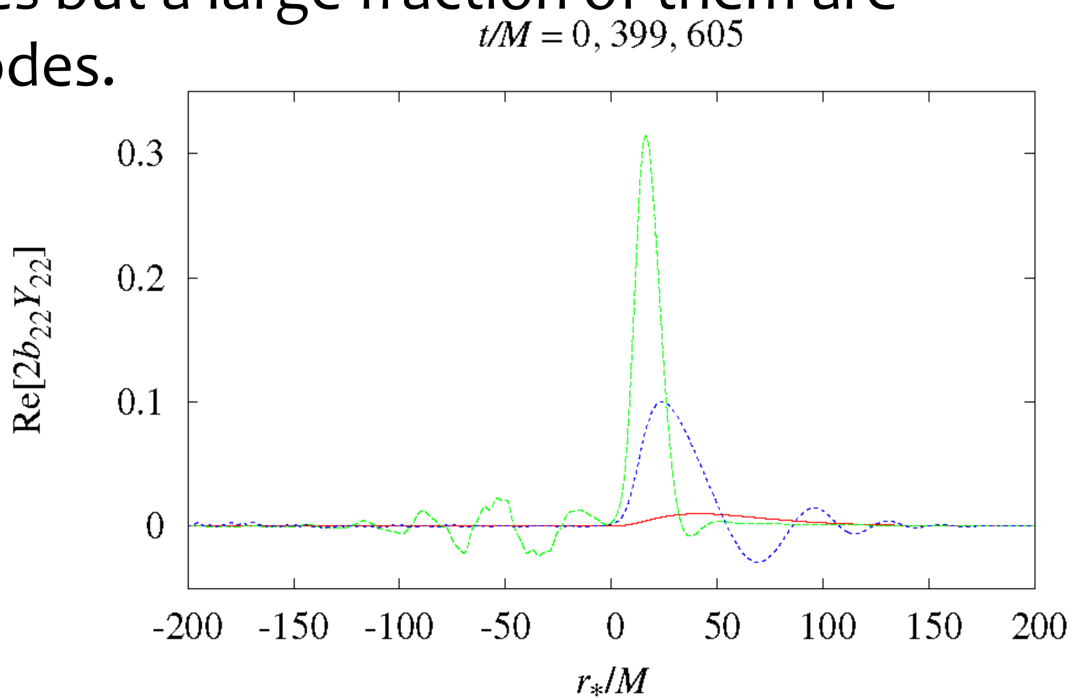

- The mixture of a tiny l=m=2 component significantly modifies the shape of the whole wave function, increases the energy infall during bosenova and decreases the angular momentum extraction.

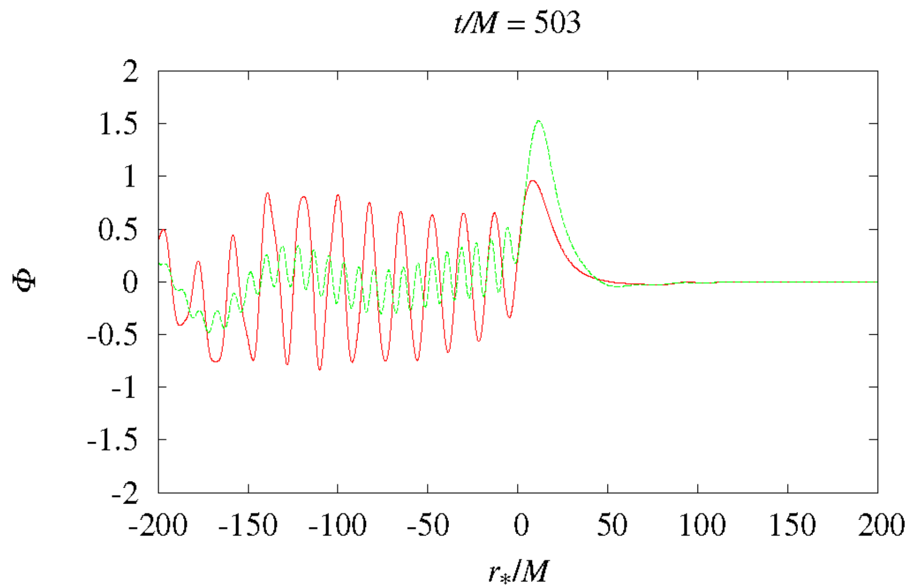

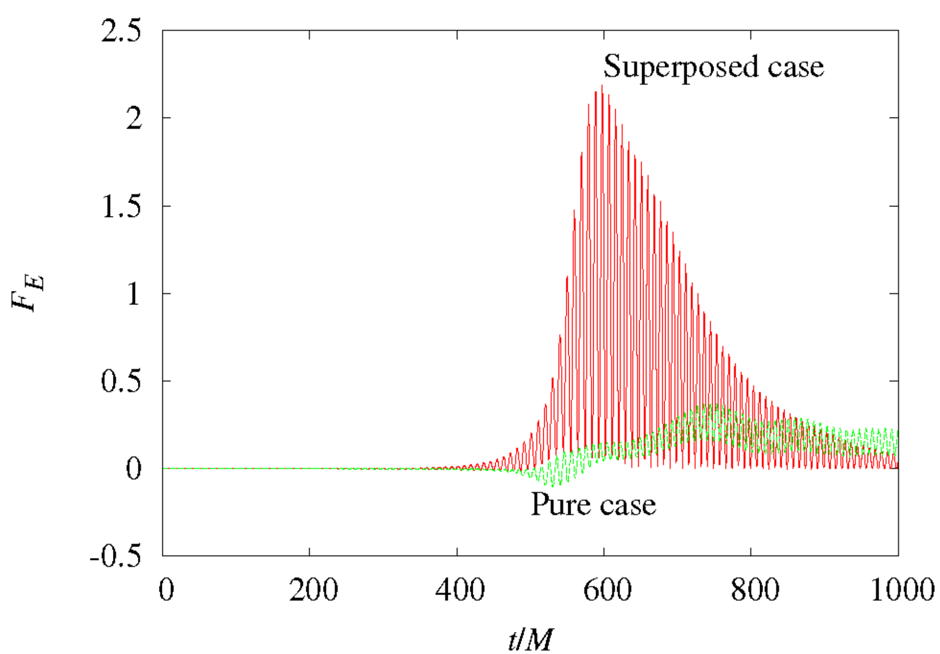

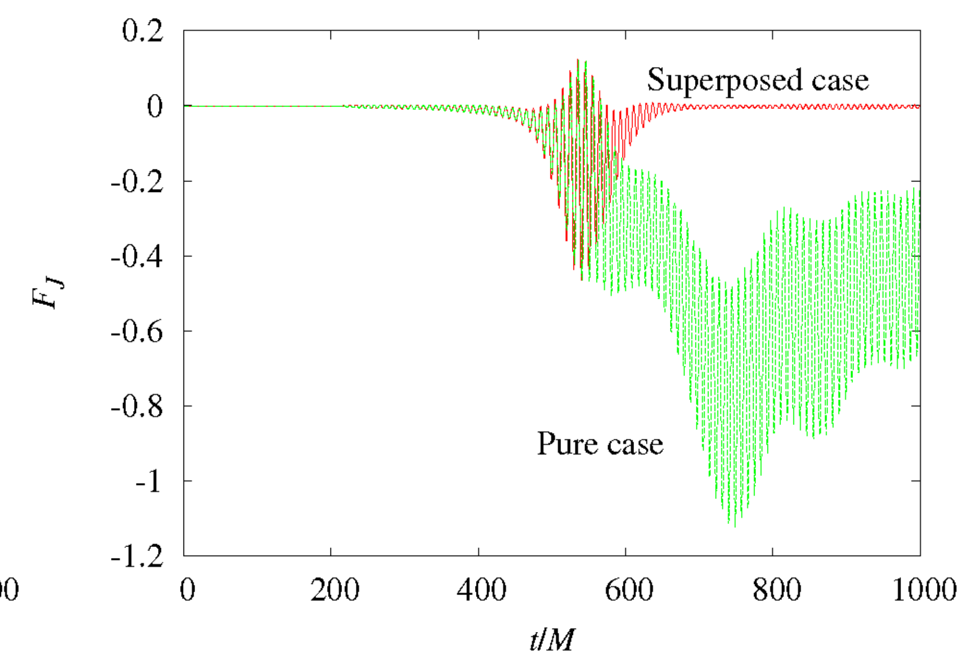

Some Consequences

- Mode interactions

  In general, large number of modes may be excited simultaneously because the age of astrophysical BHs are rather long.

  Our multi-mode simulation suggests

  – Violent bosenova can be triggered only by the l=m=1 modes.

  – l=m>1 modes do not produce violent phenomena, but still periodic bosenova-like phenomena happen.

  – The coexistence of these modes with different (l, m) changes the dynamical behavior of the BH-axion system significantly, and in particular, makes bosenova event more violent.

Methods to Estimate GW Emissions

- Semi-analytic method based on the Green's formula and the separation-of-variable solution of the source-free Teukolsky equation

$$\Box u_{\mu\nu} = 0; \quad u^\mu_\mu = 0, \quad \nabla_\nu u^\nu_\mu \sim 0 \text{ at } \mathscr{I}^+$$

$$\dot{E}_{\mathscr{I}^+} = 2\pi G \sum_{l,m,s,\tilde{\omega}} |C^s_{lm}|^{-2} \left|\langle u_{lms\,\tilde{\omega}}, T\rangle\right|^2 \qquad \langle u, T\rangle := \frac{1}{\Delta t}\int_D d^4x\sqrt{-g}u^{\mu\nu}T_{\mu\nu}$$

- Numerical integration of the Teukolsky equation in the time domain.

$$_{-2}\Psi = \sum_{\tilde{m}\in\mathbb{Z}} \frac{\Delta^2}{r}\psi^{(\tilde{m})}(t,r,\theta)\sin^{|\tilde{m}-2|}\frac{\theta}{2}\cos^{|\tilde{m}+2|}\frac{\theta}{2}\,e^{i\tilde{m}\phi} \quad \Rightarrow \quad \dot{E}_{\mathscr{I}^+}$$

$$L\psi^{(\tilde{m})} = T^{(\tilde{m})} = (\partial\Phi\partial\Phi)^{(\tilde{m})}_{\text{tf}}$$

Spin of BHs in BHBs

Middleton M: arXiv:1507.06153

	Continuum fitting					Reflection fitting
Source	Mass ($M_\odot$)	Inclination (degrees)	Distance (kpc)	a_*	Model K/K2/B	a_*
Cygnus X-1	14.8 ±1.0	27.1 ± 0.8	$1.86^{+0.12}_{-0.11}$	≥ 0.95	K2	> 0.97 [a]
XTE J1550-564	9.10 ± 0.61	74.7 ± 3.8	$4.38^{+0.58}_{-0.31}$	$0.34^{+0.37}_{-0.34}$	K2	0.55 ± 0.22
XTE J1650-500						0.79 ± 0.01
XTE J1652-453						0.45 ± 0.02
XTE J1752-223						0.52 ± 0.11
XTE J1908+094						0.75 ± 0.09
A 0620-00	6.61 ± 0.25	51.0 ± 0.9	1.06 ± 0.12	0.12 ± 0.19	K2	
4U 1543-475	9.4 ± 1.0	20.7 ± 1.5	7.5 ± 1.0	0.8 ± 0.1	K	0.3 ± 0.1
4U 1630-472						$0.985^{+0.005}_{-0.014}$
MAXI J1836-194						0.88 ± 0.03
GRO J1655-40	6.30 ± 0.27	70.2 ± 1.2	3.2 ± 0.2	0.7 ± 0.1	K	0.98 ± 0.01
GS 1124-683	7.24 ± 0.70	54.0 ± 1.5	5.89 ± 0.26	$-0.24^{+0.05}_{-0.64}$	K	
GX 339-4						>0.97 [b]
GRS 1915+105	14.0 ± 4.4	66 ± 2	11.0	≥ 0.95	K2	0.98 ± 0.01
				~ 0.7 [c]	B	
GRS 1739-278						0.8 ± 0.2 [d]
SAX J1711.6-3608						$0.6^{+0.2}_{-0.4}$
Swift J1753.5-0127						$0.76^{+011}_{-0.15}$
Swift J1910.2-0546						≤ -0.32
LMC X-1	10.91 ± 1.54	36.4 ± 2.0	48.1 ± 2.2	$0.92^{+0.05}_{-0.07}$	K2	$0.97^{+0.02}_{-0.13}$
LMC X-3	6.95 ± 0.33	69.6 ± 0.6	48.1 ± 2.2	$0.21^{+0.18}_{-0.22}$ [e]	K2	
M31 ULX-2	~10	< 60	772 ± 44	< -0.17 [f]	B	
M33 X-7	15.65 ± 1.45	74.6 ± 1.0	840 ± 20	0.84±0.05	K	

Spin of AGN BHs

Reynolds CS: SSRv 183 (2014) 277.

Object	Mass ($\times 10^6\ M_\odot$)	Spin	Mass/Spin references
Mrk335	14.2 ± 3.7	$0.83^{+0.09}_{-0.13}$	Pe04/Wa13
IRAS 00521–7054	–	>0.84	–/Ta12
Tons180	~ 8.1	$0.92^{+0.03}_{-0.11}$	ZW05/Wa13
Fairall 9	255 ± 56	$0.52^{+0.19}_{-0.15}$	Pe04/Lo12
Mrk359	~ 1.1	$0.66^{+0.30}_{-0.54}$	ZW05/Wa13
Mrk1018	~ 140	$0.58^{+0.36}_{-0.74}$	Be11/Wa13
1H0419-577	~ 340	>0.89	ZW05/Wa13
Ark120	150 ± 19	$0.64^{+0.19}_{-0.11}$	Pe04/Wa13
Swift J0501.9-3239	–	>0.99	–/Wa13
1H0707-495	~ 2.3	>0.97	ZW05/Zo10
Mrk79	52.4 ± 14.4	0.7 ± 0.1	Pe04/Ga11
Mrk110	25.1 ± 6.1	>0.89	Pe04/Wa13
NGC3783	29.8 ± 5.4	>0.88[a]	Pe04/Br11
NGC4051	1.91 ± 0.78	>0.99	Pe04/Pa12
RBS1124	–	>0.97	–/Wa13
IRAS13224–3809	~ 6.3	>0.987	Go12/Fa13
MCG–6-30-15	$2.9^{+1.8}_{-1.6}$	$a>0.98$	Mc05/BR06
Mrk841	~ 79	>0.52	ZW05/Wa13
Swift J2127.4+5654	~ 1.5	0.6 ± 0.2	Ma08/Mi09
Ark564	~ 1.1	$0.96^{+0.01}_{-0.11}$	ZW05/Wa13

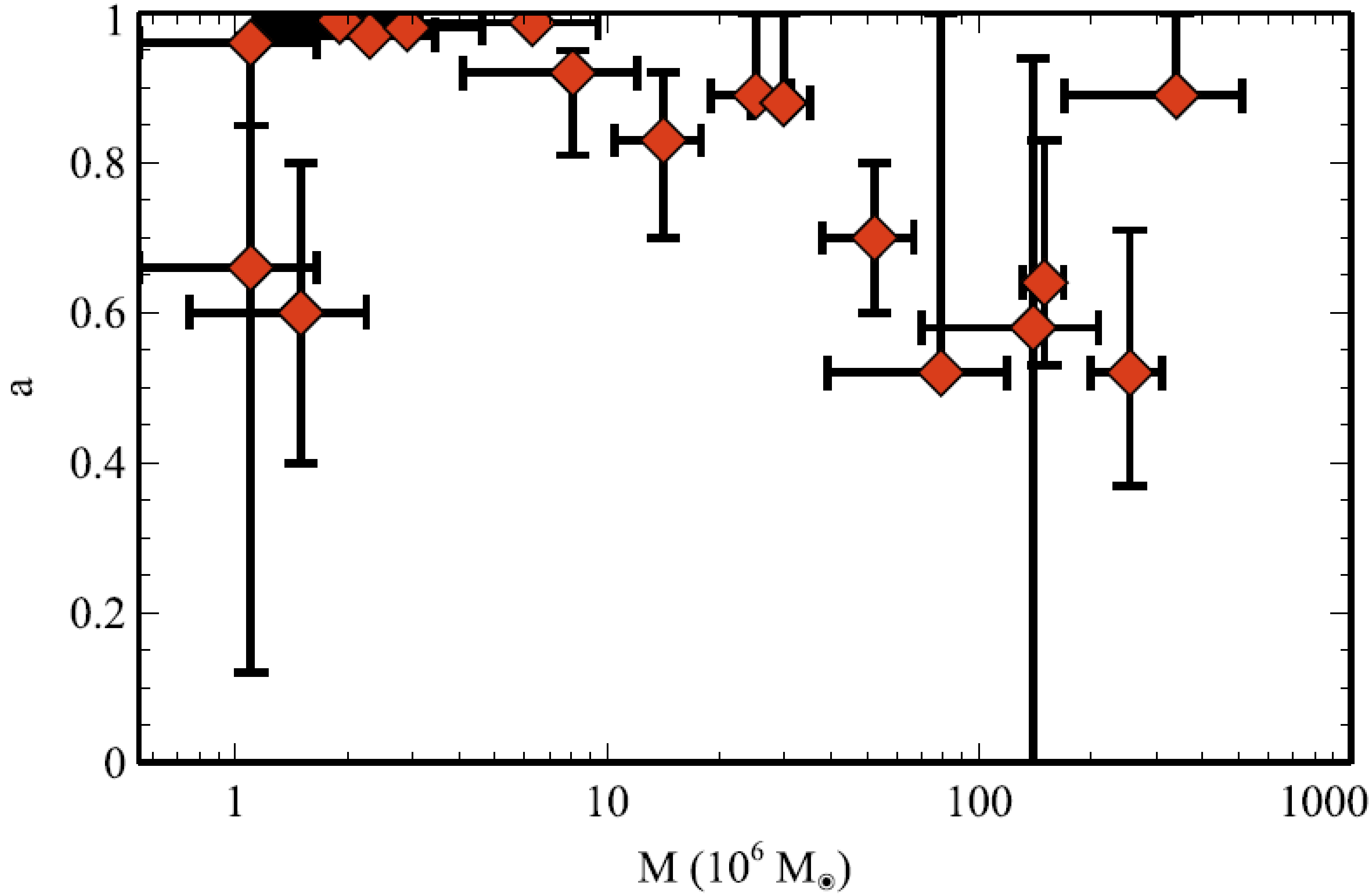

Reynolds CS: SSRv 183 (2014) 277.

Rejection of the intrinsic origin

Fig. 2. Absorption feature present in the spectra of BL Lac objects as a function of increasing redshift (data points, from top to bottom). The dashed curves show the attenuation expected for the sample of sources by averaging, in each redshift and energy bin, the opacities of the sample [the model of (*7*) was used] and multiplying this average by the best-fit scaling parameter *b* obtained independently in each redshift interval. The vertical line shows the critical energy E_{crit} below which ≤ 5% of the source photons are absorbed by the EBL. The thin solid curve represents the best-fit model, assuming that all the sources have an intrinsic exponential cutoff and that blazars follow the blazar sequence model of (*32*, *33*).

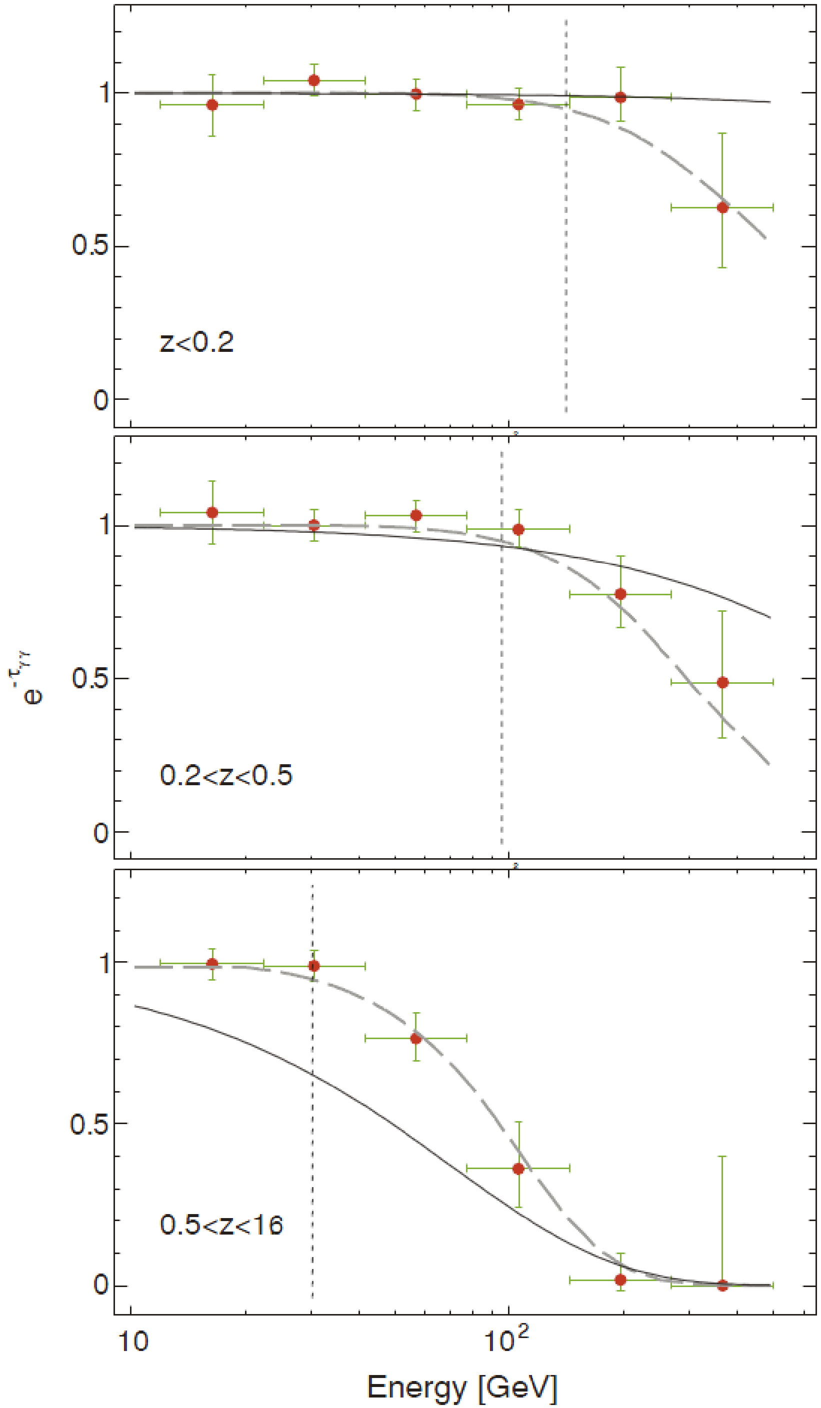

Ackermann at al (Fermi Coll):
Science 338, 1190 (2012)